

# BERICHTE

aus dem Fachbereich Geowissenschaften  
der Universität Bremen

Nr. 155

Rusch, A.

DYNAMIK DER FEINFRAKTION  
IM OBERFLÄCHENHORIZONT  
PERMEABLER SCHELFSSEDIMENTE

Max-Planck-Institut  
für Marine Mikrobiologie  
BIB 5001  
Celsiusstr. 1 • D-28359 Bremen  
Tel. 04 21 / 20 28-640

ITV-Nr. 2717  
D 040



Berichte, Fachbereich Geowissenschaften, Universität Bremen, Nr. 155,  
102 Seiten, Bremen 2000

ISSN 0931-0800

Die "Berichte aus dem Fachbereich Geowissenschaften" werden in unregelmäßigen Abständen vom Fachbereich 5, Universität Bremen, herausgegeben.

Sie dienen der Veröffentlichung von Forschungsarbeiten, Doktorarbeiten und wissenschaftlichen Beiträgen, die im Fachbereich angefertigt wurden.

Die Berichte können bei:

Frau Gisela Boelen

Sonderforschungsbereich 261

Universität Bremen

Postfach 330 440

**D 28334 BREMEN**

Telefon: (49) 421 218-4124

Fax: (49) 421 218-3116

e-mail: [boelen@uni-bremen.de](mailto:boelen@uni-bremen.de)

angefordert werden.

Zitat:

Rusch, A.

Dynamik der Feinfraktion im Oberflächenhorizont permeabler Schelfsedimente.

Berichte, Fachbereich Geowissenschaften, Universität Bremen, Nr. 155, 102 Seiten, Bremen, 2000.

ISSN 0931-0800

# Dynamik der Feinfraktion im Oberflächenhorizont permeabler Schelfsedimente

Dissertation  
zur Erlangung des  
Doktorgrades der Naturwissenschaften

im Fachbereich 5  
der Universität Bremen

vorgelegt von

*Antje Rusch*  
Bremen

2000

Mar-Planck-Institut  
für Meereskunde  
E-Mail: [rusch@zmw.uni-bremen.de](mailto:rusch@zmw.uni-bremen.de)  
Celsiusstr. 1 • 28359 Bremen  
Tel. 04 21 / 20 20-540

Tag des Kolloquiums: 13. April 2000

Gutachter:

Prof. Dr. Bo B. Jørgensen

Prof. Dr. Dieter K. Fütterer

Prüfer:

Prof. Dr. Horst D. Schulz

PD Dr. Reiner Schlitzer

## **PREFACE**

This work is part of ongoing research on the exchange of matter between marine sediments and the overlying water. The study, a subproject of the DFG graduate college "Material Flux in Marine Geosystems" at Bremen University, was conducted at the Max Planck Institute for Marine Microbiology. My project was initiated by a group of scientists there, who investigate fluxes across the sediment-water interface and their consequences for sedimentary biogeochemical processes. Supervised by Prof. Bo B. Jørgensen and with Dr. Stefan Forster and Dr. Markus Hüttl as my mentors, I focused on evidence and features of advective interfacial transport in an intertidal sandflat.

During field work near Sylt island, even most adverse weather conditions could not deter Martina Alisch from providing technical assistance. The co-workers of the BAH Wadden Sea Station in List/Sylt kindly shared their lab space and their knowledge on the study area with us. I appreciate Markus Hüttl, Stefan Forster and Bo Jørgensen for inspiring discussions, constructive criticism and experienced advice. My room-mate Jakob Zopfi and many other colleagues created a pleasant atmosphere to work in, and dear friends kept encouraging me. Finally, my parents are thanked for continuously supporting my pursuit of education.

# TABLE OF CONTENTS

## 1. Introduction

1.1. Permeable shelf sediments	1
1.2. Advective transport across the water-sediment interface	2
1.3. Organic matter in sandy sediments	3
1.4. Objectives of the study	3
1.5. Outline of the publications	4

## 2. Submitted manuscripts

2.1. Advective particle transport into permeable sediments - evidence from experiments in an intertidal sandflat	6
2.2. Transport and degradation of phytoplankton in permeable sediment	22
2.3. Spatial and temporal dynamics of particulate organic matter in permeable marine sands	48
2.4. Bacteria, diatoms and detritus in an intertidal sandflat subject to advective transport across the water-sediment interface	66

## 3. Summary

3.1. Summary and outlook	86
3.2. Zusammenfassung und Ausblick	87

## 4. References

# 1. INTRODUCTION

## 1.1. Permeable shelf sediments

Shelf seas (water depth < 200 m) cover about 8 % of the oceanic surface area, and these nutrient-rich nearshore waters contribute 18 - 33 % to the global marine primary production (Wollast 1991). High productivity in a short distance from the sea floor leads to appreciable amounts of detritus settling to the sediment. On the shelf, up to 50 % of the organic matter produced in the water column reaches the bottom (Wollast 1991), providing a high potential of sedimentary decomposition. Thus, shelf sediments, albeit marginal with respect to surface area, are considered important sites of organic matter cycling.

Shallow coastal waters are an extremely dynamic environment, where fluid motions associated with longshore and tidal currents, surface waves and internal waves reach down to the sea floor and interact with the bottom sediments. In these highly energetic areas, small and light particles are frequently resuspended, and coarser sand grains remain to form a fairly well sorted, permeable sediment. Ensuing the peculiar hydrodynamic regime of shallow waters, permeable sands are the prevalent sediment type on the continental shelves (Emery 1968, Riedl et al. 1972).

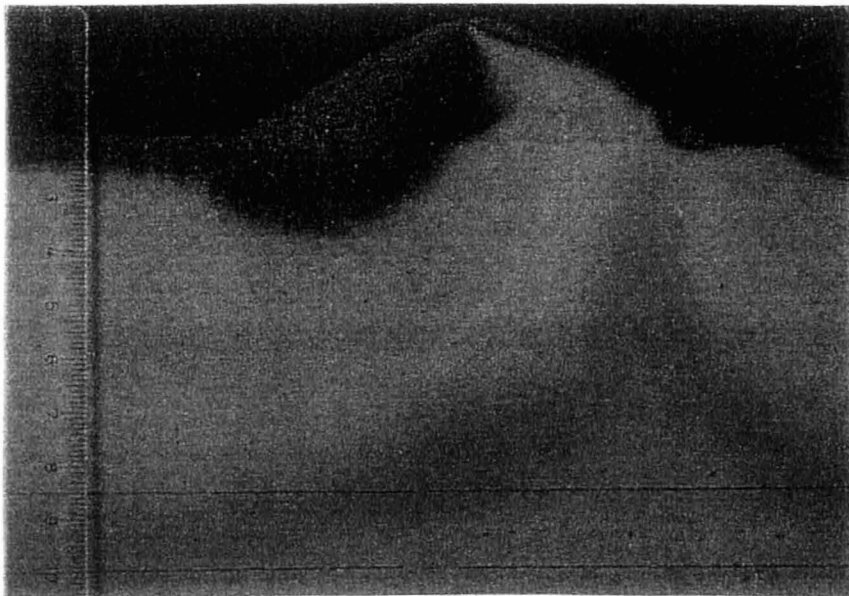
The North Sea, a shelf sea covering approximately  $6 \cdot 10^5 \text{ km}^2$ , is hydrologically coupled to the north-eastern Atlantic. Its intertidal areas, up to 20 km wide and comprising about 4600 km<sup>2</sup> (Reise 1985), the so-called "Wadden Sea", experience large variations in waves, currents, temperature and salinity on the time scales of hours to months (Kristensen et al. 1997). Near the island of Sylt in the northern part of the Wadden Sea, a shallow bay (Königshafen) harbours extensive sandy flats. The present field study was conducted in a Königshafen sandflat with small waves and moderate near-bottom currents passing over a rippled permeable sediment.



Study site in an intertidal sandflat of Königshafen, near the island of Sylt.

## 1.2. Advective transport across the water-sediment interface

Transport of solutes and particles across and near the water-sediment interface involves various processes, such as surface deposition, bedload transport, resuspension, bioirrigation, bioturbation, percolation, evaporation, and wave- or current-induced advection. Given a sufficiently permeable sediment, pressure gradients drive advective water flows into and out of the bed. Heterogeneous pressure fields are generated by the passage of currents or gravity waves over biogenic or physical bottom roughness. According to Bernoulli's law (1738), total pressure remains constant along any streamline. Locally decelerated flow, as corresponding to decreased hydrodynamic pressure, is linked to an increase of hydrostatic pressure, and flow acceleration brings about a decrease of hydrostatic pressure. Thus, areas of high (static) pressure develop at the front slope and behind protruding topographic structures, and (static) pressure is low near the top of the obstacle. Gradients of less than  $1 \text{ Pa cm}^{-1}$  can cause significant advective water flows through the upper layers of sandy sediments (Huettel & Gust 1992a).



This mound was exposed to non-erosive water flow (from left to right) in a flume experiment (Huettel et al. 1996) to demonstrate advective transport of water (pink) and small particles (black:  $1\mu\text{m}$ , blue:  $10\mu\text{m}$ ) through the interstices of a permeable sandy bed. Photo provided by Markus Hüttl.

Advective interfacial fluid exchange depends on current velocity (Forster et al. 1996), wave height and wavelength (Shum & Sundby 1996), topography height (Huettel et al. 1996), and sediment permeability (Darcy 1856). Enhancing solute fluxes between the water column and the sediment, advection can increase sedimentary oxygen utilisation (Forster et al. 1996, Reimers et al. 1996) as well as manganese, iron and nutrient dynamics (Huettel et al. 1998).

So far, the dynamics of suspended particles following interfacial and interstitial water flows have been examined in lab flume experiments using acrylic spheres (Huettel et al. 1996) and diatom cells (Pilditch et al. 1998). These studies have demonstrated that advectively moved particles penetrate the deeper into permeable sediments the smaller they are. With small particles being not only most mobile, but also enriched in fresh organic material (Bordovskiy 1965, Tanoue & Handa 1979, de Flaun & Mayer 1983, Wiesner et al. 1990, Anton et al. 1993, Mayer 1994, Lohse et al. 1995), their dynamics are of major importance to organic matter turnover in marine sediments.

### 1.3. Organic matter in sandy sediments

Sandy marine sediments generally contain relatively small amounts of particulate organic matter (POM). Their highly permeable upper layers allow for repeated supply and removal of POM, that is liable to progressive degradation alternately by planktonic and benthic organisms.

Sedimentary decomposition of organic material increases, when advective interfacial flows carry dissolved oxidants into the bottom and remove inhibitory metabolites. Recent investigations have shown that advective solute exchange can enhance early diagenetic processes in organic-poor sands (Reimers et al. 1996, Jahnke et al. 1996). Low organic carbon and nutrient concentrations in non-accumulating coastal sands, therefore, may rather reflect high turnover rates than constrain activity (Huettel et al. 1998).

### 1.4. Objectives of the study

Current-induced solute fluxes into and out of permeable sediments have been investigated using stirred chambers (Huettel & Gust 1992a, 1992b; Glud et al. 1996, Khalili et al. 1999), laboratory flumes (Forster et al. 1996, Ziebis et al. 1996b, Huettel et al. 1998), and numerical models (Khalili et al. 1997, Basu & Khalili 1999). Further flume experiments (Huettel et al. 1996, Pilditch et al. 1998) have focused on advective transport of particles into sandy bottoms. All results, however, lacked confirmation in natural settings, which became a major goal of my field study. This task was tackled by in situ experiments conducted in March 1998, using artificial sand cores exposed to the environmental conditions of a sandy tidal flat in the Wadden Sea.

In the same sandflat, the natural sediment and the overlying water were sampled periodically from July 1997 to July 1998. The resulting data set, complemented by the findings from the semi-natural setting of the in situ experiments, was intended to assess the relative importance of advective interfacial and interstitial flows in a natural marine environment. Moreover, this one-year field study aimed to elucidate the temporal and spatial dynamics of POM transport and early diagenesis in permeable shallow water sediments. My research addressed the effects of advective interfacial exchange on microbial and geochemical processes in the upper layers of a sandy shelf sediment, contributing to a better understanding of their role in marine organic matter cycling.

## 1.5. Outline of the publications

My investigations entailed four articles submitted for publication in international scientific journals. Two of them present the results of the in situ experiments (chapters 2.1. and 2.2.), and the other two present the results of the one-year field study on natural sandflat sediment (chapters 2.3. and 2.4.).

(1) Rusch, A. & Huettel, M.:

***Advective particle transport into permeable sediments - evidence from experiments in an intertidal sandflat***

Markus Hüttel initiated the experiments, and I carried them out, evaluated the data and wrote the manuscript. This article is accepted for publication in "Limnology and Oceanography".

(2) Huettel, M. & Rusch, A.:

***Transport and degradation of phytoplankton in permeable sediment***

This paper comprises chamber, flume and field experiments performed by Markus Hüttel. He wrote the manuscript and included some results from my in situ experiments. The article is accepted for publication in "Limnology and Oceanography".

(3) Rusch, A., Huettel, M. & Forster, S.:

***Spatial and temporal dynamics of particulate organic matter in permeable marine sands***

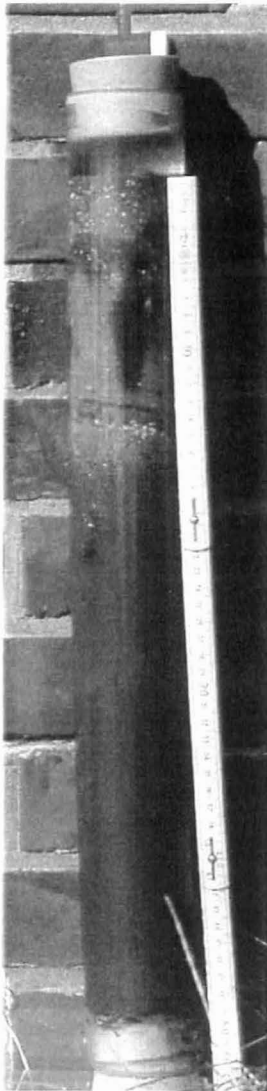
The study was initiated by Stefan Forster and Markus Hüttel. Realisation and evaluation were up to me, who also wrote the manuscript. It has been submitted to "Estuarine, Coastal and Shelf Science"

(4) Rusch, A., Forster, S. & Huettel, M.:

***Bacteria, diatoms and detritus in an intertidal sandflat subject to advective transport across the water-sediment interface***

The contributions of the authors are the same as in the previous article. The manuscript has been submitted to "Biogeochemistry".

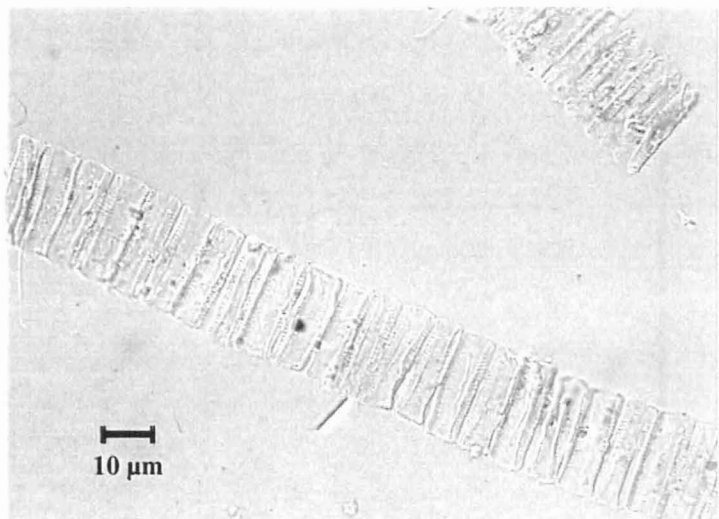
## 2. SUBMITTED MANUSCRIPTS



Sediment core taken in September 1997.



Ripples at the study site, with occasionally observed biodeposits of *Arenicola marina*.



*Brockmanniella brockmannii*, a bloom-forming diatom in Königshafen. Slide by Friedrich Hustedt, custody of AWI Bremerhaven.

## 2.1. Advective particle transport into permeable sediments - evidence from experiments in an intertidal sandflat

Antje Rusch & Markus Huettel

Advective transport of artificial and natural particles into permeable sediments was demonstrated in situ by field experiments in an intertidal Wadden Sea sandflat. Using dyed sediment, advective interfacial solute exchange was shown to reach down at least 1.5 cm below surface. Particle depth distributions depended on sediment permeability and particle size. Sandy sediments were found to efficiently trap particulate material. At the beginning of the local phytoplankton spring bloom, an average  $\text{m}^2$  of coarse-grained sediment received 850 mg organic carbon per day by filtration of 14 L of overlying water per hour. We discuss the relative importance of different transport mechanisms, and data from parallel studies on natural sediments at the same site are interpreted in close correlation to the results of the in situ experiment.

## Introduction

Deposition and resuspension are considered a major link between water column and the sediment (van Raaphorst et al. 1998), and on the inner shelf (water depth < 100 m) suspended matter concentrations in the order of 0.1-1 g L<sup>-1</sup> can occur (Eisma 1993). Here large amounts of inorganic and organic particulate matter are constantly involved in deposition/resuspension cycles, that move them into and out of the uppermost sediment layers. Friction velocities that are insufficient to cause resuspension may move particles in rolling or saltatory bedload transport (Dyer 1986). In rippled beds, material deposited on the surface is moved in the troughs towards the lee side of the ripples, where it tends to be buried by sand grains avalanching from the crest (Jenness and Duineveld 1985). Given this particular situation, the mixed depth of the sediment does not exceed the amplitude of the migrating ripples.

Apart from these purely hydrodynamic processes, also biological activity contributes to interfacial and subsurface transport. On a world-wide scale, biogeous mixing, mainly due to deposit feeding (Wheatcroft et al. 1990), reaches down to a mean depth of 9.8 cm ± 4.5 cm (Boudreau 1998), with near-surface horizontal mixing rates by far exceeding vertical ones (Wheatcroft et al. 1990). Macrofaunal sediment reworking is generally considered the prevalent biogeous mixing process, but in organically enriched muddy sediments, also the meiobenthos can be important for the rapid and shallow initial burial of sedimented phytoplankton (Webb and Montagna 1993). Periodical irrigation of macrobenthos tubes and burrows enhances interfacial solute exchange (Forster and Graf 1995; Marinelli and Boudreau 1996; Ziebis et al. 1996a), and suspended particles are cotransported with the irrigation current.

Molecular diffusion generally dominates solute transport at the sediment surface (Glud et al. 1996), in cohesive sediments (Jørgensen 1996) and at burrow walls (Forster et al. 1996; Ziebis et al. 1996b). Over larger distances, however, convective water flows transport solutes and suspended particulate matter more efficiently. Percolation of sea water by tidal filling and draining of the porous sediment is important in the intertidal and a narrow subtidal zone (Riedl et al. 1972). In coastal wetlands, evaporation and infiltration fluxes are segregated by pore size (Harvey and Nuttle 1995). Convective flow after flooding is supported by water loss and warming during exposure and by a high permeability of the sediment (Rocha 1998).

The influence of surface waves is especially pronounced in shallow water areas (Eisma 1993). Internal waves, formed by various interactions of currents, bottom topography, surface waves and tidal oscillations, can be much higher than surface waves (Kennish 1994) and may have comparable impact on the bottom of deeper waters on the outer shelf and shelf slope. Flow separations and persistent vortices, the dominant features in wave-induced oscillatory flows over sand ripples, provide an efficient mixing mechanism immediately above the sediment and enhance the vertical exchange of solutes between bottom and interstitial water (Shum 1995). Pressure variations along a rough permeable bottom, generated by the passage of currents or gravity waves, cause pore water circulation and increase solute fluxes across the sediment-water interface to an extent that depends on sediment permeability, ripple slope, wave height, and wavelength (Riedl et al. 1972; Shum and Sundby 1996).

Pressure-driven advective pore water flow into and out of permeable sediments is caused by the interaction of near-bottom currents and biogenic or physical sediment roughness (Huettel and Gust 1992a; Forster et al. 1996; Ziebis et al. 1996b). Interfacial fluid exchange depends on the permeability of the sediment (Huettel and Gust 1992a), flow velocity (Forster et al. 1996) and topography height (Huettel et al. 1996). In flume experiments, advective flow has been

shown to increase oxygen penetration (Ziebis et al. 1996b) and utilisation (Forster et al. 1996) as well as manganese, iron and nutrient dynamics (Huettel et al. 1998). Advective cotransport of fluid and suspended particles across the water-sediment interface has been demonstrated in flume studies using 1  $\mu\text{m}$  and 10  $\mu\text{m}$  acrylic spheres (Huettel et al. 1996), 8  $\mu\text{m}$  *Dunaliella* cells (Huettel and Rusch 2000, in press) and *Thalassiosira weissflogii*, a diatom of 12  $\mu\text{m}$  equivalent diameter (Pilditch et al. 1998). Moreover, field experiments have been conducted on phytopigment flux into coarse and fine sand (Pilditch et al. 1998), but results lacked depth resolution and were probably influenced by effects occurring near edges. Another approach to study advective interfacial particle transport in situ (Huettel and Rusch 2000, in press) has proved flux and penetration depth of algae to depend on sediment permeability, but failed to consider particle sizes. Nor were corresponding data of natural sediment from the same site available.

Advective transport of solutes and fine particles across the water-sediment interface, albeit well-studied in the laboratory and probably important for early diagenesis in shallow water environments, has not received much attention in field studies yet. Our in situ experiments in an intertidal sandflat consider the validity of results from flume studies, mainly addressing the influence of sediment permeability and particle size on advective interfacial transport of (organic) particles. The understanding and interpretation of data on particulate organic matter (POM) dynamics at the same site (Rusch et al. 2000, in prep.) is improved by close correlation to the in situ experiment presented here. It contributes to the discussion on the ecological role of permeable shallow water sediments.

## Methods

### *Study site*

The field study was carried out in Königshafen (55°02' N, 008°26' E), an intertidal bay of Sylt island (North Sea) with a mean tidal range of 1.7 m in its southern part (Austen 1997). Water temperatures range between -2 °C and 23 °C (Reise 1985), salinities from 23 ‰ in winter to 33 ‰ in summer (Kristensen et al. 1997). Near-bottom residual currents above the sandy tidal flats are weakly flood-dominated (Austen 1994). For further details on Königshafen see Reise (1985).

Experiments were conducted 250 m offshore on a tidal flat in southern Königshafen, where bottom topography consisted mainly of 1 - 3 cm high ripples and the predominant direction of tidal currents was SE/NW. Benthic macrofauna was comparable to that of sandflats with short exposure time, which were thoroughly studied by Reise et al. (1994). During the experiments in March 1998, current velocities at 2 cm above the bottom did not exceed 0.10  $\text{m s}^{-1}$ , waves were smaller than 0.2 m, and a phytoplankton bloom dominated by *Brockmanniella brockmannii* and *Skeletonema costatum* had recently started. Sediment permeabilities, measured in cores of 60 mm i.d. using the constant head method (Klute & Dirksen 1986), ranged between 18 and 94·10<sup>-12</sup>  $\text{m}^2$  in the uppermost 4 cm and between 18 and 52·10<sup>-12</sup>  $\text{m}^2$  in 4-8 cm depth. Median grain sizes in these depth intervals were 460 - 500  $\mu\text{m}$  and 390 - 460  $\mu\text{m}$ , respectively.

*Dye experiment to assess the depth of advective solute exchange*

Three sediment cores (36 mm diameter, 10 cm long) were taken from the study site. After staining the pore water with rhodamine, we re-inserted the cores into wells, that had been cut into the sediment using equally sized tubes, and removed the coreliners. During the procedure, no visible loss of the strongly dyed pore water occurred. Two days (i.e. 4 tidal cycles) later the cores were retrieved, and the depth of dye removal was assessed visually.

*Microbead experiment to investigate interfacial particle transport*

Two hours before low tide, 3 artificial sand cores (28 cm diameter, 20 cm depth) were carefully inserted into the natural sediment as shown in Figure 1, according to the following procedure: The PVC coreliners, on the bottom side tightly covered by PE sheets, were embedded in narrow wells and fixed by carefully consolidating the surrounding sand. Then they were filled half with particle-free local sea water, before adding cleaned marine sand until the saturated cores were level with the surrounding sediment. To ensure equal environmental conditions, we aligned the cores within 2 m, with the line perpendicular to the main current direction to avoid particle cross-contamination. We used cleaned marine coarse sand (grain size 500-1000  $\mu\text{m}$ ), fine sand (grain size 125-250  $\mu\text{m}$ ) and "Sylt sand" (grain size median: 655  $\mu\text{m}$ ), i.e. sediment from a sandy site nearby, that had been collected in September 1997, washed and oven-dried.

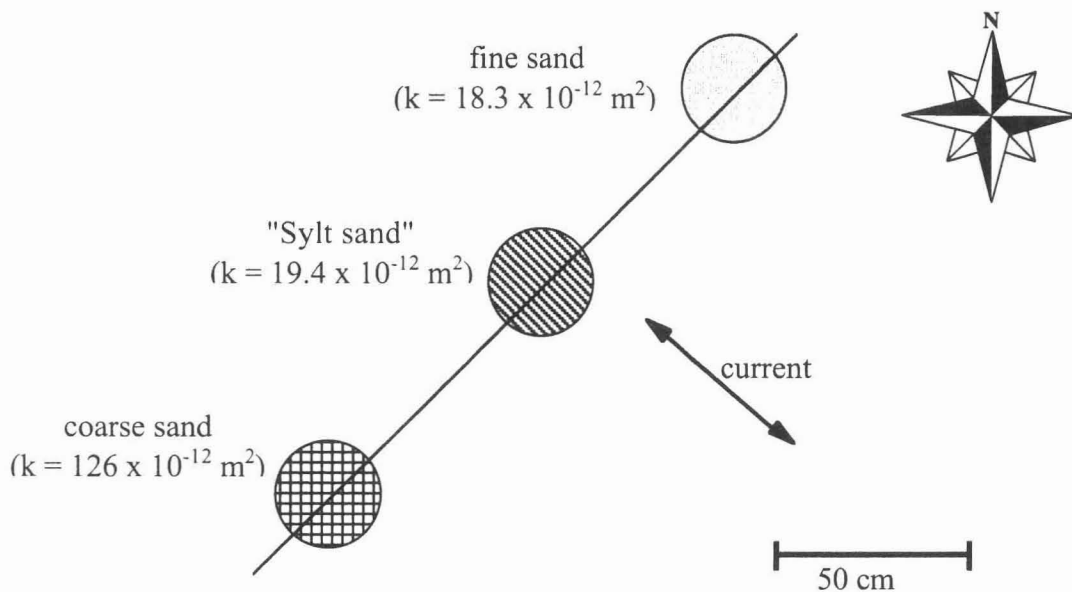


Figure 1: Experimental setup of the microbead experiment. Arrow indicates the prevailing current direction in the study area.

Fluorescent microbeads (1  $\mu\text{m}$ , 3  $\mu\text{m}$  and 30  $\mu\text{m}$  diameter; Duke Scientific Corp.) were suspended in particle-free local sea water and poured around the edges of the cores in a ring of 2.5 cm width using a template. Particle densities were  $(2.60 \pm 0.98) \cdot 10^{12} \text{ m}^{-2}$ ,  $(1.34 \pm 0.34) \cdot 10^{11} \text{ m}^{-2}$  and  $(2.56 \pm 0.70) \cdot 10^8 \text{ m}^{-2}$  for the blue (1  $\mu\text{m}$ ), red (3  $\mu\text{m}$ ) and green (30  $\mu\text{m}$ ) beads, respectively. Finally we carefully removed templates and coreliners.

After 13 hours (1.5 h before the next low tide), 5 cores (60 mm diameter) were taken from each artificial core using Plexiglas<sup>®</sup> tubes; central ones were named A/B/C, marginal ones D/E. At the same time, the water column was sampled nearby using PE-bottles, providing 6 parallels of 250 mL each. These samples were preserved by addition of glutaraldehyde (2 % final concentration) and stored at 4 °C.

#### *Pretest to estimate sampling bias*

7 dm<sup>3</sup> of each sand type described above were saturated with particle-free sea water in a bucket. Aliquots of the microbead suspension used in the main experiment were spread over the artificial sediment surfaces (particle density:  $1/_{100}$  compared to the field study) and allowed to settle for 10 minutes. Then we took 3 cores (60 mm diameter) from each bucket to quantify any particle movement not induced by natural currents.

#### *Sample treatment*

After 8h storage at 4°C, the cores were sliced into 1 cm sections down to 20 cm (pretest cores: 7 cm) depth. Each slice was carefully suspended in NaCl solution (32‰) and allowed to settle for 20 s to separate fine particles (<70  $\mu\text{m}$ ). The resulting suspensions (ca. 40 mL) were decanted into screw-cap or snap-lock glasses, the remaining sediment was once more retreated alike. After addition of glutaraldehyde (2 % final concentration) the suspensions were stored at 4 °C.

#### *Analyses*

Two aliquots (equivalent to  $1/_{80}$  -  $1/_{3}$ ) of each sample, including the water samples, were filtered on polycarbonate filters (0.8  $\mu\text{m}$  pore size; Millipore ATTP) applying gentle vacuum. The filters were examined by epifluorescence microscopy (Zeiss Axioskop), using a magnification of 100x for counting the green beads and 400x or 1300x for counting the red and blue ones. On each filter, each bead type was scored in 5 counting grids; in case of very few green beads, the complete filter was scanned.

Two more aliquots of 50 - 200  $\mu\text{L}$  of sample were stained with DAPI and filtered on polycarbonate filters (0.2  $\mu\text{m}$  pore size, Millipore GTBP) applying gentle vacuum. On each filter, epifluorescent bacteria were scored in 5 counting grids using a magnification of 1300x.

Diatom numbers and lengths > 10  $\mu\text{m}$  were obtained using a Fuchs/Rosenthal chamber and a magnification of 400x. We scored benthic and planktonic forms (Pankow 1990), each sorted into 5 length classes (10 - 15  $\mu\text{m}$ , 15 - 20  $\mu\text{m}$ , 20 - 25  $\mu\text{m}$ , 25 - 30  $\mu\text{m}$ , > 30  $\mu\text{m}$ ).

#### *Statistics*

All statistics were performed according to Sachs (1997). We applied the Kruskal/Wallis test, the Lord test, the estimation of standard deviations from the range of values and the (small) number of parallels, and the Wilcoxon matched pairs signed rank test.

The Kruskal/Wallis test is performed as a rank test to find out, if a group of random samples belong to a common total set. We had three random samples (sand types) of 5 observations (subcores) each. Possible differences between the sand types with respect to the depth

distribution and penetration depth of certain particles were examined for significance using the Kruskal/Wallis test. It was applied to microbeads in the pretest and to microbeads and diatoms in the main experiment.

After detecting a significant difference by Kruskal/Wallis, we compared the sand types by pairs using the Lord test. This test is analogous to the Student-t test and compares the mean values of two small ( $n \leq 20$ ) random samples, using ranges instead of standard deviations as a measure of variation. We applied the Lord test to the depth distribution and penetration depth of microbeads of each bead size. Moreover, this test was used for each sand type to compare planktonic and benthic diatoms of different size classes with respect to their depth distribution and penetration depth.

For small numbers of parallels (usually  $n < 15$ ), standard deviations must be estimated from the range of values using a factor tabulated in literature. We applied this procedure to the particle penetration depths given in Table 3. The Wilcoxon matched pairs signed rank test is used to find out, whether the differences within the pairs are distributed symmetrically around a median of zero. For a given pair of particle sizes, each of our 15 cores provided a pair of observations, formed by the two corresponding depth distributions or penetration depths. Applying this rank test, we set up an order of particle types with respect to particle shares below 1 cm depth and to penetration depths.

In a strict sense, the subcore parallels are not statistically independent and the tests described above therefore not applicable to our data set. The experiment would have to be conducted at least in duplicate or triplicate to gain a suitable data set allowing for statistically proven results. Hence, the outcomes of our statistical analyses should be regarded as probable trends, keeping in mind that their significance indispensably requires the subcores to be independent parallels.

## Results

### *Dye experiment*

No rhodamine was visible in the uppermost 1.0 - 1.5 cm of the cores that had been exposed to calm conditions for 2 days. The boundary towards the strongly dyed sediment below was slightly blurred (Figure 2).

### *Pretest*

Significant differences in particle depth distribution between the different sediment types could not be detected for any bead size (Kruskal/Wallis test). Thus, depth distributions in the main experiment were directly comparable to each other.

### *Microbead experiment*

After their exposure to tidal inundation, the surfaces of the artificial cores were still distinct from the adjacent sediment and unaffected by visible particle deposition and lateral sediment movement. Neither the artificial cores nor the surrounding natural sediment had a rippled surface. Transient formation of small ripples during high tide, however, was likely in spite of the calm weather. No macrofauna was found in the sliced cores.

Retrieval of microbeads, averaged over the sizes, was 9.3 % of the deployed tracer particles in the coarse sand, 0.6 % in the fine sand, and 1.0 % in the Sylt sand. Depth-integrated numbers of microbeads in all parallel cores of the different sediment types are given in Table 1. The

beads were not evenly distributed over the areas of the artificial cores. For each sand type, we considered the 3 subcores that received most tracer particles, and neither of these sets contained all central cores (A, B, C) or all marginal ones (D, E), but two central and one marginal core each.

sand type	beads	cores				
		A	B	C	D	E
coarse (500-1000 $\mu\text{m}$ )	30 $\mu\text{m}$ (green)	24.0	0.37	95.2	0.16	6.61
	3 $\mu\text{m}$ (red)	24.9	3.93	44.2	0.21	12.4
	1 $\mu\text{m}$ (blue)	29.3	1.84	47.5	0.28	12.9
fine (125-250 $\mu\text{m}$ )	30 $\mu\text{m}$ (green)	0.42	1.03	0.99	0.11	1.37
	3 $\mu\text{m}$ (red)	0.34	0.50	0.58	0.22	0.32
	1 $\mu\text{m}$ (blue)	0.42	0.83	1.16	0.38	0.63
Sylt (median: 655 $\mu\text{m}$ )	30 $\mu\text{m}$ (green)	0.36	0.11	0.06	0.03	22.1
	3 $\mu\text{m}$ (red)	0.37	0.18	0.25	0.13	6.00
	1 $\mu\text{m}$ (blue)	0.26	0.23	0.26	0.13	4.93

Table 1: Depth-integrated numbers of microbeads retrieved in coarse, fine and Sylt sand. Green beads:  $\cdot 10^3$ , red beads:  $\cdot 10^6$ , blue beads:  $\cdot 10^7$ . A - E: parallel cores.

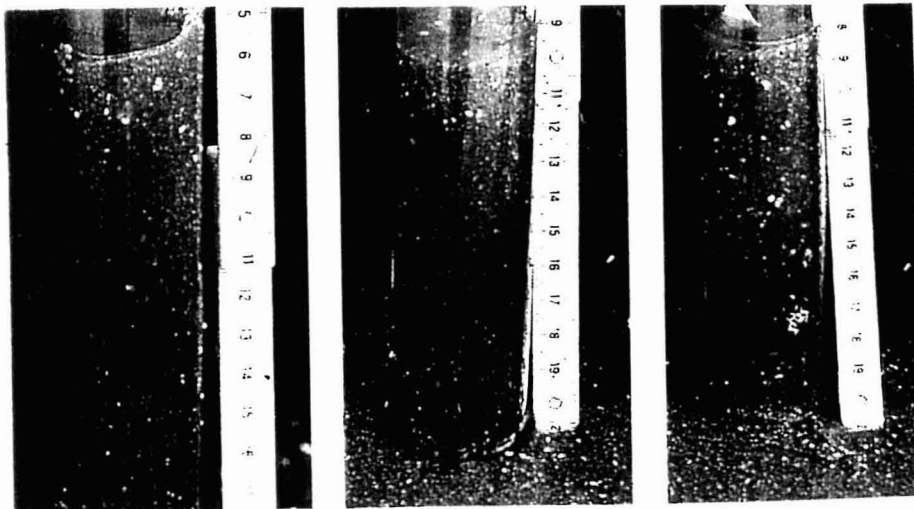


Figure 2: Retrieved cores of the dye experiment.

In the following, particle depth distributions are treated in terms of "relative particle numbers", i.e. numbers within a depth interval divided by the depth-integrated total of the respective profile. Figure 3 shows depth distributions of different artificial and natural particles found in the coarse, fine and Sylt sand cores. Differences between these sand types with respect to relative particle numbers were detected (Kruskal/Wallis test) for the green ( $\alpha = 5.1\%$ ), red ( $\alpha = 0.9\%$ ) and blue microbeads ( $\alpha = 4.9\%$ ) as well as for 10-15  $\mu\text{m}$  benthic diatoms ( $\alpha = 6.7\%$ ) and for 15-20  $\mu\text{m}$  benthic ( $\alpha = 4.8\%$ ) and planktonic diatoms ( $\alpha = 10.5\%$ ). The latter consisted mainly of the bloom-forming *Brockmanniella brockmannii*. Moreover, microbeads depth distributions were compared by pairs (Lord test); the results are compiled in Table 2. Bacteria appeared to penetrate deeper into coarse than into fine sand (Figure 3), statistical confirmation lacked parallel counts, though.

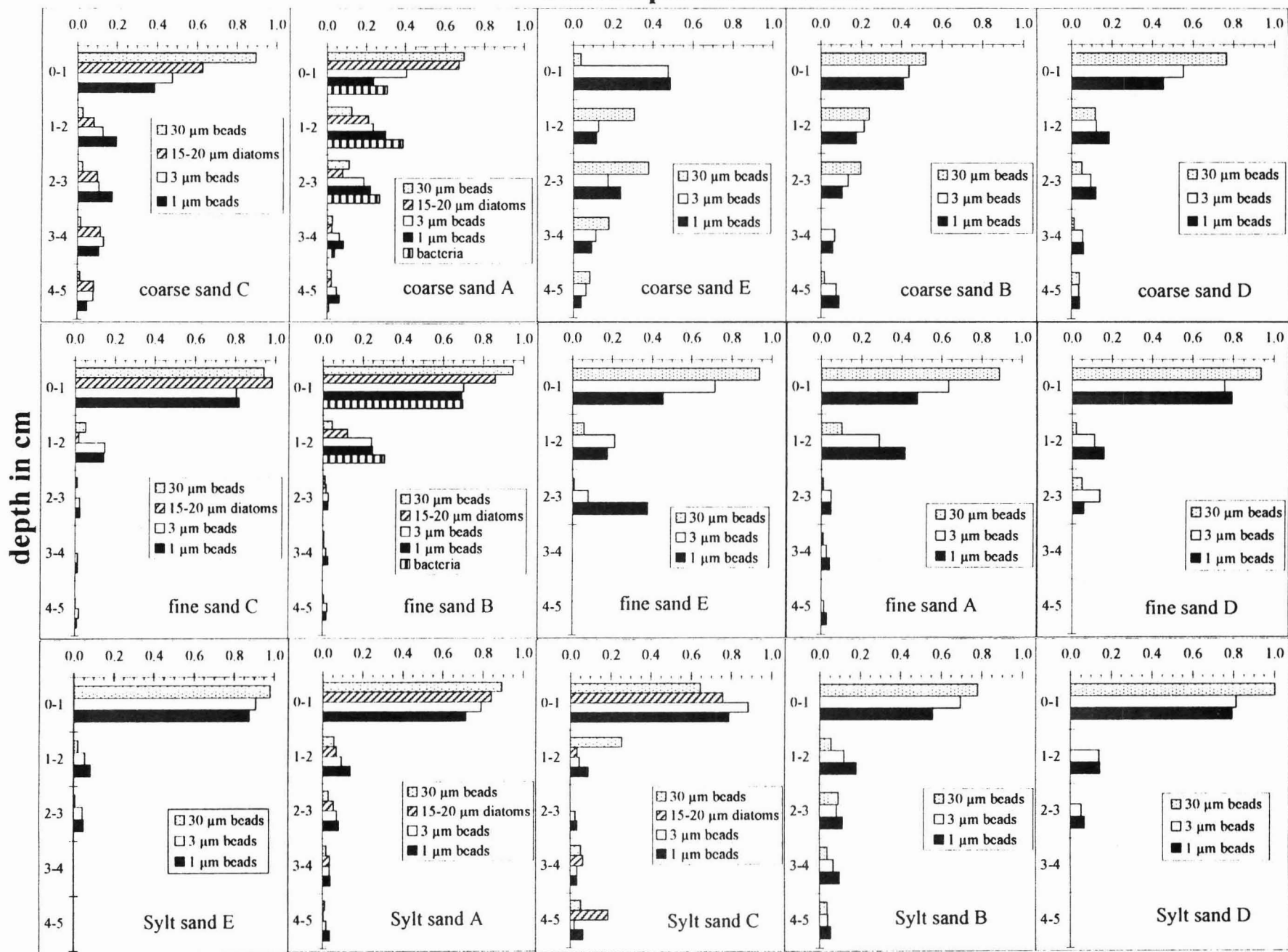
	30 $\mu\text{m}$ (green)	3 $\mu\text{m}$ (red)	1 $\mu\text{m}$ (blue)
coarse vs. fine	5 %	1 %	5 %
coarse vs. Sylt	n. s.	1 %	1%
fine vs. Sylt	n. s.	n. s.	n. s.

Table 2: Levels of significance (Lord test) of differences between particle depth distributions. n. s.: not significant ( $\alpha > 5\%$ )

Figure 3 (next page):

Depth distributions of microbeads (30  $\mu\text{m}$ : stippled, 3  $\mu\text{m}$ : white, 1  $\mu\text{m}$ : black), planktonic diatoms (15-20  $\mu\text{m}$ : hatched) and bacteria (striped) in terms of relative particle numbers in coarse, fine and Sylt sand cores. Within a row, the panels are arranged with respect to the total number of beads found in the corresponding parallel cores (cf. Table 1). Profiles from particle-rich and particle-poor cores are shown at the left and at the right, respectively.

### relative particle numbers



No significant difference in the depth distributions of diatoms could be detected (Lord test), neither between planktonic and benthic algae of the same size nor between different size classes of planktonic diatoms. For the following tests we averaged planktonic diatom numbers over all size classes and compared them to the corresponding relative particle numbers of the microbeads. The share of particles penetrating deeper than 1 cm was in the order ( $\alpha = 5\%$ , Wilcoxon matched pairs signed rank test): blue beads ( $1\ \mu\text{m}$ ) > red beads ( $3\ \mu\text{m}$ ) > green beads ( $30\ \mu\text{m}$ )  $\approx$  diatoms ( $> 10\ \mu\text{m}$ ). Relative numbers of bacteria ( $0.5 - 1\ \mu\text{m}$ ) appeared similar to that of the blue beads, though without statistical confirmation.

In nearly all profiles (exception:  $30\ \mu\text{m}$  beads in coarse sand E), relative particle numbers decreased exponentially with depth. The mean correlation coefficients were  $r^2$  (beads) = 0.848 and  $r^2$  (diatoms) = 0.668. The penetration depth was defined as corresponding to a decrease of relative particle numbers by a factor  $e^{-3}$ , i.e. 5.0% of the surface value. The penetration depths of microbeads, diatoms and bacteria in each sand type are summarized in Table 3. Red ( $3\ \mu\text{m}$ ) and blue microbeads ( $1\ \mu\text{m}$ ) penetrated significantly deeper into coarse sand than into fine and Silt sand ( $\alpha = 1\%$ , Lord test). Green microbeads ( $30\ \mu\text{m}$ ) penetrated deeper into coarse sand than into fine sand ( $\alpha = 1\%$ , Lord test), but no significant differences to the Silt sand were detected ( $\alpha = 5\%$ , Lord test).

	coarse sand (500-1000 $\mu\text{m}$ )	fine sand (125-250 $\mu\text{m}$ )	Silt sand (median: 655 $\mu\text{m}$ )
30 $\mu\text{m}$ beads	2.83 $\pm$ 0.54	1.33 $\pm$ 0.22	2.35 $\pm$ 1.38
diatoms ( $>10\ \mu\text{m}$ )	3.04 $\pm$ 0.19	2.11 $\pm$ 0.29	2.19 $\pm$ 0.29
3 $\mu\text{m}$ beads	5.27 $\pm$ 0.68	2.53 $\pm$ 0.19	2.62 $\pm$ 1.03
1 $\mu\text{m}$ beads	5.32 $\pm$ 0.77	2.59 $\pm$ 0.46	3.10 $\pm$ 1.44
bacteria	2.51 (1 core)	3.66 (1 core)	n. d.

Table 3: Penetration depths (in cm, mean of parallel cores) of differently sized particles in coarse, fine and Silt sand. As penetration depths of diatoms did not significantly differ between the size classes, they were averaged. Standard deviations were estimated according to Sachs (1997) from the range of values and the number of parallels.

No significant difference could be detected (Lord test) between the penetration depths of diatoms of different size classes. So the penetration depths of planktonic diatoms were averaged over all size classes and compared to the corresponding ones of the microbeads. The penetration depths were in the order ( $\alpha = 5\%$ , Wilcoxon matched pairs signed rank test): blue beads ( $1\ \mu\text{m}$ ) > red beads ( $3\ \mu\text{m}$ ) > green beads ( $30\ \mu\text{m}$ )  $\approx$  diatoms ( $> 10\ \mu\text{m}$ ). Bacteria ( $0.5 - 1\ \mu\text{m}$ ) appeared to penetrate approximately as deep as the blue and red beads, though without statistical confirmation.

The biovolume of planktonic diatoms, i.e. their abundance in a certain size class multiplied by the corresponding average cell volume, summed over all size classes, was determined. In the coarse sand (cores A, B, C) down to 5 cm depth it amounted to  $4.97\ \text{cm}^3\ (\text{m}^2\ \text{sediment})^{-1}$ . Provided that the cells had a density of  $1.1\ \text{g cm}^{-3}$ , a water content of 0.8 (w/w) and got into

the sediment within 13 h, the POM transport rate was  $2.02 \text{ g (dwt.) m}^{-2} \text{ d}^{-1}$ . With  $\text{POC} \approx 0.42 \cdot \text{POM}$  (Rice et al., 1986), this corresponds to a net POC input rate of  $850 \text{ mg C}_{\text{org}} \text{ m}^{-2} \text{ d}^{-1}$ .

The number of planktonic diatoms in the coarse sand (cores A, B, C) down to 5 cm depth that were filtered from the water by  $1 \text{ m}^2$  of sediment during the experiment equalled the number in  $(178 \pm 74) \text{ L}$  of bottom water. These calculations depend on the diatom size class with net filtration rates increasing with the size of diatoms. Assuming that this water volume had been passed through the sediment within the 13 h of the experiment and furthermore assuming steady state, we obtained net areal filtration rates of  $(13.7 \pm 5.7) \text{ L m}^{-2} \text{ h}^{-1}$ . These estimates are net rates, as interfacial water flows carry particles not only into, but also out of the sediment.

## Discussion

Interfacial POM transport is an important link between the biogeochemical cycles of the water column and the sediment. Our in situ experiments were designed to assess magnitude and depth penetration of advective interfacial particle transport. We first discuss several generally important transport mechanisms with respect to their possible impact on our experimental results, followed by detailed considerations on the observed features of advective transport: horizontal heterogeneity, influence of sediment permeability, and influence of particle size. Our experimental data are compared to the results of earlier laboratory studies and measurements in natural sandy sediments. Finally we discuss the implications of advective interfacial transport on the cycling of organic matter in marine ecosystems.

### *Contribution of non-advective particle transport*

We showed particle transport into sandy sediments within one tide, which generally could have been facilitated by various processes. Biogeneous transport was hardly contributing, as no macrofauna was found in the cores. Particles deposited on the sediment surface were not buried deeply by migrating sand ripples either, as only small ripples could form due to the quite calm current regime during the experiment. Nor could tidal percolation trap the microbeads, because ebb tide began 8 h after start of the experiment, i.e. more than 5 h after inundation of the study site, and during that time suspended beads would have been swept far away. Particles already trapped in the sediment at the onset of ebb tide, though, could have received some additional drag downwards by falling water levels. Convective flow caused by evaporation and warming during exposure did not apply for this experiment, because the site was exposed for less than 3 h and the sediment surface temperature was  $6 \text{ }^{\circ}\text{C}$ , differing from that of air, water and deeper sediment layers by less than  $1 \text{ }^{\circ}\text{C}$ . During exposure the wind speed was  $3.4 - 4.3 \text{ m s}^{-1}$ , corresponding to a wind force of 2 - 3 Bft. (Deutscher Wetterdienst, unpubl. data), so evapotranspiration was negligible, too.

### *Dye experiments show advective solute exchange*

The result of our dye experiment was the combined effect of bedload transport, resuspension/redeposition and advection. Under the calm hydrodynamic conditions, however, lateral transport and resuspension of the relatively coarse grains were negligible. The sediment, comparable to the Sylt sand used in the microbead experiment, was sufficiently permeable for advective pore water flow (see below), and dye removal reaching 1.5 cm down into the

sediment thus can be attributed to advective interfacial water exchange. Mixing in the interstices may have added to the dye removal by causing a dilution of the stained pore water. However, the strong colour of rhodamine is visually well perceptible even when diluted by a factor of 200 compared to our staining solution. Flushing the sediment with a water volume exceeding 200 times its pore volume within only two days was hardly probable. Diffusion and interstitial mixing could be responsible for the blurred boundary between stained and clean sediment, but fail to explain the whole observation. As the main process we rather consider advective flow pushing the stained water out of the cores without needing large water volumes. The deformation of dyed vertical pore water stripes in an even finer-grained sandy sediment (220  $\mu\text{m}$ ) exposed for merely 3 h to flume water currents slower than 0.1  $\text{m s}^{-1}$  (Huettel and Gust 1992a) showed that rhodamine dye is pushed along the pathway of advective pore water flow by the intruding and advancing front of bottom water. In finer-grained sediments, like the artificial fine sand we used, advective flushing is relatively slow due to lower permeabilities, and resuspension gains importance, as smaller grains are more easily suspended. By contrast, in coarser-grained sediments, like our artificial coarse sand, the relatively high permeabilities are expected to facilitate extensive advective flows, whereas resuspension becomes less influential.

We conclude that the Königshafen sediments permitted advective flushing and that the main particle transport process in the microbead experiment was most likely advection, too, although the two experiments were not conducted on the same day.

#### *Horizontal heterogeneity in the microbead experiment*

Each of the 3 artificial cores exhibited horizontal heterogeneity, that was consistent between all bead sizes and not related to the distance from the core edge (Table 1). This uneven distribution could be due to areas of high and low pressure created by the interaction of currents with bottom roughness. Such pressure fields have been shown in laboratory flumes for topography heights of 5-28 mm (Huettel and Gust 1992a ; Forster et al. 1996; Huettel et al. 1996; Ziebis et al. 1996b) and 70 mm (Pilditch et al. 1998). As the principle also applies to smaller topographic structures, bottom roughness and temporary ripples during our field experiment were apparently sufficient to cause pressure heterogeneities as the driving force for water and particle flows. Profiles from the coarse sand cores that trapped many particles (Table 1) showed subsurface maxima, e.g. microbeads of all sizes in core E, 1  $\mu\text{m}$  microbeads and bacteria in core A and 15 - 20  $\mu\text{m}$  planktonic diatoms in core C (Figure 3), as well as 10 - 15  $\mu\text{m}$  planktonic diatoms in core C (Huettel and Rusch 2000, in press). These profiles reflect the history of the cores with respect to pressure fields moving over them. When exposed to locally high pressure, the sand was advectively supplied with particles, whereas subsequent exposure to low pressure caused an upwelling of pore water. Apparently only close to the surface, its velocity was sufficient to overcome friction, suspend and move particles (Huettel et al. 1996). Another phase of high pressure may enter particles in the top layers again. In core E, the second deposition may have started late during the experiment, when ebb current velocities had already decreased below the threshold for remobilization of 30  $\mu\text{m}$  beads from the surrounding sediment. In core A, only small particles were affected, indicating that this area experienced weaker pressure changes, insufficient to move larger particles upwards. In core C, only diatoms were slightly more abundant in 3 - 4 cm depth than in 1 - 3 cm depth. If this subsurface maximum is significant at all, it might be caused by active rather than passive movements of the algae. Profiles from coarse sand cores that trapped less particles (Table 1)

were at first located in low pressure areas and later on received particles once, their relative numbers thus decreasing exponentially with depth (Figure 3).

Besides pressure changes, also concentration changes or a patchy distribution of particles in the bottom water are equally reasonable explanations for the observed profiles. Temporal and spatial variations of suspended particle concentrations can be caused by changes in tidal current velocity or by heterogeneous pressure fields.

Fine and Sylt sand cores probably were also exposed to migrating pressure/concentration fields (or pressure/concentration changes at a given location). Due to their lower permeability, however, advective transport was too slow to cause measurable changes in the particle profiles within 10 h of inundation. Natural sandy sediments are constantly subject to changing flow and pressure fields, and given enough time, advectively accumulate fine-grained material in subsurface layers, even if they are less permeable than our artificial coarse sand. Natural cores taken from the same study site between July 1997 and July 1998 contained maximum concentrations of particles  $< 70 \mu\text{m}$  in 4 - 8 cm depth (Rusch et al. 2000, in prep.).

#### *Sediment permeability as a key factor in advective transport*

Our in situ experiment showed how particle transport into and in the sediment depends on the permeability of the sediment. In the coarse sand, we retrieved one order of magnitude more microbeads than in the fine and Sylt sands, and artificial as well as natural particles penetrated deeper into the coarse than into the less permeable sands (Figure 3). Laboratory studies in flumes and stirred chambers have shown that highly permeable sediments compared to less permeable ones exhibit stronger and deeper-reaching influx (Forster et al. 1996) and efflux of dyed water (Huettel and Gust 1992a, 1992b), deeper penetration of oxygen (Ziebis et al. 1996b), more intense oxygen utilisation (Forster et al. 1996) and larger deposition of diatoms to the bed (Pilditch et al. 1998). Our in situ experiment demonstrated that interfacial fluxes and particle penetration depths are also increased by high permeabilities, when the sediment is exposed to a natural environment. Experiments in stirred chambers have shown that interfacial particle fluxes, penetration depths and sedimentary degradation of the trapped algal cells depended on the logarithm of sediment permeability (Huettel and Rusch 2000, in press). This key factor of advective transport is influenced not only by the grain size of the sediment, but also by its sorting and state of consolidation, animal burrows, benthic diatom mats, or bacterial mats in the so-called versicoloured sandy tidal flats (Krumbein et al. 1994). Moreover, the advectively caused subsurface accumulation of fine-grained material reduces the permeability of the affected sediment layer, hence decelerating the pore water flow and enhancing further deposition of the particles it carries. The degradation of organic fines, in permeable sediments enhanced by advective oxidant supply, restores and maintains the long-term non-accumulating feature and high permeability of sandy sediments. Enhanced organic matter turnover may give rise to the formation of subsurface microbial biofilms, which in turn decrease sediment permeability. Occasional erosion during stormy weather limits the persistence of such biofilms and therefore may be an important process in keeping the uppermost centimeters highly permeable. Contrasting our artificial sands, permeability in natural sediments is horizontally and vertically heterogeneous, resulting in internal interfaces that modify the flow and pressure field. Besides, natural sands are less well-sorted, ensuing a different spectrum of pore sizes. Therefore our Sylt sand was only as permeable as our fine sand in spite of its much higher median grain size.

The minimum permeability needed for advective interfacial fluxes of water and microalgae was  $1 \cdot 10^{-12} \text{ m}^2$  (Huettel and Gust 1992a) and  $1.5 \cdot 10^{-12} \text{ m}^2$  (Huettel and Rusch 2000, in press),

respectively. This threshold corresponds to a relatively well-sorted fine sand (Huettel and Gust 1992b). As a consequence of the shallow water hydrodynamic regime, permeable sands are the prevailing sediment type on the continental shelves (Emery 1968; Riedl et al. 1972). These areas are consequently important stages for advective interfacial transport to act on.

#### *The role of particle size*

Particles penetrated the deeper the smaller they were. Within the diatoms, depth distributions did not significantly depend on particle size, because depth resolution was insufficient to reveal differences between particles that hardly penetrated into the second slice of the cores. On average, though, their depth distribution agreed well with that of the similarly big green beads and therefore supported the finding of size-related particle penetration. Flume studies have shown the following order of penetration depths in permeable sediments: fluid > 1  $\mu\text{m}$  particles > 10  $\mu\text{m}$  particles (Huettel et al. 1996). Our in situ experiment demonstrated that the penetration depth of advectively moved particles also depends on their size, when the sediment is exposed to a natural environment. It further showed that naturally occurring particles like diatoms and bacteria fit well into the results derived from artificial particles. The calculation of penetration depths from the exponential decrease of relative particle numbers is an attempt to put into numbers the qualitative statements derived from the significantly different particle depth distributions and additional visual evaluation of the profiles. However, it may be an oversimplification and prone to errors, but careful consideration of both approaches probably yields reliable statements. From intuition and flume study results (Huettel et al. 1996) fluids are expected to penetrate deeper than particles. So water penetration down to 1.5 cm in the dye experiment (Figure 2) seems to be at odds with particle penetration 2-3 cm down into the Sylt sand (Table 3). The two experiments, however, are not directly comparable to each other, as they were conducted on different days. Besides, the stained sand had not received the same pretreatment as the Sylt sand, resulting in slightly different permeabilities. Furthermore, detection methods were different. With three quarters of even the smallest tracer particles being trapped within the first centimeter of their way downwards (Figure 3), interstitial flow velocities in the Sylt sand apparently decreased drastically in the uppermost layers. Decelerated advective flows deeper down could move small water volumes, sufficient to be traced by the particles they carried, but insufficient to push away major volumes of dyed pore water. Additionally, at the boundary between the stained and the advectively destained layers, a steep concentration gradient arose, and rhodamine could diffuse upwards, thus decreasing the apparent fluid penetration depth in the dye experiment.

#### *Rates and velocities of interfacial particle transport*

The mean net rate of bottom water filtration by the sediment calculated from our diatom data was  $(13.7 \pm 5.7) \text{ L m}^{-2} \text{ h}^{-1}$  and, thus, slightly exceeded areal filtration rates of 0.5 - 6.8  $\text{L m}^{-2} \text{ h}^{-1}$  derived from laboratory experiments with smooth sediments exposed to water flows in flumes (Huettel and Gust 1992a, 1992b; Huettel et al. 1996; Pilditch et al. 1998). These reported data points, however, were scattered over a broad range of grain sizes (170 - 1200  $\mu\text{m}$ ), flow velocities (1- 10  $\text{cm s}^{-1}$ ) and run times (5h - 7d), covering all but matching none of our experimental conditions. Thus, dealing with 3 degrees of freedom, more precise comparisons seem idle. Filtration rates calculated from planktonic diatom numbers tended to increase with cell size. Big diatoms may settle faster onto the sediment surface and be less easily resuspended than smaller ones. This difference in surficial net deposition rates could

influence the relative distribution of cells in the water column and the sediment that our calculations were based on.

Within 13h, particles penetrated at least 5 cm into our sediment cores, corresponding to a mean transport velocity of  $3.8 \text{ mm h}^{-1}$ . Vertical tracer velocities in the order of  $\text{mm h}^{-1}$  were also found in flume studies on smooth sediments under similar conditions (Huettel and Gust 1992a; Huettel et al. 1996). Not only topography and sediment permeability strongly influence the vertical progress of fluid and particles, but also the position in the pressure field (Huettel et al. 1996). In the field, the bottom currents change throughout the tidal cycle, thus adding further variability to the advective interfacial and subsurface flow velocities. Moreover, stronger bottom currents can cause the formation and migration of sand ripples. The resulting horizontal movement of the non-stationary flow field triggers additional temporal variability at a given spot.

### *Conclusions*

We have shown in an intertidal sandflat that advective interfacial flows carry suspended planktonic and benthic diatoms as well as bacteria and artificial tracer particles into permeable sediments. We found horizontal heterogeneity and an impact of sediment permeability and particle size. Several profiles showed clear signs of alternating exposure to high and low pressure and resembled fine particle profiles from natural sediments of the same study site. Our in situ experiment gives clear evidence that advective particle transport is involved in the biogeochemical budgets of sandy shelf sediments. The extent of this advective influence relative to other transport processes depends on the ecosystem under consideration. In densely populated intertidal or subtidal areas, bioturbation and bioirrigation may dominantly contribute to interfacial particle and solute fluxes. However, macrofauna also can enhance advective exchange by increasing the permeability, the water-sediment interface area and surface topography (Forster and Graf 1995; Marinelli and Boudreau 1996; Ziebis et al. 1996a). Shallow water sediments are strongly influenced by gravity waves and bottom currents and well-supplied with particulate organic matter from the euphotic zone. Therefore they are important sites of benthic mineralization to an extent that would not be possible without advective transport across and below the water-sediment interface. Recurrent resuspension and redeposition of the uppermost sediment layers gain the more importance the finer the sand. Advective flows become slower and thus less effective, and the sediment gets more selective with respect to particle size and shape. Nevertheless, dissolved oxidants, bacteria and very fine-grained or dissolved organic matter may penetrate sufficiently deep into fine sands to ensue an advectively caused increase of the sedimentary mineralization capacity. From the diatom transport into the coarse-grained artificial core we roughly estimated an advective POC input rate of  $850 \text{ mg C}_{\text{org}} \text{ m}^{-2} \text{ d}^{-1}$ . Mineralization rates of sandy North Sea sediments range between 10 and  $555 \text{ mg C m}^{-2} \text{ d}^{-1}$  (Canfield et al. 1993; Upton et al. 1993; Kristensen and Hansen 1995; Osinga et al. 1996; Boon and Duineveld 1998); in natural sands from our Königshafen study site we measured seasonally varying rates between 20 and  $580 \text{ mg C m}^{-2} \text{ d}^{-1}$  (unpubl. data). Thus, mineralization and advective input of organic carbon were in the same order of magnitude, emphasizing the important role of advective interfacial transport for the carbon turnover in sandy shelf sediments. Considering that not only carbon, but all kinds of solutes and fine-grained particulate materials are to some extent advectively exchanged between the water column and the sediment, hydrodynamic processes may co-determine the benthic ecology of the uppermost ca. 5 cm of sandy shallow water sediments.

## Acknowledgments

M. Alisch and H. Tydt are gratefully acknowledged for their help during field work. The BAH Wadden Sea Station kindly provided lab space. We appreciate discussions and valuable comments of S. Forster and B. B. Jørgensen. The critical remarks of W. van Raaphorst and an anonymous reviewer helped to improve the manuscript. This study was supported by the Max Planck Society (MPG), and A. R. received a postgraduate scholarship from Deutsche Forschungsgemeinschaft (DFG).

## 2.2. Transport and degradation of phytoplankton in permeable sediment

Markus Huettel & Antje Rusch

In flume and field experiments we demonstrate that interfacial water flows, generated when bottom currents interact with sea bed topography, provide a fast and efficient pathway for the transport of suspended phytoplankton into subsurface layers of permeable sandy sediments. The advective transport, associated with small mounds and ripples as commonly found on shelf sediments, increased penetration depth of unicellular algae (*Dunaliella spec.*) into sandy sediment (permeability  $k = 4 \times 10^{-11} \text{ m}^2$ ) up to a factor of 7 and flux up to a factor of 9 relative to a smooth control sediment. The pore water flow field produced a distinct distribution pattern of particulate organic matter in the sediment with subsurface concentration maxima and zones depleted of algae. Flux chamber simulations of advective transport of algae into sands of different grain sizes revealed increasing fluxes, algal penetration depths and degradation rates with increasing permeability of the sediment. Two experiments conducted in intertidal sand flats confirmed the importance of the advective interfacial transport of phytoplankton for natural settings, showing permeability-dependent penetration of planktonic algae into embedded sand cores of different grain sizes. The significance of our results is discussed with respect to particulate organic matter flux and mineralization in shelf sands, and we suggest the concept of a decomposition layer.

## Introduction

In contrast to muddy sea beds with low permeabilities, where transport of solutes is mainly driven by diffusion, water can flow through marine sands, providing a fast carrier for the exchange of substances between the water column and the upper sediment layers. Surface gravity waves cause pressure oscillations that increase fluid exchange at the sediment-water interface and dispersion of solutes within the bed (Harrison et al. 1983; Riedl et al. 1972; Webb and Theodor 1968). Bottom currents deflected by sediment topography create small horizontal pressure gradients that force water into the bed up- and downstream of protruding surface structures and draw pore water to the sediment surface where the pressure is lowest (Fig. 1) (Savant et al. 1987; Thibodeaux and Boyle 1987; Huettel and Gust 1992a). Huettel et al. (1996) showed that the interfacial water flows can carry particulate tracers several centimeters into sands. Shells of sea scallops on sandy sediment increase the deposition of diatoms (Pilditch et al. 1998).

Permeable sands are most common in coastal environments (Riggs et al. 1996), and relict sands cover approximately 70% of the continental shelves (Emery 1968). In these nearshore waters, high nutrient concentrations boost phytoplankton growth to generate about 30% of the total oceanic primary production in a zone covering less than 10% of the world's ocean area (Walsh 1988; Wollast 1991).

Up to 50% of the organic matter produced in the water column on the shelf is decomposed at the seafloor (Bacon et al. 1994; Rowe et al. 1988; Wollast 1991). Wind, waves and tidal currents cause deep mixing of the water column, carrying phytoplankton cells to the bottom (Jones et al. 1998). Velocity and turbulence of bottom currents in the shallow water, however, exceed the settling velocity of the organic material by far counteracting deposition (Jago and Jones 1998). Relatively high shear forces in the turbulent boundary layer break down aggregates of organic matter, decreasing their size and sinking rate (Eisma and Kalf 1987; Milligan and Hill 1998). Nonetheless, tight coupling of water column and sedimentary chlorophyll indicate a rapid transfer mechanism for the incorporation of these particles into the shelf bed (Burford et al. 1994; Buscail et al. 1995; Hansen and Blackburn 1992).

Filter feeding and bioturbation of benthic invertebrates enhance benthic-pelagic coupling (Aller 1978; Graf 1992; Rhoads 1973), but abundances of bottom dwellers decrease in frequently resuspended sandy shelf beds (Emerson 1990; Ong and Krishnan 1995; McLachlan 1996). Jenness and Duineveld (1985) suggest that in such environments, moving ripples enhance burial of material, however, this process requires that organic material could settle on the sediment surface during phases of reduced bottom currents.

The purpose of this study was to assess whether interfacial water flows, caused by boundary flow-topography interaction, increase transport and degradation of suspended phytoplankton in sands with permeabilities similar to those found in shallow shelf sediments. We conducted flume experiments to investigate the process of the interfacial algal cell transport and two *in-situ* experiments to demonstrate the effects of this process in the natural environment. A novel chamber technique was used to investigate flux and degradation of *Dunaliella* cells in sediments of different permeabilities. Based on our findings and data from the literature, we suggest a concept of organic matter degradation for sediments of different water depths.

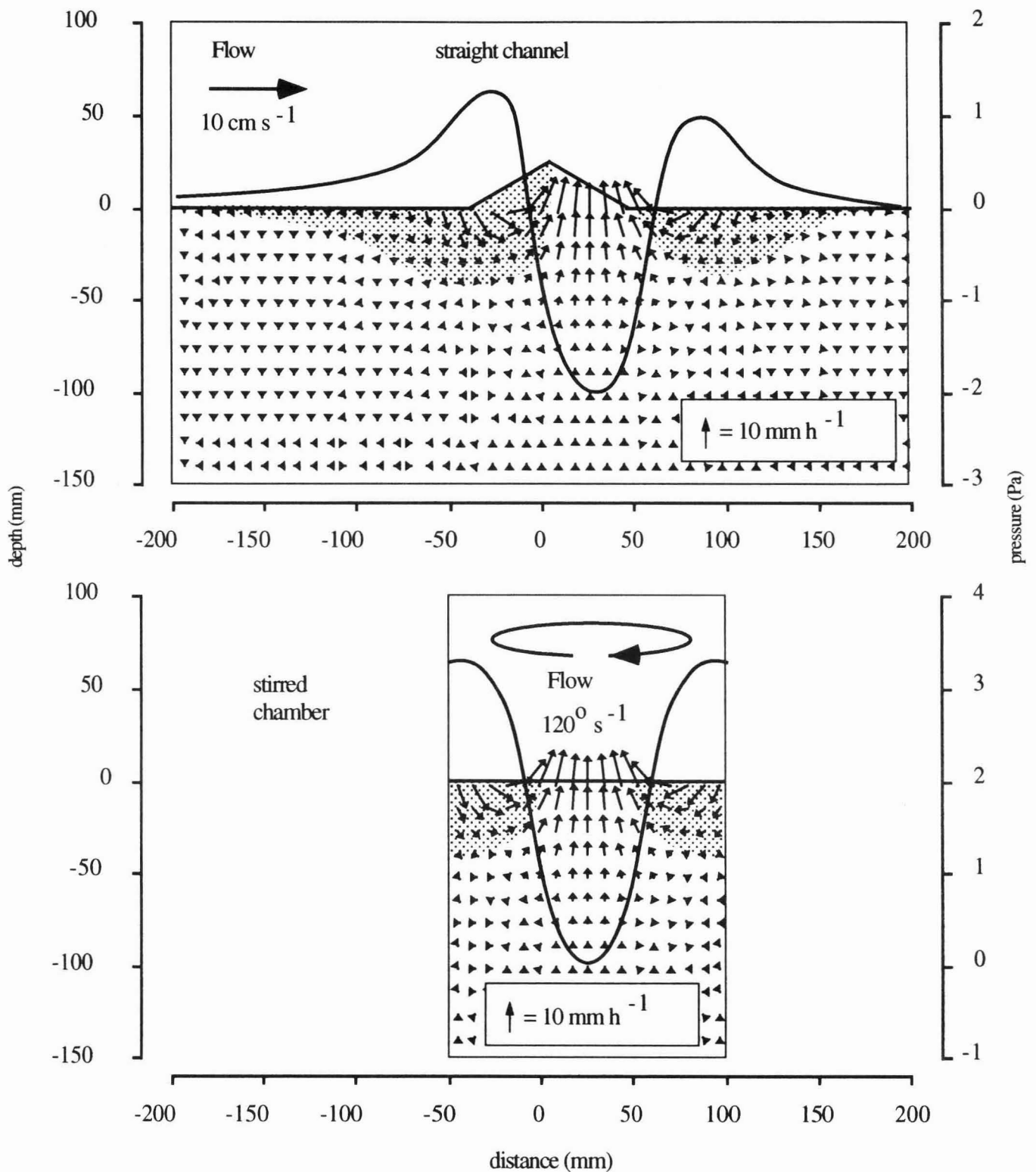


Figure 1: Schematic of the advective pore water flow field under sediment topography exposed to unidirectional flow in a straight open channel, and in sediment exposed to a rotating water column in a stirred chamber. The solid curved line depicts the pressure distribution at the sediment water interface. Shaded areas mark the intrusion zones of water, and the arrows in the sediments show direction and magnitude of the advective pore water flows.

## Methods

Four flume experiments were designed to assess a) the intrusion of algal cells into a smooth permeable sediment core (FLU-S), b) the impact of small mounds on the flux of algae from the boundary layer into the sediment (FLU-M1, FLU-M2), c) the effect of a sediment ripple on intrusion and distribution of algae cells within the sediment (FLU-R).

The recirculating flume had an open channel section of 200 cm length, 35 cm width and 12 cm height. The sediment core was placed in a drop box (60 cm long, 35 cm wide, 20 cm deep) located 90 cm downstream from the channel entrance. The sediment consisted of medium marine quartz sand (Table 1), depleted of any macrofauna and algae. Prior to the experiments, the sediment was compacted by applying low frequency vibrations, and the surface was carefully smoothed. Except for the control experiment (FLU-S), topography then was built on the surface using the same sand. In FLU-M1 and FLU-M2, 10 small mounds (60 mm base diam., 20 mm height) were built on the sediment surface, arranged to maximize the distance between the mounds and to minimize flow obstruction for each other (Fig. 2). In FLU-R the topography consisted of a sediment ripple (110 mm width, 30 mm height) built perpendicular to the flow across the center of the sediment core.

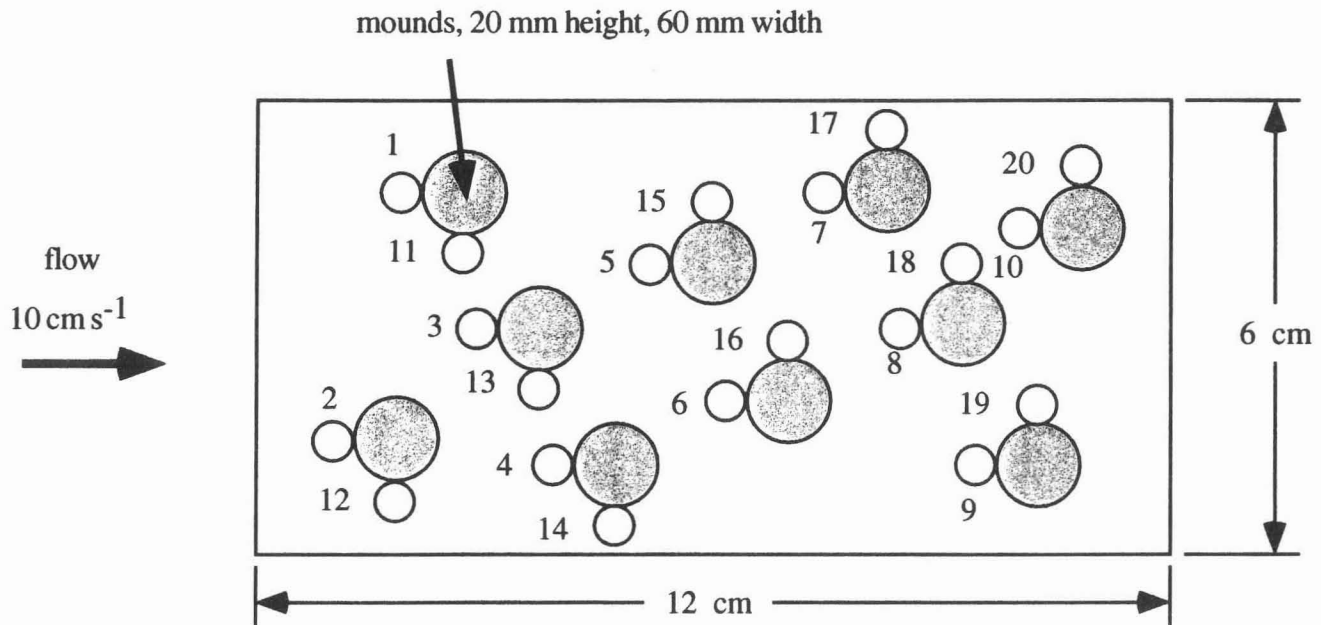
The flume was filled with 160 L of filtered artificial sea water (salinity 35), to a water depth of 10 cm. A large propeller (17 cm diam.) located in the return circuit of the flume generated flow without damaging suspended algae. The flow velocity in the open channel was adjusted to  $10 \text{ cm s}^{-1}$  using a Mini Water™ flow sensor mounted 8 cm above the sediment surface at the downstream end of the core (shear velocity:  $0.33 \text{ cm s}^{-1}$ , shear stress:  $0.11 \text{ g cm}^{-1} \text{ s}^{-1}$ ). The turbulent boundary layer (boundary layer Reynolds number  $Re_b = 3400$ ) above the smooth control core had a thickness,  $z_b$ , of  $\geq 3.8 \text{ cm}$ . A thin opaque PVC sheet that covered the flume prevented algal growth and evaporation, and a cooling unit kept the water temperature at  $20 \text{ }^\circ\text{C} \pm 0.1 \text{ }^\circ\text{C}$ . Oxygen concentration in the flume remained  $> 95 \%$  air saturation at all times. Before addition of algae in FLU-S and FLU-M2, we measured oxygen concentration profiles in the sediment with Clark-type microelectrodes as described by Revsbech (1989).

Suspensions of the planktonic unicellular algae *Dunaliella* spec. ( $8 \pm 6 \text{ } \mu\text{m}$  diameter, Chlorophyceae) were added to the flume at the beginning of each experiment to produce initial chlorophyll *a* (Chl. *a*) concentrations in the recirculating water of 68, 103, 161 and  $74 \text{ } \mu\text{g L}^{-1}$  for FLU-S, FLU-M1, FLU-M2 and FLU-R, respectively. After 3 (FLU-S, FLU-R, FLU-M2), and 5 (FLU-M1) days, the flume water was drained and sediment subcores (26 mm diam., 180 mm length) were taken at the locations depicted in Fig. 2; in the smooth control core (FLU-S), 12 subcores were sampled from random locations. The subcores were sliced in 5 mm (FLU-S), or 10 mm (FLU-M1, FLU-M2) intervals down to 60 mm depth; in FLU-R, the subcores were analyzed down to 70 mm depth (5 mm and 10 mm intervals). Algal cells and sand grains were separated by resuspending the individual sediment slices four times in 50 ml of filtered seawater and filtering the supernatant after 20 s deposition time. In the ripple experiment (FLU-R), the supernatant was drawn on black polycarbonate membranes (Nuclepore,  $0.2 \text{ } \mu\text{m}$  pores) and *Dunaliella* cells were counted under a Zeiss Axiophot epifluorescence microscope (excitation wave length 450-490 nm, magnification of 160x). In all other flume experiments, Chl. *a* concentrations were used to quantify the concentration of algae. Here, the supernatant was filtered through GF-F filters (Whatman,  $2.2 \text{ } \mu\text{m}$ ), and subsequent rinsing with filtered sea water assured that only Chl. *a* contained in algal cells was measured. The Chl. *a* content of the filters was analyzed spectrophotometrically according to Rowan (1989).

	median ( $\mu\text{m}$ )	sorting P75/P25	permeability ( $\times 10^{-12} \text{ m}^2$ )	porosity (% of vol)
<b>flume experiments</b>				
<b>FLU-S, FLU-R, FLU-M1, FLU-M2</b>				
all cores	350	1.5	40.5	32
<b>chamber experiments</b>				
<b>CHA-1</b>				
core 1	187	1.4	7.1	20.8
core 2	187	1.4	7.0	21.0
core 3	375	1.4	28.5	20.2
core 4	375	1.4	30.5	20.0
core 5	750	1.4	113.9	20.1
core 6	1500	1.4	455.4	20.4
<b>CHA-2</b>				
core 1	105	2.4	0.2	47.2
core 2	150	1.9	4.6	35.6
core 3	600	2.3	72.3	32.1
core 4	1050	3.2	223.1	32.2
<b>field experiments</b>				
<b>FLD-1</b>				
core 1	200	1.6	11	20.8
core 2	500	1.7	67	20.5
core 3	1150	1.9	346	20.0
core 4	2000	1.7	1027	20.4
core 5	200	1.6	11	20.5
core 6	500	1.7	70	21.5
core 7	1150	1.9	350	20.5
core 8	2000	1.7	1015	20.0
<b>FLD-2</b>				
core 1	187	1.4	18	20.8
core 2	750	1.4	126	20.4

Table 1: The characteristics of the sands used for the flume and field experiments.  
Permeabilities were measured with a standard constant head permeameter.

## FLU-M1, FLU-M2



## FLU-R

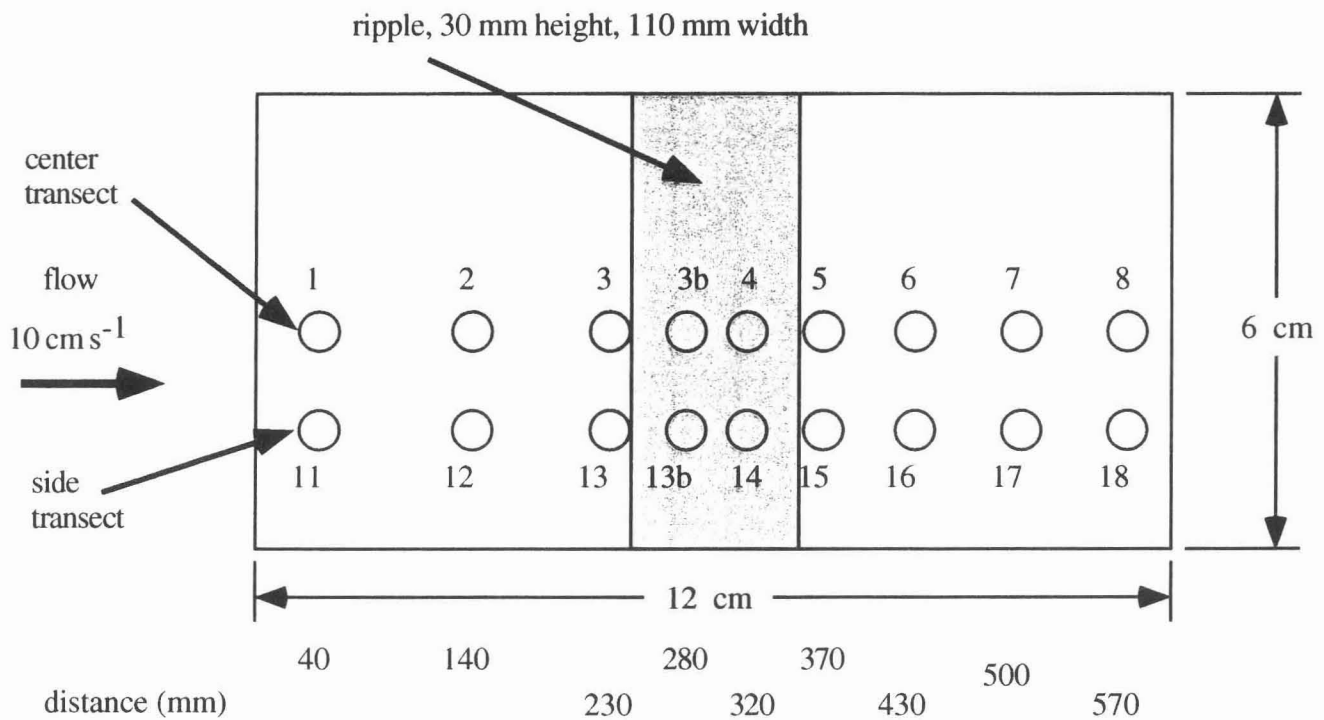


Figure 2: Top view of the sediment cores in the flume experiments. The upper panel shows the positions of the mounds (large shaded circles) and the locations of the sediment subcores taken after the experiments (small open circles). The lower panel depicts the positions of the ripple and the sediment subcores taken after the experiment.

In two chamber experiments we investigated a) the penetration of algal cells into sieved sands of selected grain sizes (CHA-1), b) the penetration of algae into natural sediments of different permeabilities (CHA-2), c) the degradation of algal cells in the sieved and natural sediments (CHA-1, CHA-2).

In a centrally stirred chamber, a pore water flow field can be generated in the incubated sediment core that is similar to that produced by bottom currents interacting with sediment topography (Fig. 1). The rotating water column over the smooth sediment core creates a radial pressure field with lowest pressure at the center of the sediment surface and highest pressure at the outer rim (Huettel and Gust 1992b). The pressure distribution along the diameter of the incubated sediment compares to that along the cross-section of a sediment ripple (perpendicular to crest) exposed to two-dimensional flow (Huettel and Gust 1992a). By selecting the appropriate diameter and stirring speed, the chamber, thus, can be used to mimic the pressure gradients at a ripple of common size. In permeable sands, the radial pressure gradient in the chamber forces water into the sediment at the outer rim of the incubated core. The water flows on a curved path through the sediment towards the center of the sediment surface, where the pore water emerges (Huettel and Gust 1992b). Tracer experiments and calculation of the vorticity vectors show that the rotational movement of the water column is not transferred to the pore water (Khalili et al. 1997). For further details of flow and pressure fields in cylindrical chambers we refer to Basu and Khalili (1999); Glud et al. (1996); Glud et al. (1995).

We combined six (CHA-1) and four (CHA-2) cylindrical chambers (19 cm i. diam., 28 cm i. height, 8 L volume) for sediment incubations (Table 1). One additional chamber was divided horizontally by a false bottom with two pressure ports (one in the center, one 8.5 cm away from the center) into an upper compartment containing the water and a lower compartment housing a differential pressure gauge (Effa GA 63) connected via stiff tubing to the ports. The water in all chambers (2.5 L each) was stirred by flat disks (17 cm diameter) rotating 7 cm above the sediment cores (5 dm<sup>3</sup> each). All axes of the stirring disks were connected via toothed belts to a DC servo-motor and rotated at exactly the same constant angular velocity. The motor was controlled by a computer that used the signal of the pressure gauge to adjust the rotation of the stirring disks to the selected pressure differential (0.1 Pa cm<sup>-1</sup>) that equaled the differential previously measured at a ripple exposed to two-dimensional flow (Huettel et al. 1996). All chambers were kept in a temperature bath (20°C) and covered by an opaque sheet excluding all light.

In CHA-1, we incubated 4 different sieved sands of selected grain sizes, with grain size medians ranging from 187 µm to 1500 (Table 1), and the control chamber with false bottom simulated an impermeable sediment core. After insertion of the water-saturated sand cores, filtered seawater (S = 35) with *Dunaliella* was carefully added to each chamber producing an initial Chl. a concentration of 100 µg L<sup>-1</sup>. A plastic sheet covering the sediment prevented mixing of algal cells into the sands during the filling procedure. After 72 hours, the overlying water in each chamber was drained and analyzed for Chl. a content. In addition, 7 sediment subcores (20 mm diam., 100 mm length) were taken across each chamber. These cores were sliced (5 and 10 mm intervals), and sediment slices of the same depth layer were pooled to average Chl. a concentrations over the core diameter. *Dunaliella* cells were extracted from each depth layer as described for FLU-S. Extraction efficiencies were assessed by adding *Dunaliella* suspension of known concentration to 250 ml bottles containing the different sands and subsequent extraction, yielding 80 ± 6% for 175 µm sand, 83 ± 5% for 375 µm sand, 86 ± 6% for 750 µm sand and 86 ± 6% for the 1500 µm sand.

In CHA-2, 4 natural sand cores with different grain sizes (Table 1) were placed in the chambers. These cores that originated from the German Bight (North Sea, 54° 8' N; 7° 32' E) were mixed and kept in a dark cold room for 7 months prior to the experiment to allow decomposition of algal material and chlorophyll. The initial Chl. a concentration in the chamber water after addition of *Dunaliella* was 540  $\mu\text{g L}^{-1}$ . After 144 h, the entire sediment cores were sliced (1, 2, 5 and 10 mm intervals), and the algal cells were extracted from each slice and analyzed for Chl. a as described for FLU-S.

*Two field experiments* were conducted to investigate algal transport into sediment under field conditions. The experiments were performed in intertidal sand flats at the German North Sea coast that combined accessibility and natural current and wave conditions. The first field experiment (FLD-1) was carried out in a sand flat close to Sahlenburg (53° 9' N; 8° 6' E), mean tidal range in this area is 1.2 m. Two sets of 4 different sand cores (280 mm diameter, 300 mm height, grain sizes: Table 1) that were saturated with filtered sea water were inserted into the sediment approximately 100 m seaward from the mean high tide line. During the following high tide, 3  $\times$  500 ml water samples were collected and preserved (2% glutaraldehyde) for POC analyses. After 12 h, including one inundation period of 10 h, one (seaward set) and two (landward set) sediment subcores (36 mm diameter, 200 mm length) were taken from the center of each imbedded sand core. These subcores were sliced immediately into 10 mm (one set) and 5 mm (two sets) intervals, down to 100 mm depth. The subcore segments were brought to the laboratory in a cooler, and algal cells were extracted within 2 h after retrieval following the same procedure as described for FLU-R. All intact fluorescent algal cells were counted.

The second field experiment (FLD-2) was carried out in Königshafen (55°02'N, 8°26'E), an intertidal bay of Sylt island with a mean tidal range of 1.7 m (Reise 1985). Two artificial sand cores (grain sizes: Table 1) were inserted at low tide into the exposed sand flat sediment approximately 250 m offshore. In order to trace penetration of particulate matter into the experimental cores, fluorescent microbeads (3  $\mu\text{m}$  diameter, density 1.05  $\text{g cm}^{-3}$ ; Duke Scientific Corp.) suspended in particle-free North Sea water were poured on the sediment surface around the cores in a ring of approximately 25 mm width and leaving 20 mm distance from the outer edge of the core using a template. Tracer particle abundance in the rings was  $(1.34 \pm 0.34) \times 10^{11} \text{ m}^{-2}$ . After one tidal inundation of 10 h, 2 subcores (60 mm diam., 200 mm length) were taken from each artificial core and sliced into 10 mm sections down to 200 mm depth. Algae and beads were extracted from the segments and counted as described for FLU-R. Benthic and pelagic algae were counted separately, and here we report the results for the planktonic diatoms in the size range of 10 to 15  $\mu\text{m}$ , which was the size range closest to that of *Dunaliella*. In field and chamber experiments, the maximum penetration depths of algae was defined as the depths where the exponential functions fitted to the Chl. a depth distributions reached 0.01  $\mu\text{g cm}^{-3}$ .

## Results

### *Reference flume experiment (FLU-S).*

Advective pore water transport in the smooth sediment core was relatively small. Oxygen penetration into the core did not exceed 7 mm depth (Fig. 3), while diffusive oxygen penetration under stagnant water conditions reached to 3-5 mm. However, the sediment subcores taken at the end of the experiment revealed that algal cells had penetrated into the sand. 72% of these cells were trapped in the upper 5 mm, the rest were found between 5 and 10 mm depth (Fig. 4). Integrated over the whole depth of the subcores, we recorded  $11.1 \pm 3.7$  mg Chl.  $\text{a m}^{-2}$ , which corresponds to a flux of  $3.7 \pm 1.2$  mg C  $\text{m}^{-2} \text{d}^{-1}$  (Table 2).

*Flume sediment cores with mounds (FLU-M1, FLU-M2).* Oxygen penetrated 25 mm deep at the upstream edge of the mounds (FLU-M2, Fig. 3) revealing intrusion of oxygen-saturated flume water into the sediment core. With these interfacial flows, suspended algae were carried into subsurface sediment layers (Fig. 4). Consistent with the oxygen distribution, maximum penetration depths of *Dunaliella* were recorded at the upstream edge of the mounds, however, algae penetrated deeper than oxygen and cells were found down to 40 (FLU-M1) and 50 mm (FLU-M2). Due to the interfacial transport, topography increased the trapping efficiency of the sediment. Advective infiltration of algae produced carbon fluxes exceeding that of the smooth reference FLU-S by factors of 2.1 (FLU-M1) and 1.7 (FLU-M2, Table 2).

	average in water column	average in sediment core	normalization factor	normalized flux	increase by factor	tracer derived flushing rate	normalized flux calculated using flushing rate
	mg C L <sup>-1</sup>	mg C m <sup>-2</sup>		mg C m <sup>-2</sup> d <sup>-1</sup>		L m <sup>-2</sup> d <sup>-1</sup>	mg C m <sup>-2</sup> d <sup>-1</sup>
<b>FLU-S</b>	0.8 ± 0.7	11.1 ± 3.7	1.0	3.7 ± 1.2	1.0	7	5.6
<b>FLU-M1</b>	0.5 ± 0.3	13.2 ± 7.6	1.7	7.6 ± 4.4	2.1	28	23.8
<b>FLU-M2</b>	2.4 ± 1.1	53.7 ± 33.2	0.4	6.3 ± 3.9	1.7	28	26.9
<b>FLU-R</b>	1.0 ± 0.8	113.8 ± 88.8	0.9	33.5 ± 26.2	9.1	60	54.0

Table 2: Organic carbon imported into the sediment calculated using the chlorophyll data recorded in the sediment cores and a chlorophyll to carbon ratio of 1:20 (Sims 1993; Verity et al. 1993). The normalized flux column lists the fluxes calculated assuming same average flume water carbon concentration in all experiments. For this normalization we divided the average water carbon content measured in FLU-S by the average water carbon content of the respective experiment. For flux calculations in FLU-M1, which ran longer than the other flume experiments, we took the average water carbon content measured in the last 3 days of the experiment. The average carbon content in the sediment was calculated by integrating the carbon content of all subcores, and in the ripple experiment by integrating the areas of equal concentration (Fig. 5) and subsequent summation. The tracer-derived flushing rates were calculated from dye tracer experiments performed in similar sediment with similar topography (Huettel and Gust, 1992, Huettel et al. 1996).

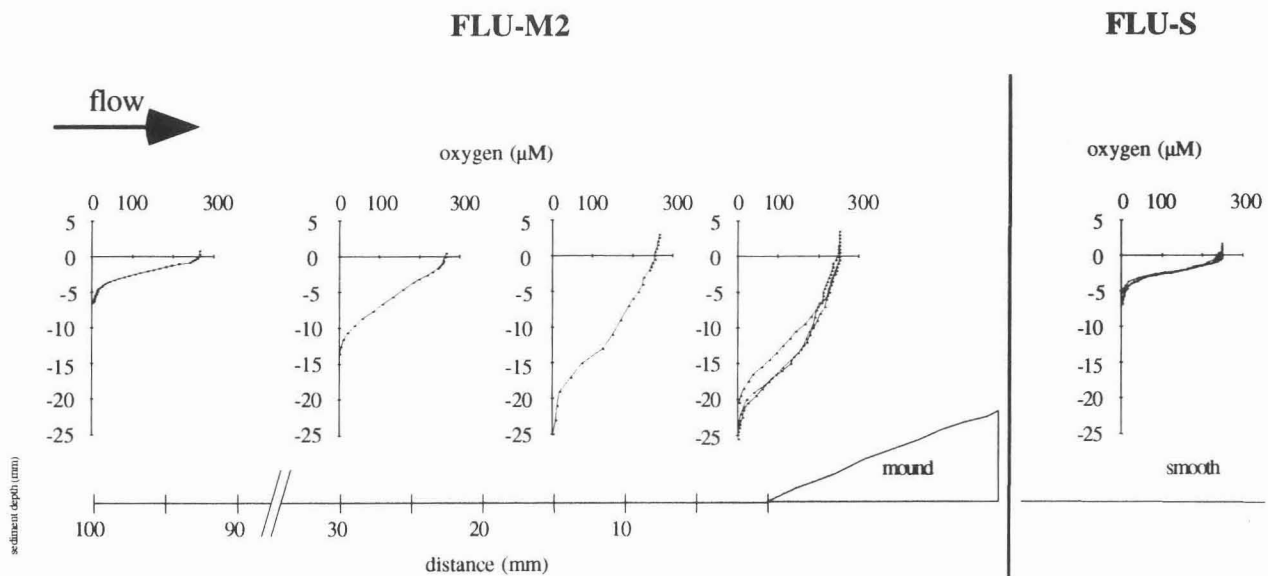


Figure 3: Oxygen penetration depths measured with microelectrodes in the second mound experiment (FLU-M2) and the in the smooth surface experiment (FLU-S).

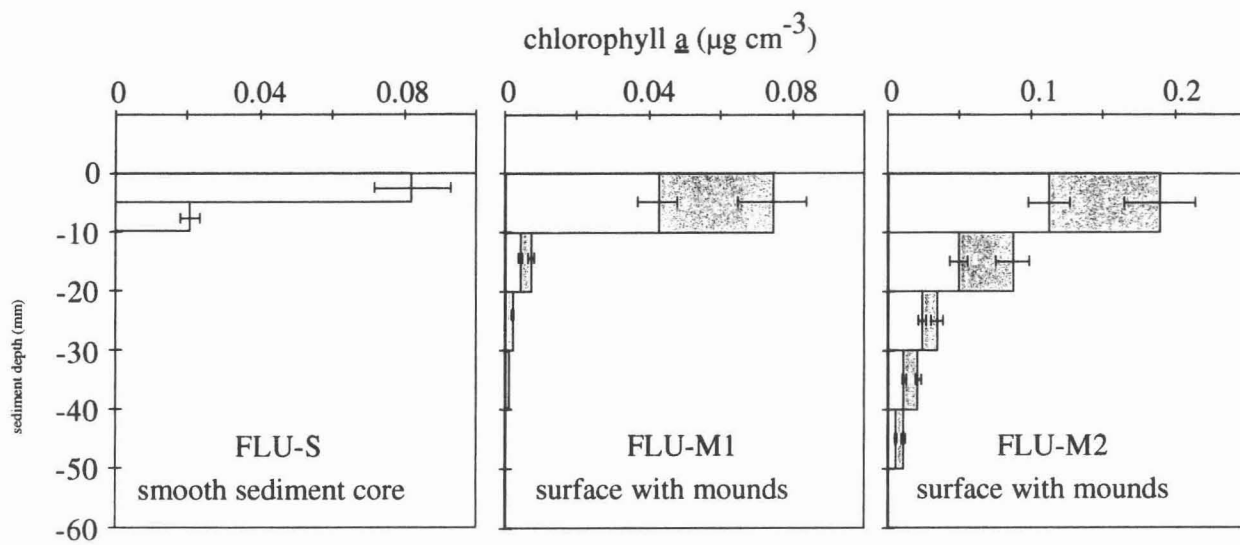


Figure 4: Chlorophyll  $a$  concentrations in the sediment cores with smooth surface and surface with mounds. Dark-gray bars represent Chl.  $a$  in sediment subcores taken in the center of the intrusion areas, upstream of the mounds, light-gray bars Chl.  $a$  in sediment subcores taken perpendicular to the mounds (compare Fig. 2).

#### *Flume sediment core with ripple (FLU-R).*

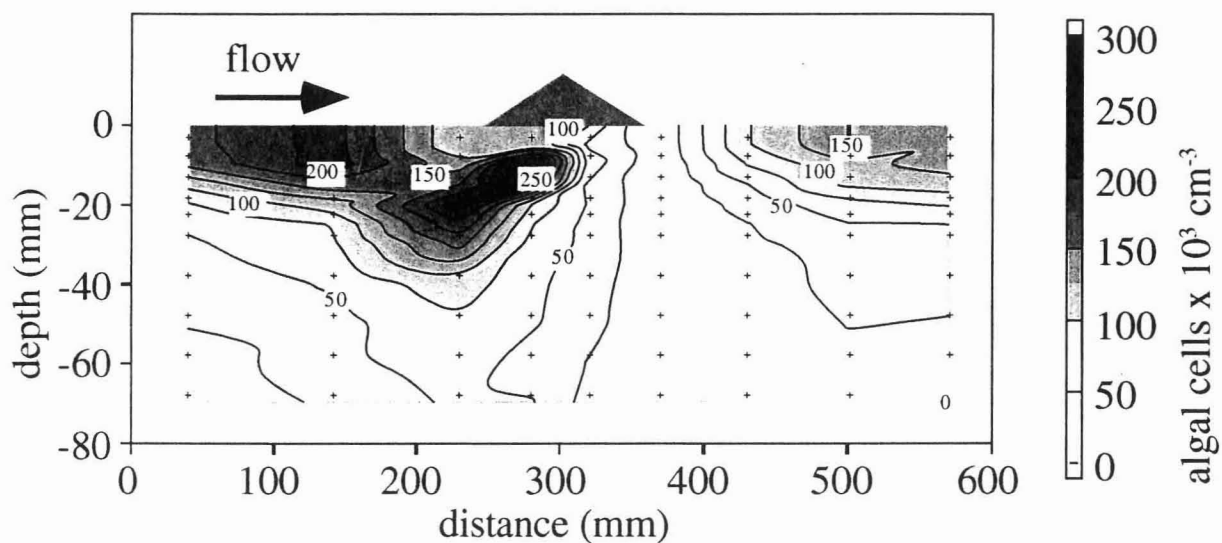
Upstream of the ripple, where water intrusion was strongest, algal cells were transported down to at least 70 mm depth (Fig. 5, the lower boundary of algal distribution was not reached by the subcores). The downstream penetration was less pronounced and restricted to the upper 50 mm of the core. In the center transect, maximum cell concentrations were recorded at 10 mm depth, below the upstream slope of the ripple ( $299 \pm 43 \times 10^3$  cells  $\text{cm}^{-3}$ ). Low numbers ( $< 6 \times 10^3$  cells  $\text{cm}^{-3}$ ) were counted where pore water from deeper sediment layers was drawn to the surface. The side transect showed a similar distribution of algae, but due to the side wall effect in the flume (reduced flow speeds and pressure gradients), the advective transport of *Dunaliella* into the sediment was not as strong (maximum  $219 \pm 25 \times 10^3$  cells  $\text{cm}^{-3}$  at 5 mm depth) and reached less deep (Fig. 5). Integration of the cell numbers found in the center and side transect resulted in a flux of  $33.5 \pm 26.2$  mg C  $\text{m}^{-2} \text{d}^{-1}$ , the 9.1- fold of that recorded in the smooth control core.

#### *Chamber experiments (CHA-1 and CHA-2).*

Algal penetration depth increased with grain size (Fig. 6) and sediment permeability (Fig. 7). In CHA-1, algae reached 18, 26, 42 and 56 mm depth in the 187, 375, 750 and 1500  $\mu\text{m}$  sands, respectively. Because the natural sediments were less well sorted (Table 1), penetration depths in CHA-2 were lower (5, 12, 18, 26 mm for 105, 150, 600 and 1050  $\mu\text{m}$  sands). The coarser the sands, the more algae were transported into the sediment cores. The different filtration rates could be observed visually during the experiments (Fig. 8). At the end of CHA-1, the algal concentration in the water overlying the coarse sand had dropped to 4 % of the initial concentration, while in the very fine sand the concentration had decreased to only 31% (Fig. 9, Table 3). The amount of Chl. a trapped by the sediment surface layer (upper 5 mm) dropped with increasing grain size and accounted for 9% to 6% of the Chl. a decrease in the chamber water. Some sedimented algae accumulated in the "calm zone" in the center of the surface of the 187  $\mu\text{m}$  and 375  $\mu\text{m}$  sands (these algae were included in the final water column Chl. a content), no such accumulations formed on the 750  $\mu\text{m}$  and 1500  $\mu\text{m}$  sands. The total volume of Chl. a found below 5 mm sediment depth increased with permeability, and accounted for 8% (187  $\mu\text{m}$  sand) to 13% (1500  $\mu\text{m}$  sand) of the Chl. a decrease in the chamber water. The coarsest sand contained twice as many cells as the finest sand. CHA-2, with the natural sediments from the North Sea, confirmed the results of CHA-1 (Fig. 9, Table 3). Final concentrations of algae in the water overlying the coarse sand had decreased to 6% and in the muddy silt to 33% of the initial concentration. Sedimentary Chl. a reached maximum values in the coarsest sand. In contrast to CHA-1, the relative number of algae trapped by the surface proper increased with grain size.

The total number of phytoplankton cells that could be recovered from the chambers decreased with increasing permeability of the sediments (Fig. 9, Table 4). While 61% and 34% of the initially added cells could be regained from the chambers with "impermeable" bottom (CHA-1: chamber with false bottom, CHA-2: chamber with 105  $\mu\text{m}$  sand), only 24% (CHA-1) and 17% (CHA-2) were found in the chambers with coarsest sands. Due to the longer duration, the total number of cells recovered from the chambers in CHA-2 was relatively lower than in CHA-1.

center transect (FLU-R)



side transect (FLU-R)

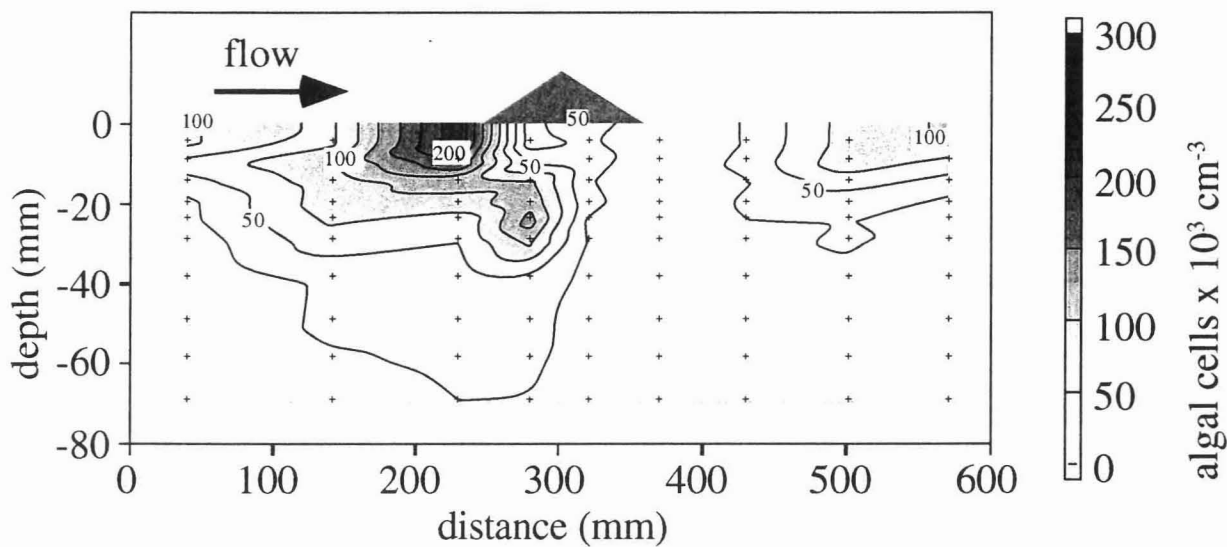


Figure 5: Isoline diagrams generated from algal cell counts in subcores retrieved along center and side transect upon termination of the ripple experiment (FLU-R).

Sediment permeability m <sup>2</sup>	final C content of water and surface µg C	difference to "impermeable" µg C	flux into sediment mg C m <sup>-2</sup> d <sup>-1</sup>	found in sediment µg C	POC degradation in sediment mg C m <sup>-2</sup> d <sup>-1</sup>
<b>CHA-1</b>					
4.6 x 10 <sup>-10</sup>	551	2515	30	669	22
1.1 x 10 <sup>-10</sup>	1053	2013	24	648	16
2.8 x 10 <sup>-10</sup>	1838	1227	14	470	9
7.1 x 10 <sup>-12</sup>	1981	1084	13	407	8
0	3066	0	0	0	0
<b>CHA-2</b>					
2.2 x 10 <sup>-10</sup>	2613	6244	37	1916	25
7.3 x 10 <sup>-11</sup>	3991	4867	29	750	24
4.6 x 10 <sup>-12</sup>	5809	3049	18	654	14
2.3 x 10 <sup>-13</sup>	8858	0	0	0	0

Table 3: Carbon fluxes and sedimentary POC degradation rates (degradation = cell loss) calculated for the chamber experiments and assuming 30 pg C per *Dunaliella* cell (Sims 1993; Verity et al. 1993). Initial POC input in each chamber was 5 mg in CHA-1 and 27 mg in CHA-2. For CHA-1 sediments with same permeabilities the average values are listed.

<b>CHA-1</b>							
			impermeable bottom	fine sand	medium sand	coarse sand	very coarse sand
	permeability	m <sup>2</sup>	0	7.1E-12	2.95E-11	1.1E-10	4.6E-10
not degraded		%	61	48	46	34	24
max. degraded in water		%			39		
min. degraded in sediment		%	0	13	15	27	37
<b>CHA-2</b>							
			cohesive mud	fine sand	medium sand	coarse sand	
	permeability	m <sup>2</sup>	2.2E-13	4.6E-12	7.2E-11	2.2E-10	
not degraded		%	34	25	18	17	
max. degraded in water		%			66		
min. degraded in sediment		%	0	9	16	17	

Table 4: Degradation (= cell loss) of algae in the different chambers. Calculations are based on the numbers of intact *Dunaliella* cells found in the chambers. The number of cells that was degraded in the chambers with "impermeable" bottom/sediment provided the maximum number of cells that were degraded in the water columns and surface. For CHA-1 sediments with same permeabilities the average values are listed.

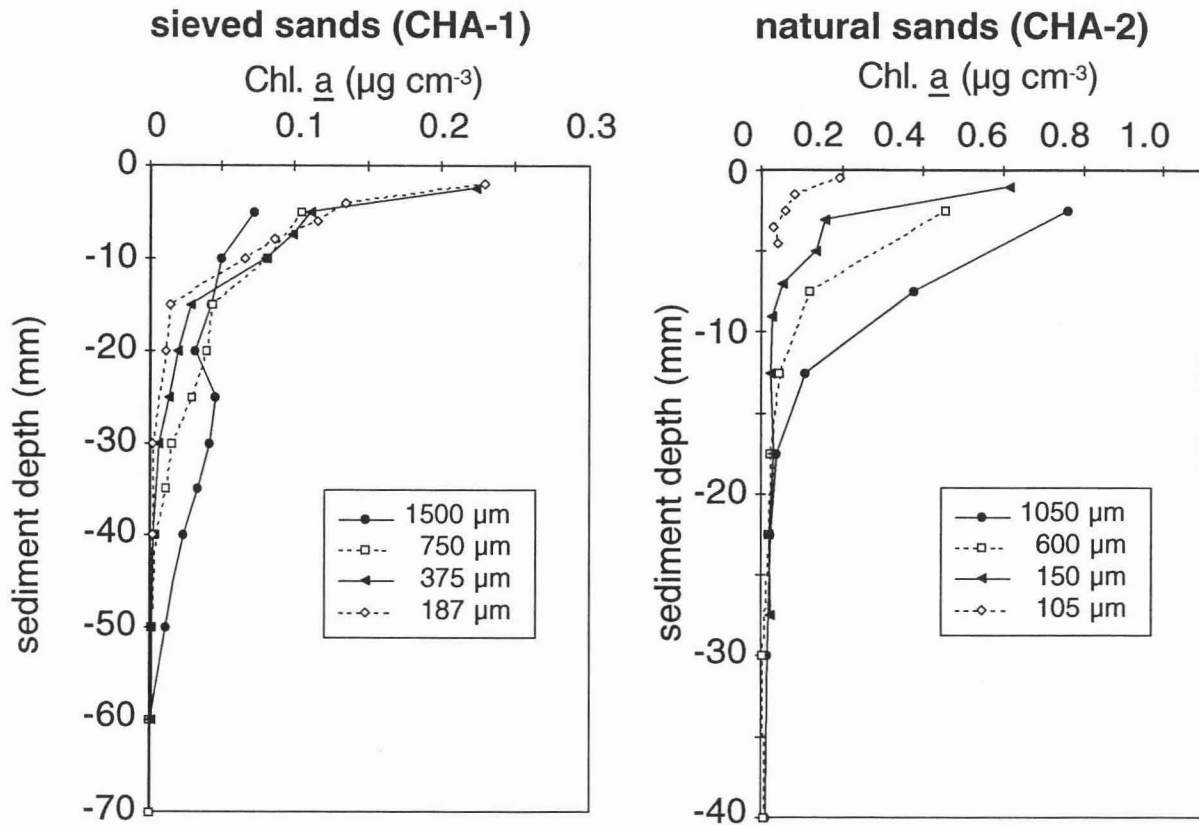


Figure 6: Penetration depths of *Dunaliella* cells in the sediments incubated in the stirred chambers of experiments CHA-1 and CHA-2. Please note different depth scales.

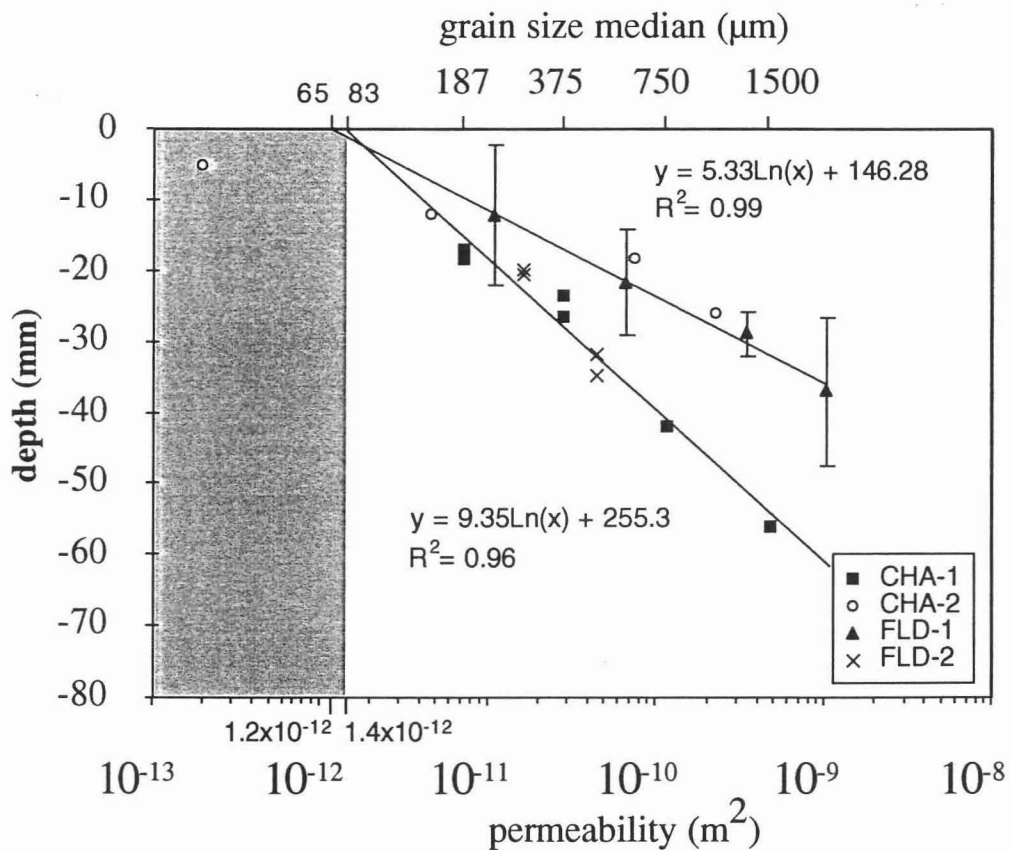


Figure 7: Penetration depth vs. permeability for chamber and in-situ experiments. No advective particle transport is possible in the gray zone. Grain size median values are given for comparison.

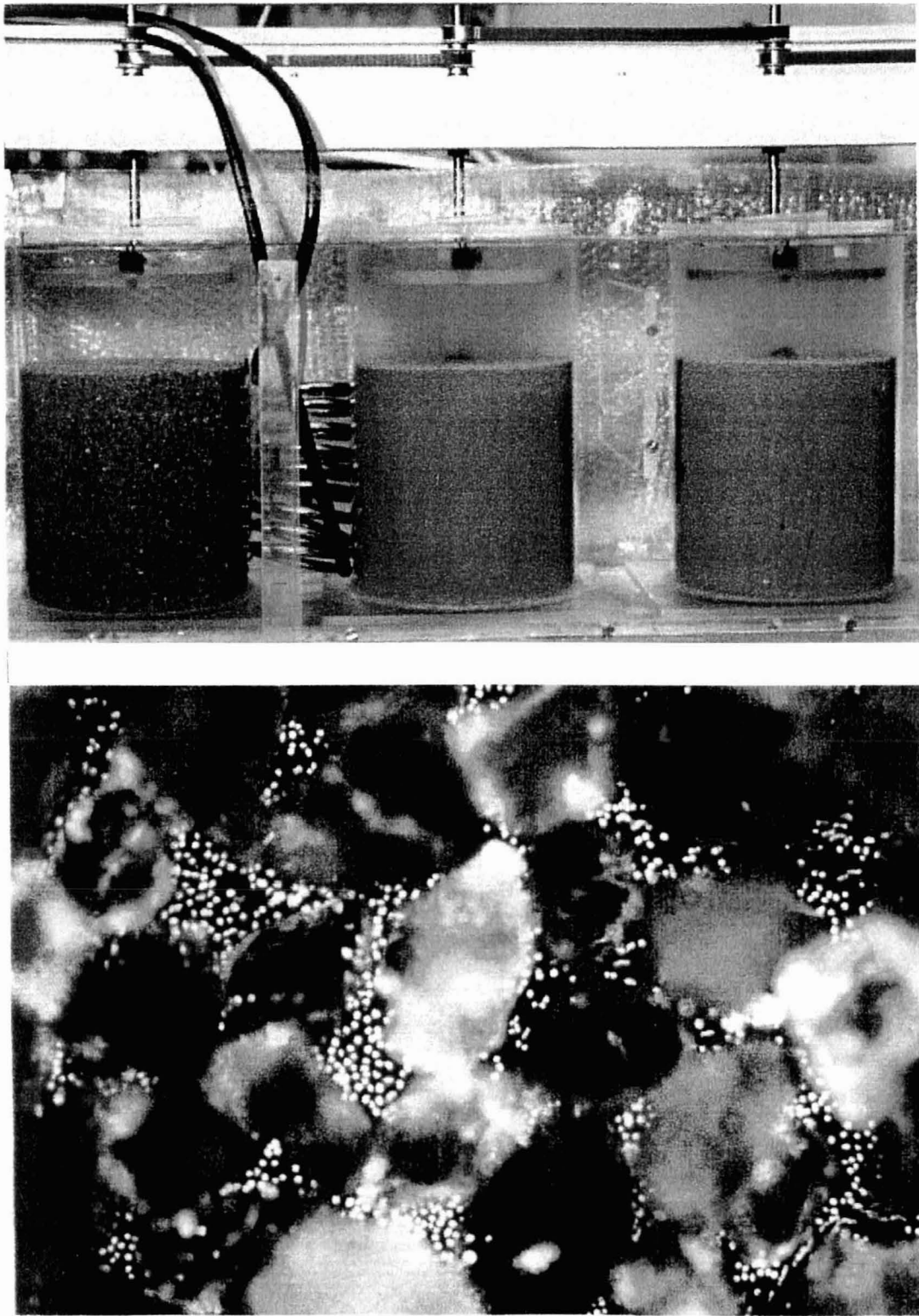


Figure 8: The upper picture shows the chambers with 1000-2000  $\mu\text{m}$  (left), 125-250  $\mu\text{m}$  (middle) and 250-500  $\mu\text{m}$  (right) sands on the last day of CHA-1. In the chamber with the coarsest sand, the *Dunaliella* cells had almost disappeared from the water column, while in the fine sand (middle chamber) most cells were still in the water and alive. The lower graph depicts *Dunaliella* cells in the interstices of 125-250  $\mu\text{m}$  sand demonstrating the space available for the algal transport with pore water flows.

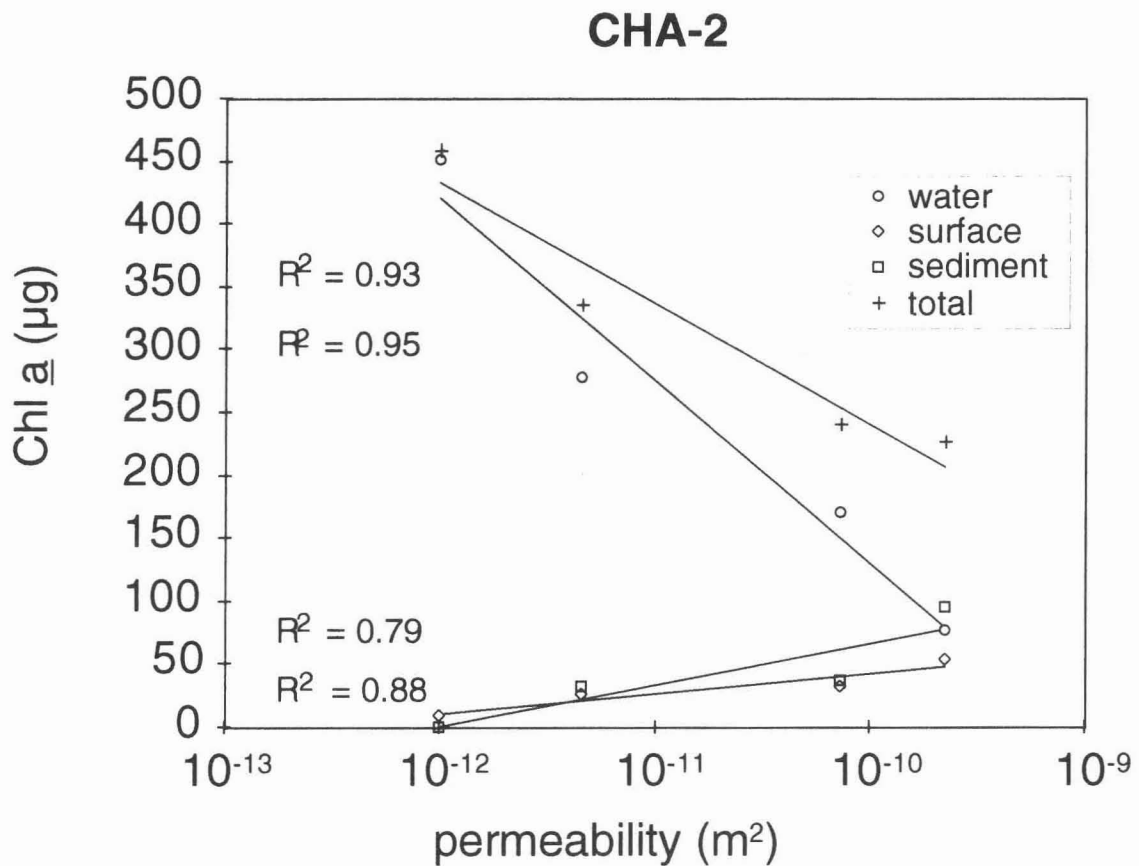
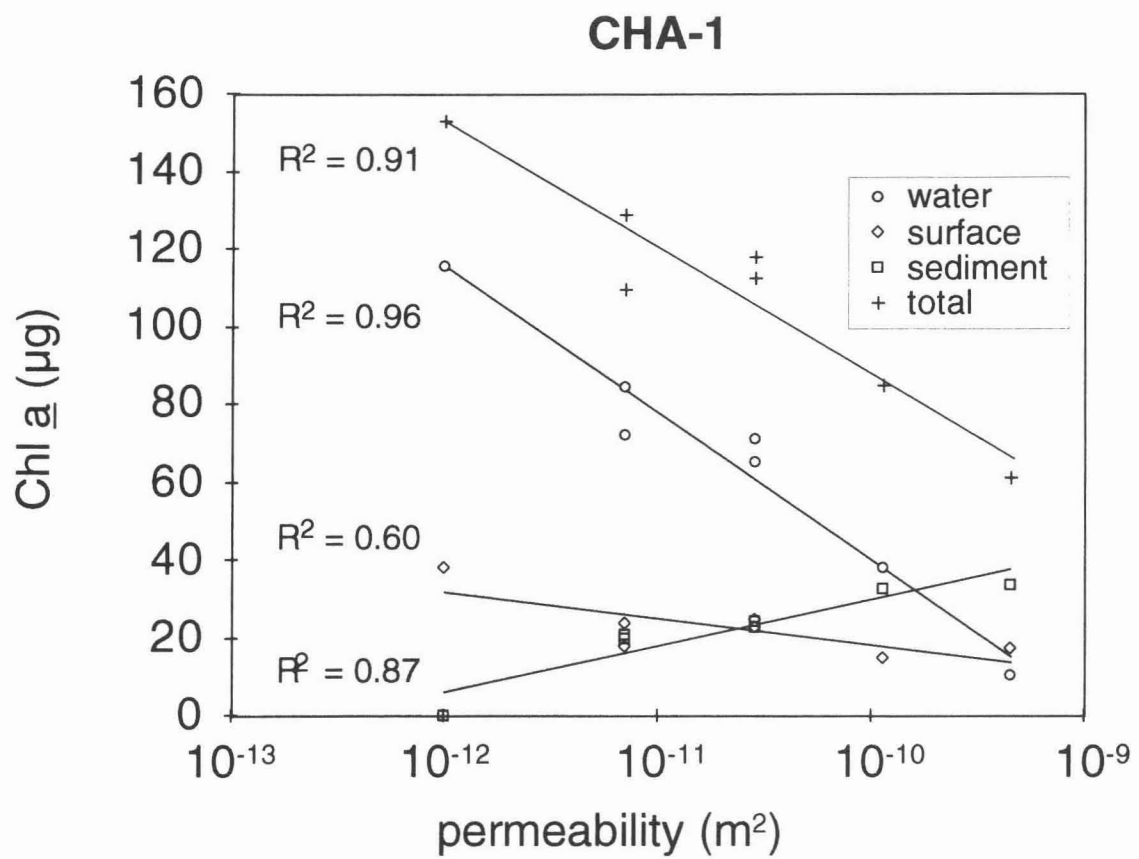


Figure 9: Total chlorophyll and chlorophyll concentrations found in water, surface and subsurface layers upon termination of CHA-1 and CHA-2.

*Field experiments (FLD-1, FLD-2).*

At the time of experiment FLD-1, wave amplitudes were less than 20 cm and tidal currents at the study site reached maximum velocities of  $18 \text{ cm s}^{-1}$  at 10 cm above the sediment surface. Water samples taken at 5 cm above bottom had a particulate organic carbon (POC) content of  $177 \pm 19 \text{ mg C dm}^{-3}$ . Lateral sediment movement was negligible; at the end of the experiment, the surfaces of the embedded cores were not covered by surrounding sediment, however, small wave ripples had formed on the sands (amplitude  $< 15 \text{ mm}$ ). During submergence, benthic and planktonic algal cells were transported into the embedded sand cores (Fig. 10). As found in the laboratory chamber experiments, penetration depth of algae grew linearly with the logarithm of sediment permeability (Fig. 7) and reached  $12 \pm 10 \text{ mm}$  (200  $\mu\text{m}$  sand),  $22 \pm 7 \text{ mm}$  (500  $\mu\text{m}$ ),  $29 \pm 3 \text{ mm}$  (1150  $\mu\text{m}$ ), and  $38 \pm 10 \text{ mm}$  (2000  $\mu\text{m}$ ). The total number of algae cells found in the sediments increased from  $(20 \pm 15) \times 10^3 \text{ cells cm}^{-2}$  in the 200  $\mu\text{m}$  sand to  $(496 \pm 637) \times 10^3 \text{ cells cm}^{-2}$  in the 2000  $\mu\text{m}$  sand (Table 5).

Weather and current conditions during FLD-2 were very similar to those in FLD-1; wave height was less than 20 cm, bottom currents did not exceed  $15 \text{ cm s}^{-1}$  and sediment erosion was minimal. A water sample taken shortly after inundation contained  $238 \times 10^5$  phytoplankton cells per liter. Penetration depths of phytoplankton cells of the 10 to 15  $\mu\text{m}$  size class increased from  $20 \pm 1 \text{ mm}$  in the 187  $\mu\text{m}$  sand to  $35 \pm 2 \text{ mm}$  in the 750  $\mu\text{m}$  sand. The fluorescent tracer beads (3  $\mu\text{m}$ ) were transported deeper, reaching  $27 \pm 3 \text{ mm}$  and  $65 \pm 7 \text{ mm}$  sediment depth in the 187  $\mu\text{m}$  and 750  $\mu\text{m}$  sands, respectively. The 750  $\mu\text{m}$  sand contained 1.8 times as many algal cells as the 187  $\mu\text{m}$  sand (Table 5).

	permeability ( $\text{m}^2$ )	algae per area ( $\times 10^3 \text{ cells cm}^{-2}$ )	flux ( $\text{mg C m}^{-2} \text{ d}^{-1}$ )	factor
<b>FLD-1</b>				
	1.0E-09	$496 \pm 637$	$297 \pm 382$	24.7
	3.5E-10	$58 \pm 68$	$35 \pm 41$	2.9
	6.7E-11	$21 \pm 24$	$13 \pm 14$	1.0
	1.1E-11	$20 \pm 15$	$12 \pm 9$	1.0
<b>FLD-2</b>				
	1.3E-10	$159 \pm 86$	$95 \pm 52$	1.8
	1.8E-11	$89 \pm 6$	$54 \pm 4$	1.0

Table 5. The number of algal cells found in the sediment cores embedded in the intertidal sand flats. In FLD-1 all algal cells were counted. The counts listed for FLD-2 include only the planktonic diatoms in the size class 10-15  $\mu\text{m}$ . Carbon fluxes were calculated assuming an average C content of 30 pg per cell.

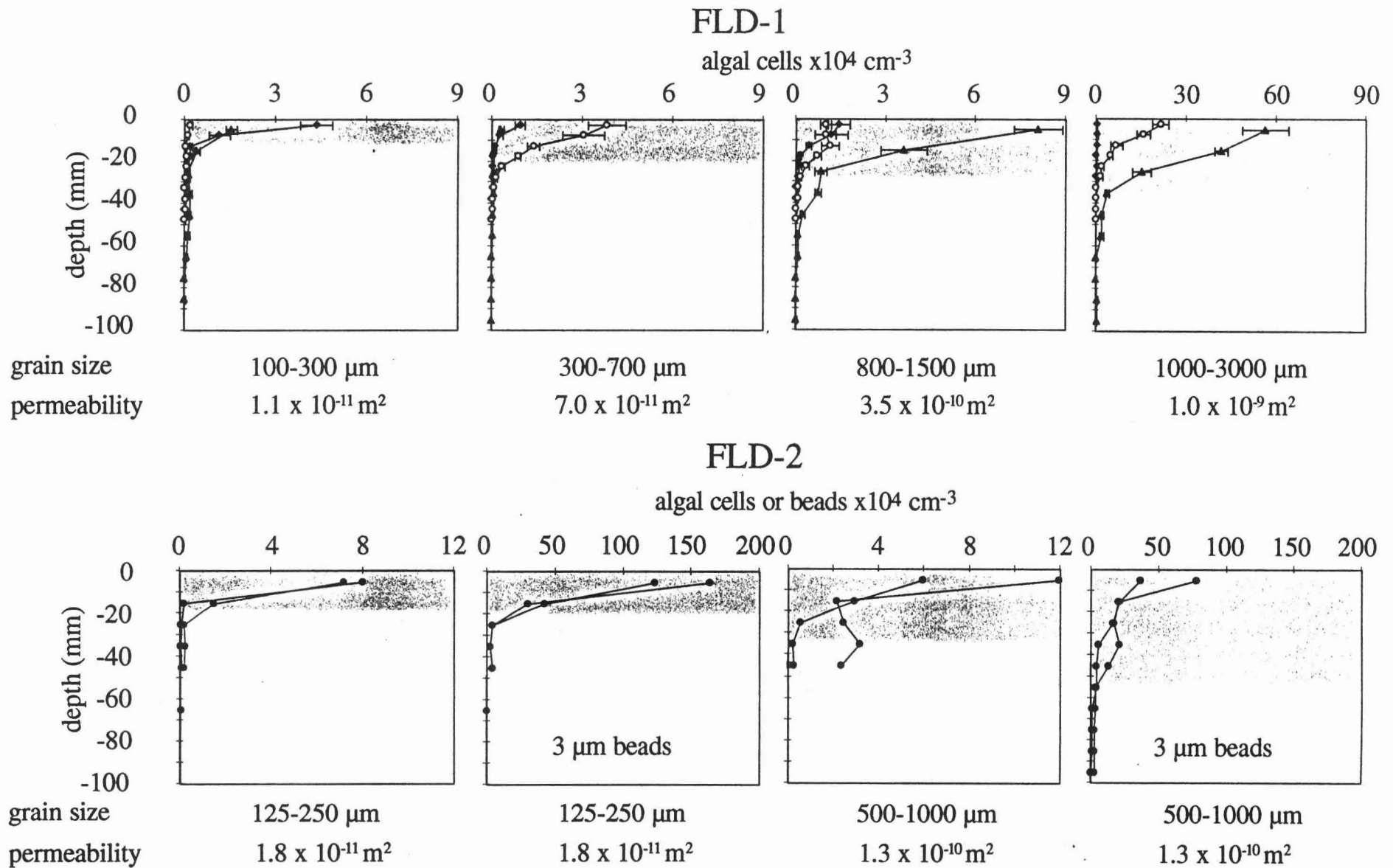


Figure 10: Penetration of algal cells in the sediment cores inserted in intertidal sand flat sediment. In FLD-1, we lost the pore water of one of the subcores taken in the coarsest sediment due to a leak, causing almost a complete loss of infiltrated algae. Gray areas depict the maximum penetration depths of algal cells and microbeads, respectively.

## Discussion

Due to their specific weight close to that of sea water, sedimented planktonic algae are resuspended by even the slightest boundary flow. In the shallow shelf, waves and strong bottom currents, thus, hinder the deposition of sinking phytoplankton. Frequent resuspension of the upper sediment layers periodically removes fine particles (Churchill et al. 1994; Grant et al. 1997) and exopolymeric substances from the sandy sea bed and impedes settling of benthic organisms, thereby maintaining high permeability and "clean" appearance of the sands. Our experiments demonstrate that in such an environment advective interfacial water flows provide a rapid and direct pathway for suspended phytoplankton cells into permeable sediment. With a particle Reynolds number of approximately  $6 \times 10^{-5}$ , path and velocity of the algal cells in our flume water were mainly controlled by the turbulent flow. The latter kept the algae in suspension, and visible accumulation of algal cells on the sediment surface did not occur. Contrasting this visual appearance of a "non-accumulating", "clean" sand bed, the analyses of the sediment revealed infiltration and deep penetration of algae into the sand when topography was present. The sand acted as efficient POM trap.

### *Interfacial transport.*

Two mechanisms were responsible for the transfer of algal cells into the sediment: Interfacial water exchange caused by shear and water exchange driven by topography-related pressure gradients. The relatively high permeability of the sediment permitted extension of the boundary layer velocity profile into the sand, with shear generating pore water flows in the upper 2 to 3 millimeters of the sand (Beavers and Joseph 1967; Brinkman 1947). Ensuing dispersion in this porous layer enhanced fluid exchange with the overlying water (Webster and Taylor 1992). The oxygen profiles measured in the smooth flume core (Fig. 3) were shaped by this exchange process; concentrations in the upper 2 millimeters of the sand did not decrease but below that flushing depth they dropped sharply. This shear-driven interfacial water exchange was responsible for the penetration of algae into the upper 5 mm of the sediment we found in the smooth control core (FLU-S, Fig. 4). Penetration of some algal cells below 5 mm in this core is attributed to surface heterogeneities. Huettel and Gust (1992a) showed that even surface roughness in the millimeter-scale can enhance interfacial transport in permeable sands exposed to flow. Algae penetrated more than 70 mm into flume sediment with topography. In contrast to the shear-induced exchange that is dominated by surface-parallel pore water flows, the topography-related pressure areas force water at steep angles into the sand up- and downstream of protruding surface structures (Fig. 1). The ensuing pore water flow field causes a distinct distribution of POM in the sediment with concentration maxima and minima (Fig. 5).

### *Limiting factors.*

Transport of suspended algae into and within the sediment is limited by the size of open pores in the sand and the characteristics of the cells. Extrapolation of the recorded penetration depths sets the limit of advective algal transport to sand with a permeability of  $1.4 \times 10^{-12} \text{ m}^2$  and approximately 100  $\mu\text{m}$  grain size (Fig. 7). An increase of interfacial solute fluxes due to advective pore water flows can be measured when sediment permeabilities exceed  $1 \times 10^{-12} \text{ m}^2$  (Huettel and Gust 1992a; Huettel et al. 1998). Transport of algal cells into the sediment, thus, was found for almost the same permeabilities that facilitate detectable advective pore water flows, emphasizing the role of tight coupling between cell and water movement. In a well-sorted sediment with relatively spherical sand grains of 350  $\mu\text{m}$  diameter, like the one we used

in the flume experiments, the pores have a diameter of about 30-50  $\mu\text{m}$ . With an average diameter of  $8 \pm 6 \mu\text{m}$ , the *Dunaliella* cells could easily be transported through these pores (compare relation to pore space in 125-250  $\mu\text{m}$  sands, Fig. 8). Penetration depth was determined by size, shape, density, and surface characteristics of the algae, and in case of living cells, also their own movement. The spherical shape of *Dunaliella*, its elasticity and smooth, non-sticking cell surface reduced the friction between algae and sand grains. We found moving *Dunaliella* cells in the sediment samples, showing that living cells were transported into the sand. Motility facilitates advective transport of living cells within the sediment by increasing the fraction of time the cells spend in a detached versus an attached state (McCaulou et al. 1995). However, *Dunaliella* cells can move considerably faster (ca. 200  $\mu\text{m s}^{-1}$ , Aleev 1991; Marano et al. 1989; Schoevaert et al. 1988) than the maximum velocity of the advective pore water flows (ca. 100  $\mu\text{m s}^{-1}$  in the uppermost 3 mm of the sediment core), and phototaxis and negative geotaxis should keep healthy cells from being carried into the sediment. *Dunaliella* cells transported into our sands may have been alive but probably were not fully motile any more. Less or non-motile planktonic organisms should be affected more strongly by the interfacial transport.

#### *Subsurface maximum.*

The velocity of the advective flows gradually decreases with sediment depth (Huettel et al. 1996) and limits the penetration of algae to the depth where pore water moves too slowly to overcome the friction retarding the cells in the interstitial space. Algae can accumulate in that layer (Fig. 11). This process is responsible for the subsurface maxima we recorded in the flume experiment at the upstream edge of the ripple, where water intrusion was strongest (Fig. 5). In our relatively short chamber experiments, algal subsurface accumulation could only be observed in the coarsest sediment, where pore water flows were sufficiently strong to carry enough cells into the sand to produce a measurable maximum (Fig. 6, CHA-1, 1500  $\mu\text{m}$ ). In the second field experiment, concentration profiles of algae and tracer beads showed a subsurface maximum in the 750  $\mu\text{m}$  sand at 30 to 40 mm depth (Fig. 10). Ripples that form on sandy shelf sediments due to bottom currents slowly move with or against the current direction. Because the pore water upwelling associated with ripples is too weak to efficiently remove particles from the deeper sediment layers, moving ripples can produce a subsurface layer of organic matter. In sand cores collected from the shallow South Atlantic Shelf and in laboratory incubations of these sediments, Marinelli et al. (1998) regularly observed ammonium and silicate peaks at 20 to 80 mm sediment depth that indicate decomposition of subsurface accumulations of organic matter.

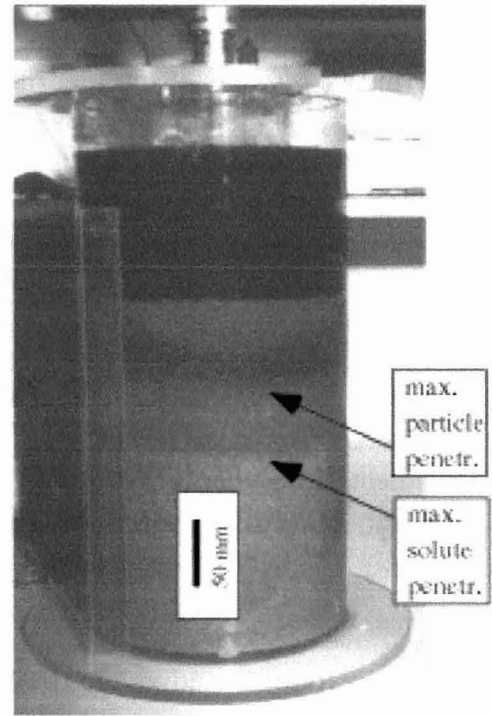
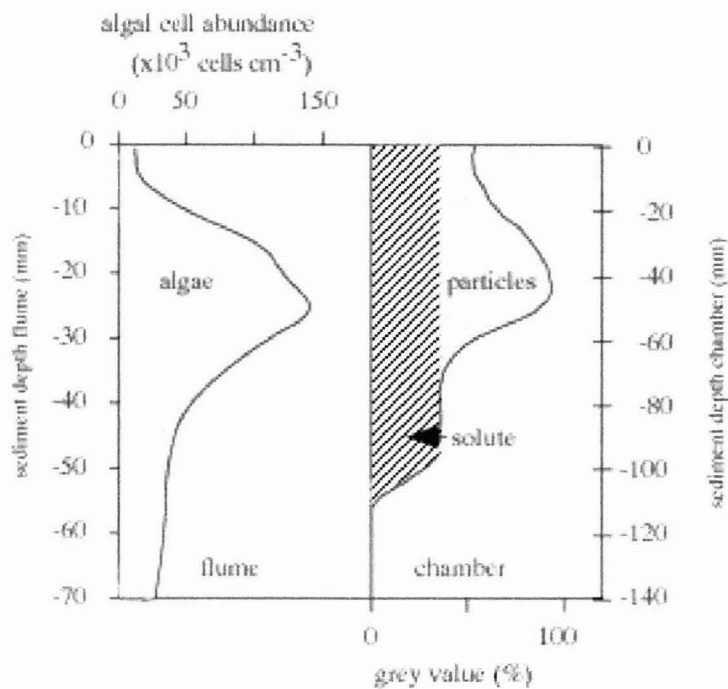


Figure 11: Particle accumulation at a specific sediment depth demonstrated in a chamber experiment with solute (red) and particle (black) tracers, and in the flume ripple experiment (FLU-R) with algae. In the cylindrical chamber, the radial pressure gradient forces Rhodamine WT dye and black acrylic particles (1  $\mu\text{m}$ ) into the sediment (750  $\mu\text{m}$ ). Particles were transported downward until the pore water flow was too slow to overcome the friction between particles and sand grains. The particles accumulated in that layer, while the solute tracer was transported deeper into the core (right graph and photo). The same process caused the accumulation of algal cells in the flume sediment upstream of the ripple (left graph).

#### Field validation.

The field experiments showed the same linear relationship between penetration depth of algae and the logarithm of sediment permeability as the laboratory results, indicating that the same transport process was responsible for the interfacial particle flux (Fig. 7). Currents and waves caused negligible sediment mixing, as shown by the small penetration depth of algae into the 100-300  $\mu\text{m}$  sand that had the lowest erosion threshold of the tested sediments. As there were no benthic animals in the embedded sand cores, we conclude that the dominant process transporting algae into the sand cores was advective pore water flow generated by the interaction of the small ripples on the cores and the tidal water currents. This conclusion is supported by the strong variability between the concentration profiles in each core. Sediment mixing by waves or currents would have produced a uniform distribution of algae in the sediments, while pore water up- and downwelling associated with sediment topography results in a patchy distribution of the imported material.

### *Flux enhancement.*

Our experiments demonstrate that permeable sediments with topography are efficient POM traps. Mounds, similar in size and abundance to those built by the polychaete *Arenicola marina* in intertidal sand flats, can double the flux of suspended unicellular algae into permeable sediment. The ripple had an even stronger effect because it narrowed the free water flow more efficiently than the scattered mounds (Table 2). The real flux enhancements by mounds and ripple were even higher than the ones calculated from the concentrations of algae found in the flume sediments because these concentrations were reduced due to degradation of cells in the sands (Table 2). From experiments with inert tracers, we know the approximate volumes of water that is forced through the sediment at small mounds or ripples (Huettel and Gust 1992a; Huettel et al. 1996). Calculations using these flushing rates suggest that topography enhanced POC fluxes to the sediment up to factors of 5 (mounds) and 10 (ripple). The flux of algal cells into the sediments increased with permeability, and in the field experiments roughly doubled when permeability changed from  $10^{-11} \text{ m}^2$  to  $10^{-10} \text{ m}^2$  (Tables 3 and 5). A larger volume of water was forced through the coarser sands (Darcy 1856) transporting more algae into the sediment.

Recent investigations in sandy shelf beds support our experimental results. Bacon et al. (1994) reported that in permeable Atlantic Bight shelf sediments (>90% sand), where no net accumulation of sediment and organic matter presently occurs, the excess  $^{210}\text{Pb}$  inventories are nearly in balance with the atmospheric supply. Because  $^{210}\text{Pb}$  only enters the sediment adsorbed to particles, these findings imply that the sands efficiently retain fine particulate matter due to a trapping mechanism. Bacon et al. (1994) suggested that benthic organisms may be responsible for this particle uptake; we propose that advective filtration of bottom water through the upper layers of the sands contributed significantly to the particle trapping. Marinelli et al. (1998), in their recent investigations of nutrient profiles in South Atlantic Bight shelf sediments, found evidence that advective pore water exchange dominates interfacial solute fluxes over bioturbation in these sands. The time-averaged rate of mass transfer for nonlocal exchange in these permeable sediments exceeded that for diffusive exchange by as much as 50-fold. As suspended particles are tightly linked to the interfacial water flow, these findings strongly suggest that in these South Atlantic Bight sediments, that have a median grain size up to twice as large as those used in our flume experiments, advective POM trapping is an important process.

### *Decomposition.*

With increasing permeability, the total number of algal cells that could be recovered from the chambers decreased. Penetration of algae into the sands accelerated the degradation process, cells disintegrated faster in the sediment than in the water column (in the following, when using "decomposition" or "degradation" in context with our experiments, we mean this disintegration of the algal cells and not complete mineralization). The contribution of phytoplankton degradation in subsurface layers of the sediments increased from 0% in the chambers with "impermeable" bottom to 37% (CHA-1) and 17% (CHA-2) in the chambers with the coarsest sands (Fig. 12). In the latter, more than twice as many algae were degraded within the same time period than in the chambers with "impermeable" bottom (Table 4). Increased mechanical stress, contact with bacteria-covered sand grain surfaces (Clement et al. 1997) and exposure to higher enzyme concentrations in the pore water could explain this result. Advective transport of oxygen into (Lohse et al. 1996; Ziebis et al. 1996b) and

decomposition products out of the sand (Gehlen et al. 1995; Huettel et al. 1998) further accelerate POM degradation. Oxygen consumption rates in non-accumulating sands can be as high as in relatively impermeable accumulating muds (Andersen and Helder 1987; Marinelli et al. 1998). In the organic-poor sands at 12 to 30 m depth of the Middle Atlantic Bight, Reimers et al. (1996) measured oxygen consumption rates as high as  $15 \text{ mmol m}^{-2} \text{ d}^{-1}$ . Low organic content of permeable sediments, thus, may be also a consequence of high turnover rates.

These findings may have significant implications for the cycling of organic matter in the shallow shelf. The closer the sediments are to the euphotic zone, the more important they become for the mineralization of sedimenting primary production, because more labile material can reach the sea floor (Buscail et al. 1995; Olesen and Lundsgaard 1995; Wollast 1991). Moreover, total primary production increases up to an order of magnitude towards the coast due to nutrient input from land, atmosphere and coastal upwelling (Galloway et al. 1996; Jickells 1998; Rowe 1975; Seitzinger and Kroeze 1998). Despite highest concentration of POM in the water column, sedimentary POC and nutrient concentrations in large areas of the shallow shelf are very low (Bacon et al. 1994; Marinelli et al. 1998). The increasing hydrodynamic forces acting on the sea bed with decreasing water depth result in a coarsening of the sediment towards the shore, culminating in highly permeable beach gravel. The smaller specific surface area of the coarser sediments may explain a lower organic matter content (Hargrave 1972). However, the intensity of advective flushing of bottom water through the coarsening sediments increases towards the coast, and at less than 100 m depth is additionally enhanced by gravity wave induced pore water exchange (Harrison et al. 1983; Malan and McLachlan 1991; Riedl et al. 1972; Shum and Sundby 1996). Our experiments demonstrate that these interfacial flows filter suspended POM from the water column, permeable shelf sands, thus, represent gigantic filter systems. How efficient these filters are is revealed by the excess  $^{210}\text{Pb}$  inventories in sandy shelf sediments measured by Bacon et al. (1994). The distributions of  $^{210}\text{Pb}$  in suspended particulate matter and in the fine fraction of the Atlantic Bight shelf sediments indicate that the particles undergo several cycles of deposition/short-term-burial/resuspension that cause a far longer residence time in the shelf than predicted from the flushing time of shelf waters. We show that cycling of the POM through the sands accelerates the decomposition of this organic matter. With efficient particle trapping, acceleration of degradation and fast nutrient release, the non-accumulating permeable sediments become important sites of POM decomposition, tightening the cycling of matter in the shelf (Fig.13). This could explain why organic production on the Middle Atlantic Bight shelf, where non-accumulating sandy sediments dominate, is balanced primarily by consumption on the shelf and only 2 to 20% of the primary production are exported (Bacon et al. 1994; Rowe et al. 1986; Walsh 1988).

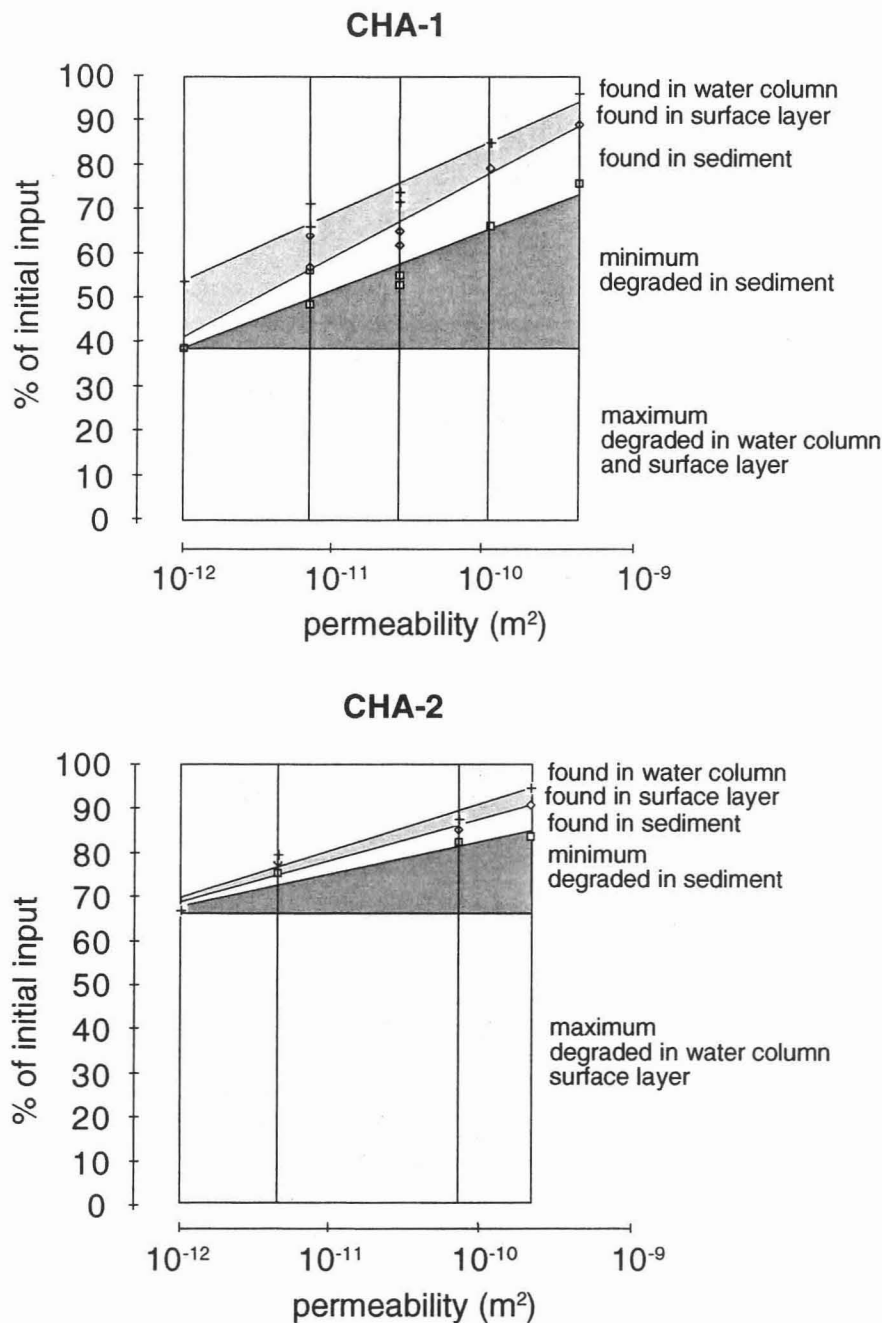


Figure 12: Cumulative plots of the chamber results given in % of initial *Dunaliella* input. The number of algae that were degraded (= disintegrated) within the sediment (dark triangular areas) is equal or larger than the difference between the total number of algae found in a chamber at the end of the experiment (upper part of plots) and the maximum number of algae that could have been degraded in water column and sediment surface of that chamber (lower part of plots). The latter number was provided by the chambers with “impermeable” bottom, where degradation in sediment subsurface layers was excluded. Because filtration reduced the number of algae in the water of the chambers with permeable sediment, the number of cells degraded in these water columns probably was smaller and certainly not larger than in the chambers with “impermeable bottom”.

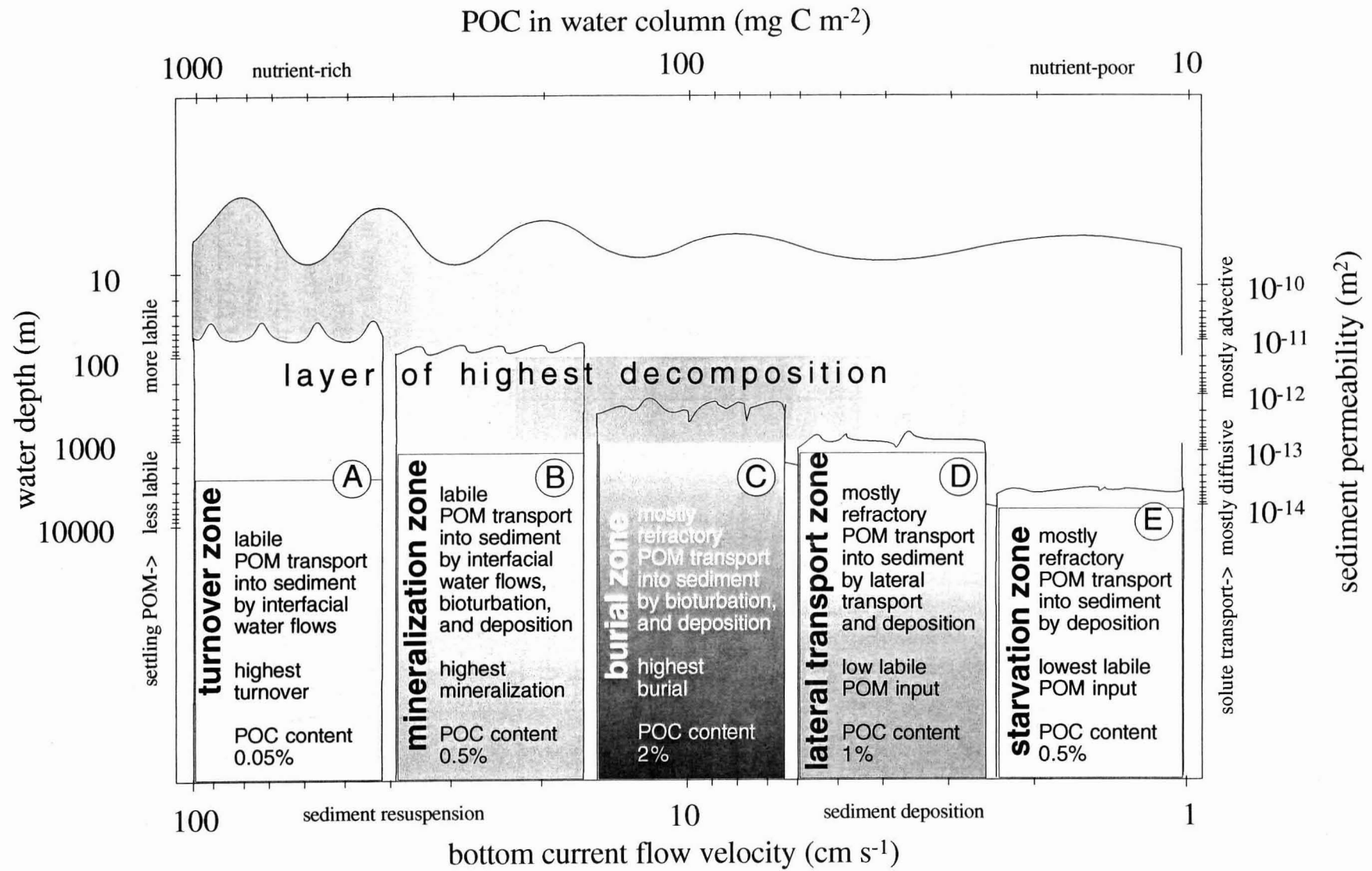


Figure 13 (previous page):

A simplified scheme of the layer of accumulation and highest decomposition of sedimenting particulate organic matter demonstrating the increasing importance of sedimentary mineralization in the shelf. The layer of highest decomposition gradually moves into the sediment with decreasing water depth. (A) In the shallow shelf wave and strong bottom currents cause frequent resuspension that keep the sediment highly permeable but also suppress bioturbation due to mechanical stress. Labile POM mixed down from the highly productive photic zone is transported deep into the sands by strong advective pore water flows. Burial of organic matter is nil due to rapid turnover promoted by the interfacial flows of oxygen-saturated water. (B) Total sedimentary mineralization peaks between the shallow non-accumulating shelf with highest turnover rates and the depocenter in the deeper shelf slope with the highest burial rates. In this zone, sporadic resuspension keeps the sediment sufficiently permeable to permit limited advective transport, but the bottom currents are weaker and allow occasional settling of organic particles and an abundant macrofauna to grow. Hydrodynamical and biological filtering and mixing mechanisms combine resulting in maximum uptake and decomposition rates of labile POM in the sediment. (C) The depocenter in the upper shelf slope receives mainly refractory organic material, and the slow bottom currents permit deposition of fine particles causing low sediment permeability. Ensuing lack of advective oxidation and reduced bioturbation promote anaerobic decomposition and highest burial rates. (D) Below the depocenter, POM input and the relative importance of the sediment for mineralization gradually decreases. Downslope POM transport gains importance. (E) Bacterial growth on sinking particulate organic matter peaks at 500 m water depth where studies of  $^{210}\text{Pb}$  reveal also the greatest break-up of particles.

*In conclusion*, we propose that permeable shelf sands are efficient POM filters and act as biocatalysts, accelerating mineralization of organic carbon and recycling of nutrients. High flushing rates, preventing the build-up of nutrients and refractory POM in the pore space, maintain their oligotrophic and non-accumulating character. Benthic primary production, however, producing up to 6-times more Chl. *a* in the surface 5 mm of the South Atlantic Bight shelf sands than the entire overlying water column (Nelson et al. 1999), indicates intensive sedimentary mineralization with high nutrient release from these beds. Non-accumulating sandy sediments that cover extensive areas of all continental margins, thus, may play an important role in the cycling of matter in the shelf.

## Acknowledgments

We thank Susanne Menger and Martina Alisch for assistance with the experimental set-ups, sampling, phytoplankton counting and chlorophyll analyses. The comments of two anonymous reviewers helped to improve the manuscript.

## 2.3. Spatial and temporal dynamics of particulate organic matter in permeable marine sands

Antje Rusch, Markus Huettel & Stefan Forster

Transport and degradation of particulate organic matter (POM) were investigated in a North Sea intertidal sandflat. Bimonthly from July 1997 to July 1998, we measured the amount of fine-grained ( $< 70 \mu\text{m}$ ) material in the permeable sand matrix, its N,  $C_{\text{org}}$  and chlorophyll content as well as porewater DIC,  $\text{NO}_x^-$  and  $\text{NH}_4^+$  concentrations. Depth profiles of fine particle concentrations indicated hydrodynamic influence down to 4 - 8 centimetres below the sediment surface. Worst case calculations on the macrofaunal contribution to particle transport resulted in a biodiffusion coefficient of  $D_B \leq 1.85 \cdot 10^{-6} \text{ cm}^2 \text{ s}^{-1}$ , implying only minor impact of bioturbation. Chl and POC contents and DIN concentrations exhibited summer/autumn and winter/spring characteristics in their profiles, revealing the seasonal importance of early diagenesis and advective transport, respectively. In the upper 5 cm, seasonal variation in the particle, POC, PN and Chl contents of the sediment was 1.4 - 5.3 times as large as below. Areal inventories of POC, PN and Chl indicated dominance of degradation and hydrodynamic removal of organic material during autumn/winter and fresh POM input throughout spring and summer. Calculations based on POC loss or short-term DIC accumulation yielded estimates of annual carbon turnover rates ranging between 55.2 and 123  $\text{g C m}^{-2} \text{ a}^{-1}$ . Possible implications of POM dynamics on the role of permeable sands in the marine carbon cycle are discussed.

## Introduction

Permeable sands, which are the dominant sediment type on continental shelves (Emery, 1968; Riedl et al., 1972), generally contain a relatively small amount of organic matter. Nevertheless, low organic carbon and nutrient concentrations in non-accumulating coastal sands may reflect high turnover rates rather than low activity (Huettel et al., 1998).

Particulate matter passes through many cycles of settling and resuspension during transport over the shelf (van Raaphorst et al., 1998), is seized by ripple migration (Jenness & Duineveld, 1985), bioirrigation and bioturbation, thus facing progressive degradation alternately by planktonic and benthic organisms. Moreover, advective co-transport of fluid and particles across the sediment-water interface is caused by the interaction of topography and bottom flows over permeable sediments (Huettel et al., 1996; Pilditch et al., 1998). The shallow coastal zone is an extremely dynamic region, where the fluid motions associated with both surface waves and currents reach down to the sea floor and interact with the bottom sediments. Recent investigations indicate that advectively accelerated solute exchange across the sediment-water interface (Lohse et al., 1996; Huettel et al., 1998) causes high oxygen consumption rates of organic-poor sands (Reimers et al., 1996) and makes early diagenetic processes in non-accumulating sediments very active and variable (Jahnke et al., 1996).

Shelf seas, especially their intertidal areas, are subject to large variations in waves, currents, temperature and salinity on the time scales of hours to months (Kristensen et al., 1997). The mineralisation of organic matter in shallow water sediments therefore can be expected to be highly variable both in time and in space (Shum & Sundby, 1996). However, little attention has been paid to the dynamics of suspended particles following interstitial flows in these sediments, so far mainly in lab experiments (Huettel et al., 1996; Pilditch et al., 1998). In natural sands, particulate organic matter (POM) constitutes the most fine-grained and easily suspendable part of the sediment and is therefore likely to follow pore water flows through the sand matrix.

We present the results of a one-year field study in an intertidal sandflat with respect to particulate organic matter (POM) dynamics. Its vertical distribution and seasonally varying composition is explained as a consequence of hydrodynamical and biogeochemical processes. Carbon turnover rates are estimated and compared to data from different marine sediments.

## Materials and methods

### *Study site*

Our study site was located in the southern North Sea near Sylt island (55°02' N, 008°26' E). Near-bottom residual currents above the sandy tidal flats of Königshafen Bay are weakly flood-dominated (Austen, 1994); semidiurnal tides have a mean range of 1.7 m (Austen, 1997), and the study site was exposed on average for 2.5 hours during low tide. Königshafen is sedimentologically relatively stable (Austen, 1994), and we found no indications of local erosion or net sedimentation during the study period. Water temperatures in this area range from -2 °C to 23 °C (Reise, 1985), salinities from 23 to 33 in winter and summer, respectively (Kristensen et al., 1997). Reise (1985) gives a more detailed description of the study area.

The study area was exposed to waves of less than 20 cm height and to currents of 0 - 0.32 m s<sup>-1</sup> (for details see Table 4), measured 2 cm above the sediment surface. Ripples of up to 2 cm height formed on the sediment surface. The upper 15-20 cm of the sediment column consisted of moderately well sorted medium to coarse quartz sand (grain size median: 400 - 750 µm),

with permeabilities ranging between  $3 \cdot 10^{-12} \text{ m}^2$  and  $20 \cdot 10^{-12} \text{ m}^2$ . Benthic macrofauna was typical for Königshafen sandflats with short exposure time at low tide, that were thoroughly studied by Reise et al. (1994). There was no benthic diatom bloom at the sediment surface.

### Sampling

Sampling dates were: 17 Jul 97, 17 Sep 97, 18 Nov 97, 13 Jan 98, 15/17/19/23/25/27 Mar 98, 12 May 98 and 7 Jul 98.

Each time, we took 8 sediment cores of 60 mm i. d., 1 core of 36 mm i. d., with core lengths of at least 20 cm, and 400 ml of overlying water. The respective sampling spots (0.5 m diameter) were chosen within a selected circular area of 4 m radius (Figure 1). All cores were carefully transported to the nearby lab and cut at depth intervals of 2.5 mm (0-1 cm depth), 5 mm (1-2 or 4 cm depth) and 10 mm (2 or 4 - 15 cm depth).

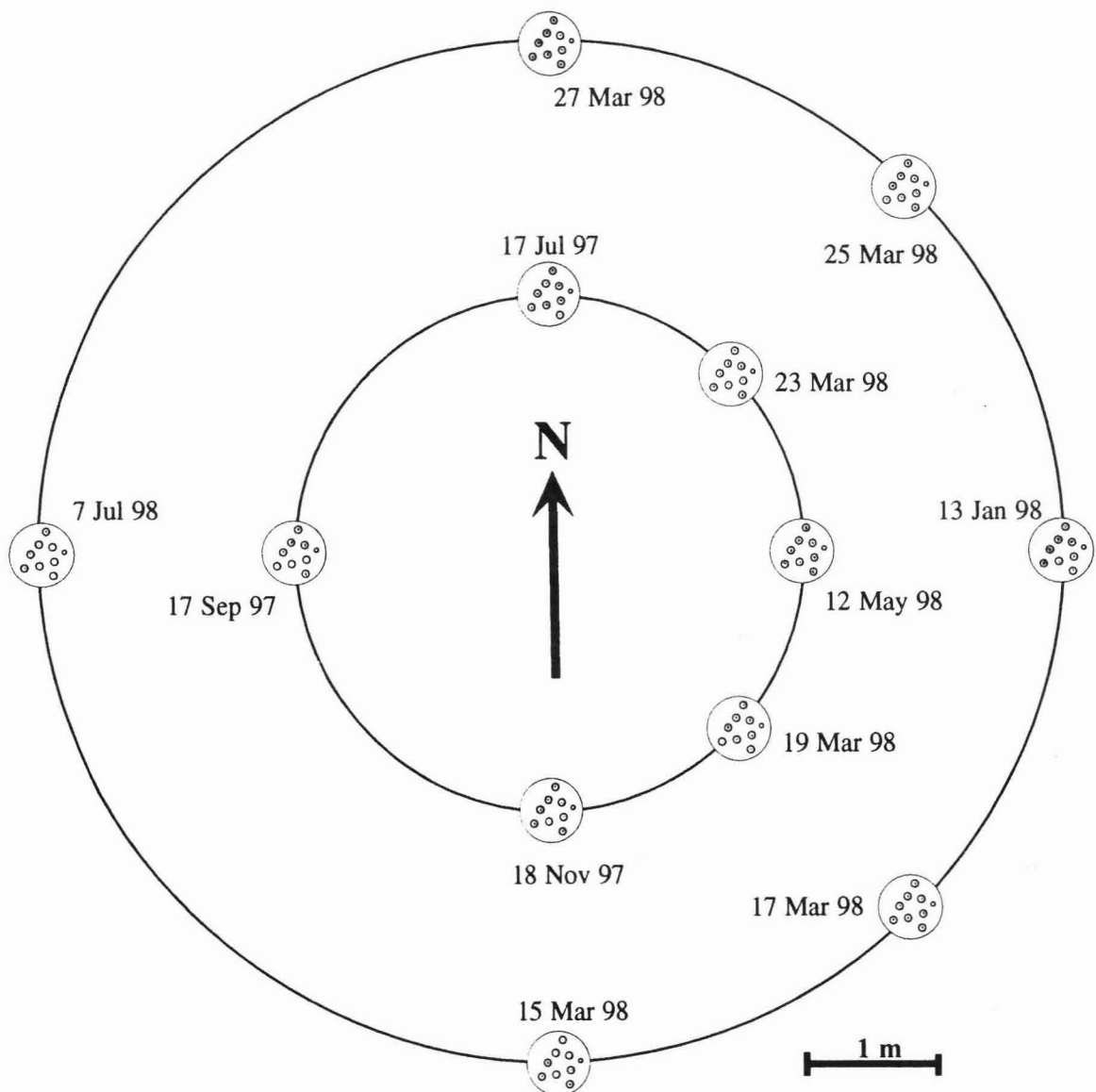


Figure 1: Study site and arrangement of the sampling spots (light shading). Dark shading: approximate arrangement of the cores within the sampling spot.

#### *Extraction of porewater*

Equivalent slices of 3 parallel cores (60 mm diameter) were pooled. Porewater was obtained by centrifugation (500·g, 10 min, 15 °C) through GF-F filters in a Beckmann TJ-6 centrifuge. Our centrifuge tubes were fabricated according to Saager et al. (1990), with minor changes to improve tightness.

For DIC analysis performed shortly after extraction, 1.5 ml aliquots of pore water were kept at 4 °C in gas-tight glass vials containing 75 µl of NaMoO<sub>4</sub> (0.5 M). Molybdate reduces the interference of dissolved sulphides (Lustwerk & Burdige, 1995). Two more 1.5 ml aliquots were stored in PE vials at -20 °C for NH<sub>4</sub><sup>+</sup> and NO<sub>x</sub><sup>-</sup> analysis.

#### *Extraction of the fine fraction*

Equivalent slices of 3 parallel cores (60 mm diameter) were pooled, carefully suspended in NaCl solution (32 g l<sup>-1</sup>, 3 ml per cm<sup>3</sup> of sediment), and allowed to settle. After 20 s, the supernatant was decanted and the remaining sediment once more retreated alike. The decanted suspensions, containing the particulate matter of an effective diameter less than 70 µm (hereafter referred to as "fine fraction"), were centrifuged (1200·g, 5 min, 15°C) using an Eppendorf 5416 centrifuge. The pellet was freeze-dried, weighed and stored at 4 °C in the dark.

#### *Porewater analyses*

Dissolved inorganic carbon (DIC) was measured using a flow-injection system according to Hall & Aller (1992). For calibration we used freshly prepared NaHCO<sub>3</sub> solutions. The detection limit was 0.05 mM, analytical precision 0.01 mM.

Ammonium concentrations were measured using a similar flow-injection system (Hall & Aller, 1992), with NH<sub>4</sub>Cl solutions serving as calibration standards. The detection limit was 2 µM, the analytical precision 0.05 µM.

NO<sub>x</sub><sup>-</sup> (nitrate/nitrite) was determined by vanadium (III) reduction at 80 °C and subsequent chemiluminescence detection (Braman & Hendrix, 1989). We used a Thermo Environmental Instruments 42C NO<sub>x</sub>-analyser and a HP3395 peak integrator. The detection limit was 1 µM, and replicates agreed within 2%.

#### *Solid phase analyses*

Particulate carbon (PC) and nitrogen (PN) contents were measured using a Fisons NA1500N elemental analyser with sulphanilamide as calibration standard. For particulate organic carbon (POC) determination, samples were pre-treated with 6N HCl for 15 min, washed twice with distilled water and dried. Weight loss by this pre-treatment was calculated assuming complete conservation of nitrogen, and POC contents were corrected accordingly.

For chlorophyll analyses, we prepared extracts from the fine fraction by dark incubation with 90% acetone at 4 °C for 16 h and subsequent centrifugation (1620·g, 7 min, 4 °C) using a Heraeus Metafuge 1.0 R. The supernatant was syringe-filtered through 0.45 µm pores (Nalgene 199-2045 PTFE). Chlorophyll equivalent concentrations were determined fluorimetrically without acidification using a Hitachi F-2000. For calibration, we used solutions of Chl a in 90% acetone.

### *Auxiliary measurements*

Daily data on the local weather conditions throughout 1997 and 1998, in particular wind speed and air temperature, were kindly provided by Deutscher Wetterdienst (DWD).

On all sampling days we recorded the temperatures of air, water and sediment at the sampling site. Current velocities 2 cm above the sediment surface were measured 1-1.5 h before low tide using a Schiltknecht turbine anemometer.

Throughout the study period, Königshafen Bay was monitored with respect to phytoplankton cell numbers and species as well as Chl concentrations in the water column. P. Martens (BAH Wadden Sea Station, Sylt) kindly placed these unpublished data at our disposal.

Smear-slides of the fine fraction were prepared according to Haq & Boersma (1978) using filtered Balsam Canada as fixative. We inspected them by light microscopy to qualitatively survey the types of fine particles found in the sediment samples.

## Results

### *Fine fraction*

The fine fraction extracted from the cores consisted mainly of silt-sized quartz grains, detritus, and fragments of diatom and foraminifera shells.

As an overall feature of the depth profiles of fine particles, we observed high concentrations at the very surface, a minimum mostly located between 1.0 and 2.5 cm depth, and a further maximum in 4 to 8 cm depth, in most cases close to the visually localised redox horizon (Table 1). The bandwidth of concentrations within a profile amounted to 42 - 87 % of the corresponding maximum value, and gradients from the minimum both towards smaller and towards greater depths were steep (Table 1). A Wilcoxon matched pairs signed rank test (Sachs, 1997) was applied to reveal significant differences between fine fraction concentrations in the depth intervals selected according to the profile characteristics described above. The results are summarised in Table 2.

	depth of minimum cm	depth of maximum cm	redox horizon cm	gradient downwards mg cm <sup>-4</sup>	gradient upwards mg cm <sup>-4</sup>	(max-min)/max
17 Jul 97	0	4 - 5	5	4.45	n. a.	0.67
17 Sep 97	1.5 - 2.0	4 - 5	3.5	3.55	6.67	0.65
18 Nov 97	0.75 - 1.0	7 - 8	3.5	1.18	4.29	0.55
13 Jan 98	3 - 4	5 - 6	5	7.38	2.36	0.87
March 98	0.5 - 2.5	5 - 8	4 - 9	1.85	2.01	0.82
12 May 98	1.5 - 2.0	3.5 - 4.0	3	58.4	n. a.	0.87
7 Jul 98	3.0 - 3.5	4 - 5	8	17.0	6.10	0.42

Table 1: Columns 2-4: Location of minimum and maximum fine particle concentrations compared to the depth of changing sediment colour (visual redox horizon). Columns 5 and 6: Concentration gradients downwards (from the minimum towards the maximum below) and upwards (towards the sediment surface), respectively. Last column: Relative bandwidth of concentrations in the profile.

	1.0 - 2.5 cm	2.5 - 5 cm	4 - 5 cm	5 - 10 cm	10 - 15 cm	5 - 15 cm
0 - 0.25 cm	n. s.					
0 - 1.0 cm	n. s.					
1.0 - 2.5 cm	-	0.1 %	0.1 %			
2.5 - 5 cm		-	n. s.	1 %	n. s.	n. s.
4 - 5 cm			-	n. s.	n. s.	n. s.
5 - 10 cm				-	n. s.	

Table 2: Results of Wilcoxon matched pairs signed rank test applied to fine particle concentrations in different depth intervals. Percentages specify the level of significance; n.s.: not significant ( $\alpha > 5\%$ ).

### Impact of bioturbation

Bioturbating macrofauna species found in the sliced cores were *Nereis* spec. and *Scoloplos armiger*. Additionally, not more than 1 lugworm (*Arenicola marina*) per sampled area ( $0.24 \text{ m}^2$ ) was present. In March 98, wet-sieved sediment contained  $647 \text{ ind m}^{-2}$  *Nereis*,  $117 \text{ ind m}^{-2}$  *Scoloplos* and  $< 11 \text{ ind m}^{-2}$  *Arenicola*. Judged from the species occurring during the study period, their approximate abundances in spring, organic content, grain size and exposure time of the sediment, our study site belonged to a habitat type covering about 50 % of intertidal Königshafen Bay (Reise et al., 1994). Macrofaunal biomass data from that more comprehensive study were used for the following calculations, constraining biological particle transport.

Species-specific biodiffusion coefficients at  $15 \text{ }^\circ\text{C}$  and the corresponding biomasses were taken from Huettel (1988). Conversion based on the biomasses given by Reise et al. (1994) resulted in biodiffusion coefficients of  $D_B(\textit{Arenicola marina}) = 1.43 \cdot 10^{-6} \text{ cm}^2 \text{ s}^{-1}$ ,  $D_B(\textit{Nereis diversicolor}) = 0.18 \cdot 10^{-6} \text{ cm}^2 \text{ s}^{-1}$ , and  $D_B(\textit{Scoloplos armiger}) = 0.24 \cdot 10^{-6} \text{ cm}^2 \text{ s}^{-1}$ .

The particle flux ( $J$ ) is related to porosity ( $\varphi$ ), biodiffusion coefficient ( $D_B$ ) and the vertical component of the particle concentration gradient ( $\frac{\partial}{\partial z} B$ ) by Equation 1 (Boudreau, 1997):

$$J = -(1 - \varphi) \cdot D_B \cdot \frac{\partial}{\partial z} B \quad (\text{Equation 1})$$

With  $\varphi = 0.34$  and  $\frac{\partial B}{\partial z} \approx 6 \text{ mg cm}^{-4}$  in our study, biogeochemical transport of fine particulates accounted for  $J = 6.33 \text{ g m}^{-2} \text{ d}^{-1}$ . The amount of fine particles in the top 5 cm varied between  $146 \text{ g m}^{-2}$  in winter and  $2533 \text{ g m}^{-2}$  in summer. To accumulate the difference within half a year, a net particle flux of  $13.1 \text{ g m}^{-2} \text{ d}^{-1}$  was needed. Less than half of it could be explained by biogeochemical transport.

*Biogeochemically labile components*

To characterise the composition of the fine fraction, we measured its Chl content and C:N (w/w) ratio. The summer and autumn chlorophyll equivalent concentration profiles (Figure 2: Jul 97, Sep 97, Nov 97, May 98, Jul 98) could in major parts be described by the following equation:

$$[\text{Chl}](z) = [\text{Chl}]_0 \cdot e^{-\lambda \cdot z} \quad (\text{Equation 2})$$

with  $[\text{Chl}]_0$ : content at sediment surface,  $z$ : depth and  $\lambda$ : decay constant. Constants and correlation coefficients for the best fits are given in Table 3.

The winter and spring  $[\text{Chl}]$  profiles (Figure 2: Nov 97, Jan 98, March 98) were shaped differently: Relatively Chl-rich material penetrated down to 5 - 9 cm depth, below contents rapidly dropped to background values. Chl contents were highest in the depth interval of minimum C:N ratios. We consider the Nov 97 profiles intermediate between the "summer shape" and the "winter shape".

C:N ratios of the fine fraction ranged between 7.5 and 11, in the sediment total between 14 and 36.

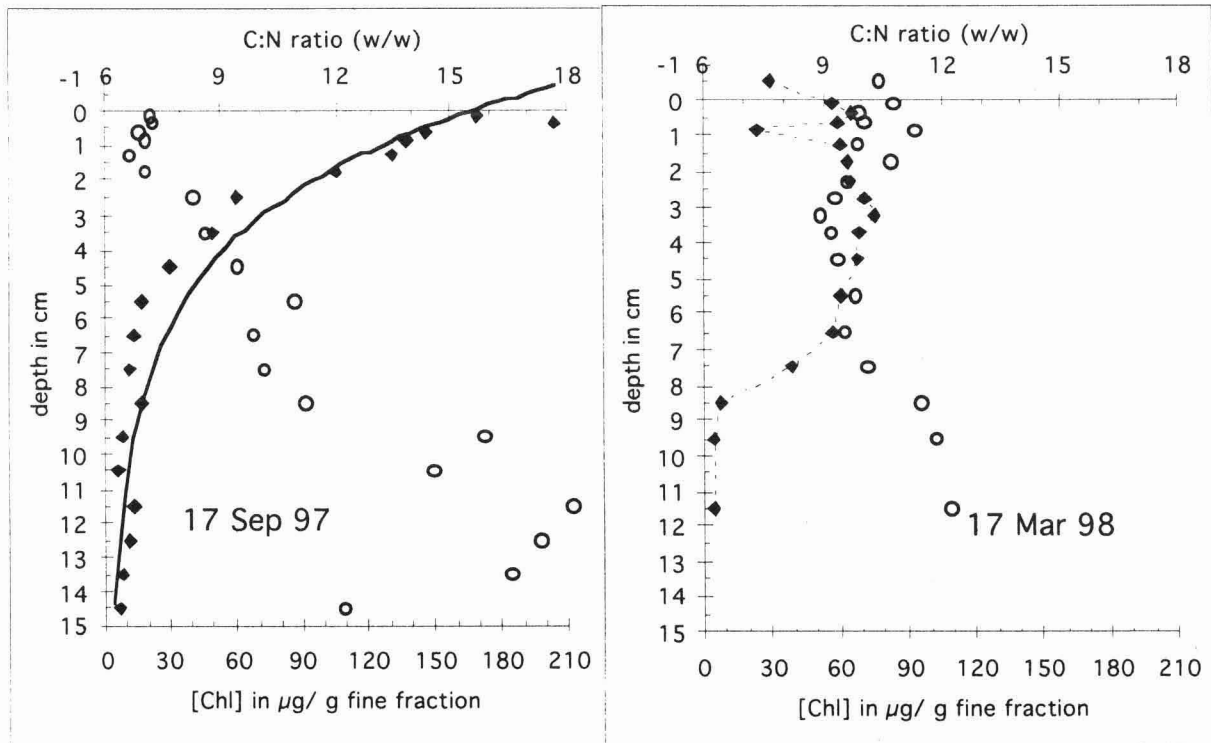


Figure 2: Depth profiles of Chl content (diamonds) and C:N ratio (circles) of the fine fraction. Left: summer/autumn, represented by 17 Sep 97; right: winter/spring, represented by 17 Mar 98. The complete data set for all profiles is available from the authors.

	[Chl] <sub>0</sub> in $\mu\text{g g}^{-1}$	$\lambda$ in $\text{cm}^{-1}$	$R^2$	
17 Jul 97	259	0.207	0.9532	
17 Sep 97	164	0.278	0.8607	
18 Nov 97	176	0.175	0.9233	$z > 2.5 \text{ cm}$
12 May 98	102	0.269	0.8240	$z > 1.5 \text{ cm}$
7 Jul 98	141	0.222	0.9831	$z \leq 6 \text{ cm} \vee z \geq 11 \text{ cm}$

Table 3: Parameters of the summer/autumn [Chl] profile fits according to Equation 2: surface concentration, decay constant, correlation coefficient. Last column: depth interval, if not all data were included.

### Carbon

The fine fraction was  $47.5 \pm 34.4$  ( $n = 15$ ) times as rich in POC (by weight) as the sediment it was extracted from. It contained ( $28.2 \pm 28.3$ )% of the sedimentary organic carbon.

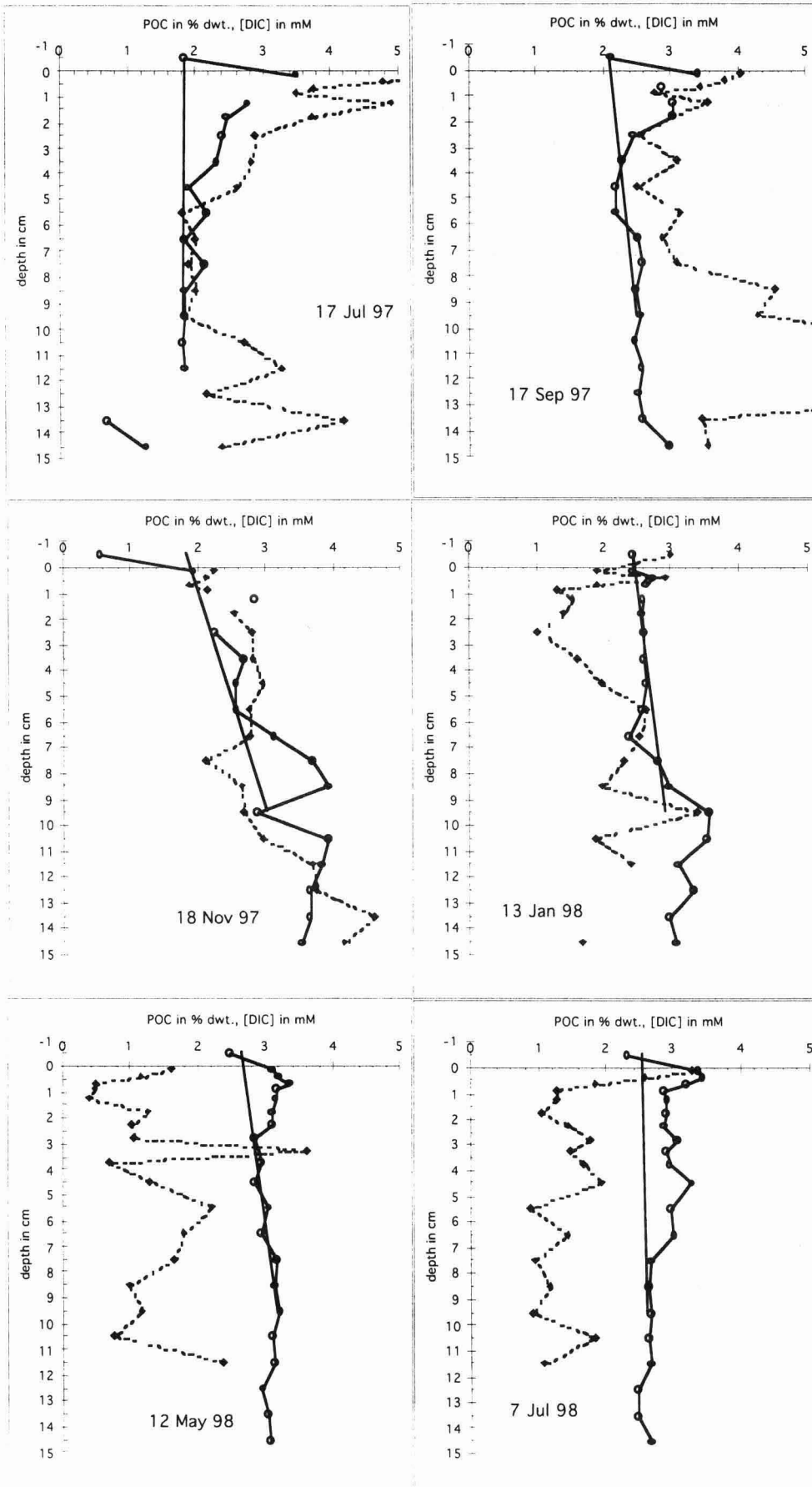
In Figure 3a/b, fine POC as the starting-point of decomposition is opposed to pore water DIC as its final product. Most DIC profiles could be described as the superposition of linear increase with depth and a local, cap-shaped surplus within the top 5 cm. The slope of the gradient and the depth-integrated size of the cap varied seasonally.

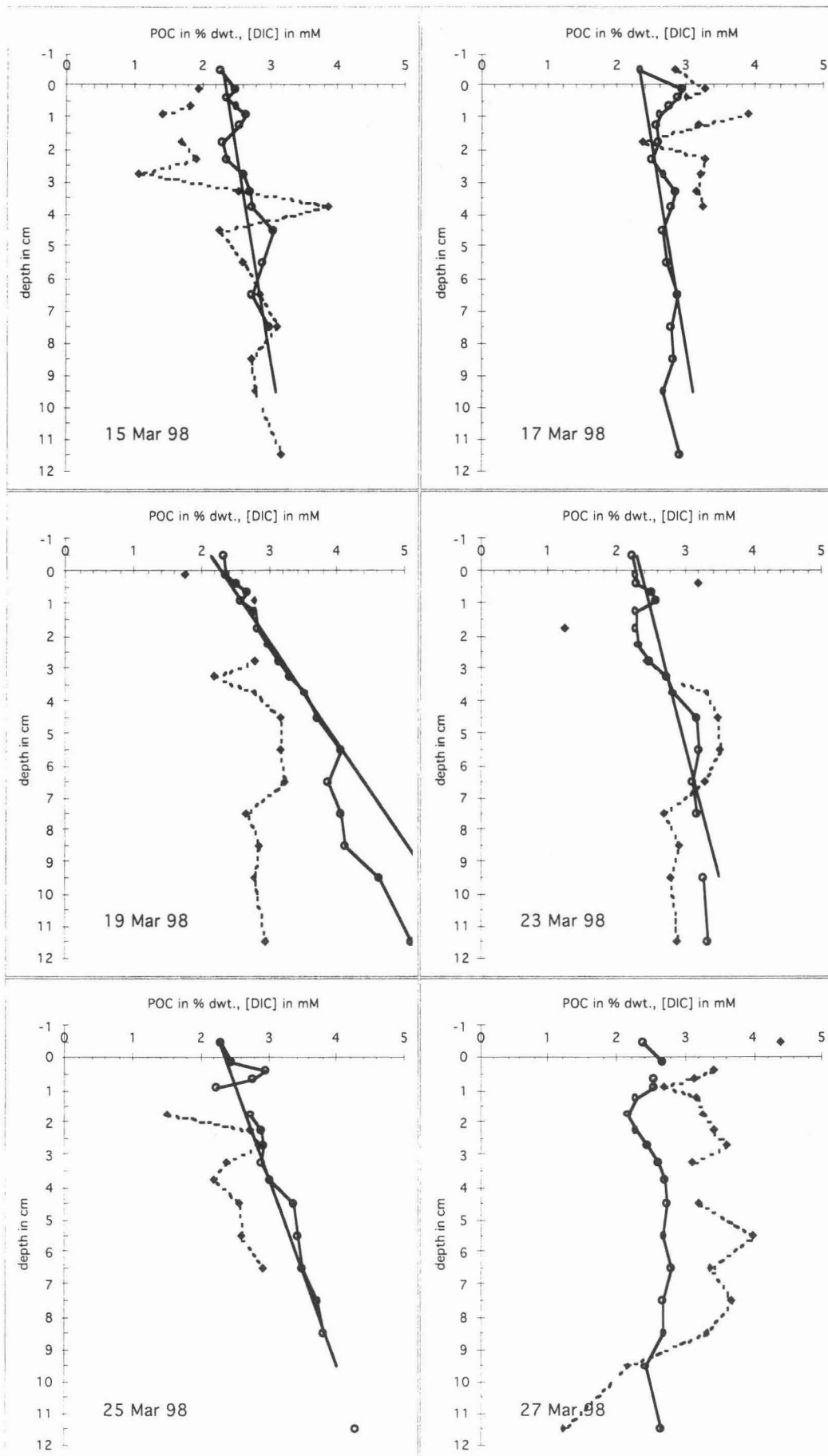
POC contents markedly decreased towards greater depths in summer and autumn (Fig. 3a: Jul 97, Sep 97, May 98, Jul 98), whereas in winter and spring (Fig. 3a: Nov 97, Jan 98, Fig. 3b) they appeared constant or slightly increasing with depth. In the May profile, the value in 11-12 cm depth was an outlier due to locally higher amounts of fine particles, that were rich in POC and PN, but poor in Chl. As a common feature of all POC profiles we observed a minimum within the uppermost 2-3 cm.

Figure 3 (following pages): Depth profiles of POC content of the fine fraction (diamonds) and pore water DIC concentration (circles). Bold lines: supposed DIC gradient.

a (p. 56): Jul 97 through Jan 98, May 98, Jul 98

b (p. 57): March 98





### Nitrogen

The fine fraction was  $19.1 \pm 10.4$  ( $n = 94$ ) times as rich in nitrogen (by weight) as the sediment it was extracted from. It contained  $(12.3 \pm 11.3)\%$  of the sedimentary nitrogen.

Figure 4 compares the profiles of different nitrogen species: fine particulate nitrogen (PN), oxidised DIN (nitrate/nitrite) and reduced DIN (ammonium). As examples for the summer and winter situation we show Sep 97 and 17 Mar 98, respectively.

In general, there was a slight decrease in the PN content of the fine fraction below 5 cm depth. Temporal changes virtually affected only the top 5 cm. Minimum PN contents were mostly found in the uppermost 2 cm.

Except for occasionally a very narrow peak in the top 1-2 cm, pore water nitrate/nitrite ( $\text{NO}_x^-$ ) concentrations during summer and autumn were mostly below  $5\text{--}10 \mu\text{M}$  throughout the sediment column and overlying water. Comparatively high concentrations of up to  $70 \mu\text{M}$   $\text{NO}_x^-$  were recorded in winter and spring, with pore water profiles appearing dominated by oxidant supply from and DIN release into the water column.  $\text{NO}_x^-$  penetration as well as  $\text{NH}_4^+$  removal reached down to 3 to 8 cm depth.

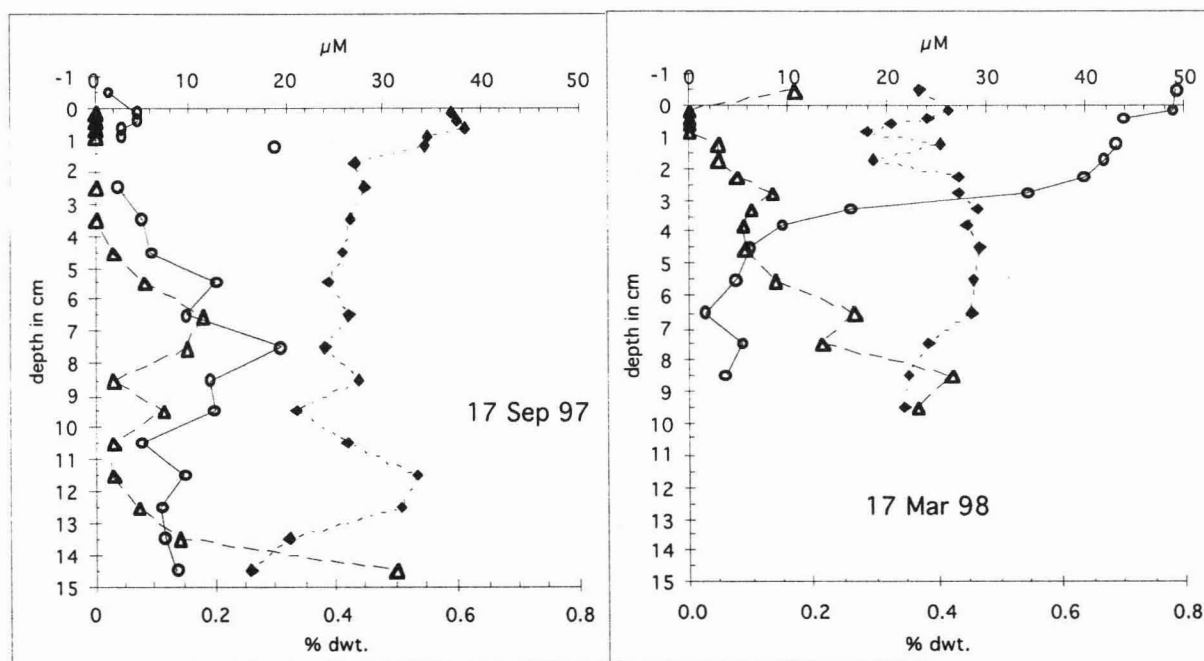


Figure 4: Depth profiles of PN content of the fine fraction (diamonds) and pore water DIN concentrations ( $\text{NO}_x^-$ : circles;  $\text{NH}_4^+$ : triangles). Left: summer/autumn, represented by 17 Sep 97; right: winter/spring, represented by 17 Mar 98.

### *Seasonal variation*

The phytoplankton and weather conditions for each sampling date are compiled in Table 4. Throughout the year, only minor changes occurred below 5 cm depth, whereas above marked seasonal variation was observed in the profiles of fine particulates, POC, PN, and Chl, with contents decreasing from summer 97 to winter and increasing again until summer 98. The mean contents between 5 and 10 cm depth over all seasons amounted to  $(13.6 \pm 5.0) \text{ mg cm}^{-3}$  ( $n = 46$ ) for the fine fraction,  $(363.2 \pm 88.5) \mu\text{g cm}^{-3}$  ( $n = 55$ ) for POC,  $(48.2 \pm 19.4) \mu\text{g cm}^{-3}$  ( $n = 25$ ) for PN, and  $(0.409 \pm 0.411) \mu\text{g cm}^{-3}$  ( $n = 51$ ) for Chl. In the following, these values are referred to as the refractory part of the respective material. We defined a dimensionless "relative amplitude" according to Equation 3:

$$\text{relative amplitude} := \frac{\text{summer content} - \text{winter content}}{\text{refractory part}} \quad (\text{Equation 3})$$

with winter meaning Jan 98 and summer the mean of Jul 97 and Jul 98. The resulting depth profiles of the relative amplitudes are compared in Figure 5. The amount of fine particles did not vary significantly more in the upper 5 cm than below ( $\alpha > 5 \%$ , Lord test; Sachs, 1997). By contrast, the relative amplitude of POC and PN contents abruptly and significantly decreased at 5 cm depth ( $\alpha < 1 \%$ , Lord test), with the variation of PN generally exceeding that of POC. The most pronounced seasonality was found in Chl contents, with relative amplitudes of up to 12 near the surface. Unlike the other parameters, Chl amplitudes decreased with depth rather exponentially than abruptly at a certain depth. Significant differences between the depth intervals 0-1 cm and 1-5 cm were found for Chl ( $\alpha < 1 \%$ ), but not ( $\alpha > 5 \%$ ) for fine particle, POC and PN amplitudes (Lord test).

The contents of POC, PN and Chl in the upper 5 cm exceeding the refractory part were integrated separately for each sampling date (March: mean). The resulting areal inventories are listed in Table 5. The pool sizes gradually decreased from summer 97 until Jan 98 and afterwards increased again. Negative inventories show that not only labile, but also part of the refractory organic matter was removed during winter.

### *Mineralisation rates*

Annual carbon mineralisation rates of the studied sandy sediment were calculated using 4 different approaches, A-D. In approach A, the loss of POC between maximum inventory in summer and minimum inventory in winter was divided by 0.5 years, resulting in  $55.2 \text{ g C m}^{-2} \text{ a}^{-1}$  (summer: Jul 97) or  $63.7 \text{ g C m}^{-2} \text{ a}^{-1}$  (summer: Jul 98). More elaborate approaches treated each DIC profile separately, integrating the amount of accumulated mineralisation product in the way schematically illustrated in Figure 6. Considering sea water penetration down to 5 cm depth, there was a DIC background to be deducted from the total amount in the uppermost 5 cm. Annual mean ( $2.26 \text{ mM} \pm 0.16 \text{ mM}$ ) and momentary sea water DIC concentrations were used in approach B and C, respectively. In approach D, the DIC gradient (Figure 3 a/b) concentrations were regarded as background, and only the superimposed surplus DIC was depth-integrated. We assumed that the maximum time for DIC accumulation was the span between highest near-bottom tidal current velocity in the first third of the flood cycle (Austen, 1994) and sampling, i.e. 7 h, used in the calculation. The rates obtained that way for every second month were integrated over the year, yielding annual rates of  $123 \text{ g C m}^{-2} \text{ a}^{-1}$  (B),  $116 \text{ g C m}^{-2} \text{ a}^{-1}$  (C) and  $75 \text{ g C m}^{-2} \text{ a}^{-1}$  (D), respectively.

	wind speed (daily mean)	current speed	T (air)	T (water)	[Chl] (water)	algal cells	recent development
	m s <sup>-1</sup>	m s <sup>-1</sup>	°C	°C	µg dm <sup>-3</sup>	cm <sup>-3</sup>	
17 Jul 97	7.3		15.9	17	40.7	56	T constant, wind rising, start of bloom ( <i>Rhizosolenia imbricata</i> )
17 Sep 97	9.0	0.24	14.1	14	64.4	103	gradually calming and cooling, shortly after bloom ( <i>Chaetoceros spec.</i> )
18 Nov 97	10.8	0.13	3.4	4	68.7	16	after mild weather suddenly stormy and colder
13 Jan 98	4.7	0.21	4.3	2	34.7	26	T constant, wind unsteady
March 98							T and wind unsteady, spring bloom ( <i>Brockmanniella brockmannii</i> , <i>Skeletonema costatum</i> )
15 Mar 98	6.8	0.15	5.7	4			
17 Mar 98	6.7	0.05	5.9	5			
19 Mar 98	10.4	0.12	5.1	6			
23 Mar 98	9.1	0.16	3.0	8	107.7	805	
25 Mar 98	7.2	0.07	5.9	3			
27 Mar 98	7.1	0.07	7.0	5	96.7	511	
12 May 98	8.5	0.10	13.2	13	51.7	121	wind rising, start of bloom ( <i>Phaeocystis globosa</i> )
7 Jul 98	11.2	0.17	12.0	12			slowly calming after gale

Table 4: Weather conditions at each sampling date. Wind speed, air temperature: data provided by Deutscher Wetterdienst (DWD). Phytoplankton, water column Chl concentrations: data provided by P. Martens. Current speed, water temperature: own measurements, 1-1.5 h before low tide, 2 cm above the sediment surface.

	inventory (0 - 5 cm) in µg cm <sup>-2</sup>		
	POC	PN	Chl
17 Jul 97	1349	279	11.4
17 Sep 97	-303	-2	2.2
18 Nov 97	-507	-78	2.6
13 Jan 98	-1411	-175	-1.1
March 98	-1137	-151	-0.8
12 May 98	874	72	5.4
7 Jul 98	1774	344	17.2

Table 5: Areal inventories of POC, PN and Chl in the top 5 cm of the sediment, refractory part deducted.

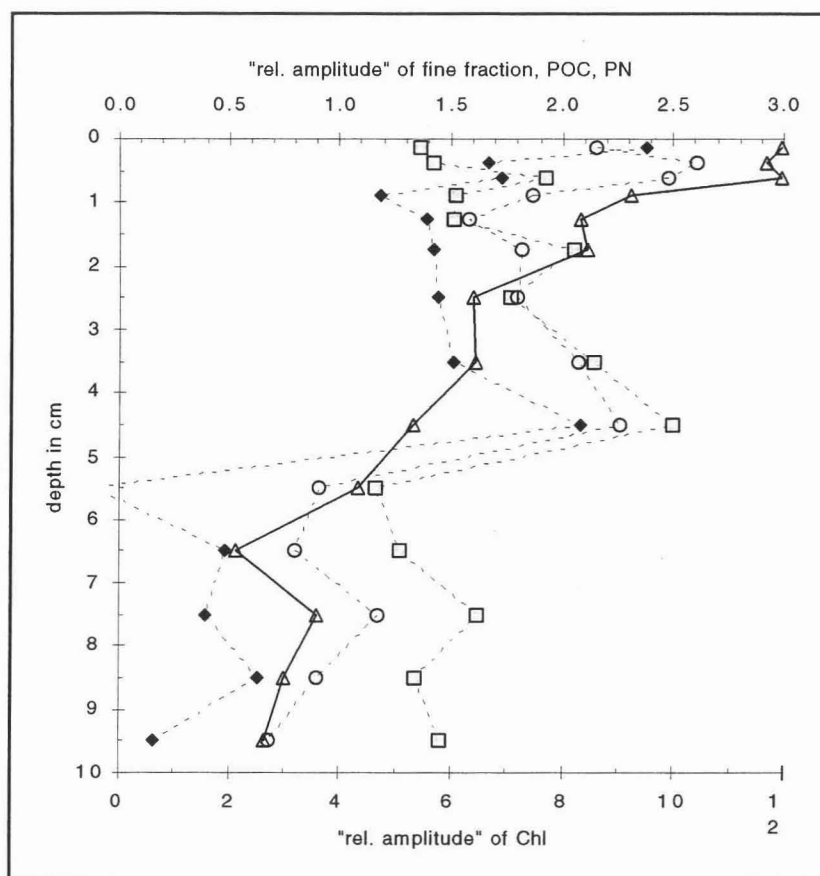


Figure 5: Depth profiles of the "relative amplitude" (defined by Equation 3) of fine particle (squares), POC (diamonds), PN (circles) and Chl (triangles) concentrations in the sediment.

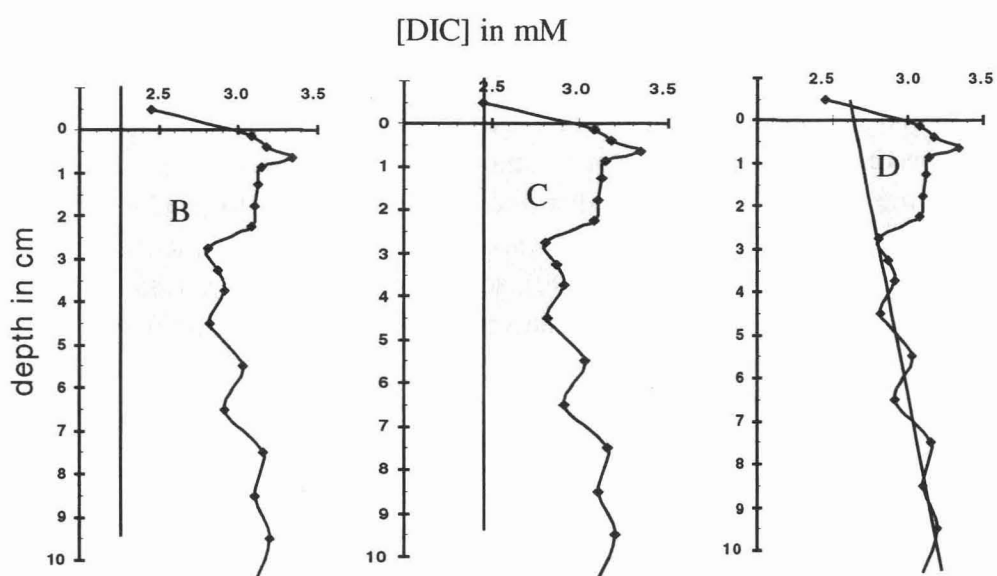


Figure 6: Schematic of the DIC integration approaches B (left), C (centre) and D (right).

## Discussion

The studied marine sediment was exposed to near-bottom currents, and its relatively high permeability facilitated hydrodynamic influence down to 4-8 cm depth. The sediment colour suggested, that there was sufficient pore water flushing to keep the upper 3.5-9 cm of the sediment oxidised. This reach of pore water exchange was in many cases close to the horizon of maximum concentration of fine particles (Table 1). With concentrations in 2.5-5 cm depth significantly lower than in 5-10 cm depth (Table 2), we state that not only pore water but also small particles were hydrodynamically removed from the sediment. The closer to the surface, the more material was displaced by advective flows or waves propagating into the sediment. Fine particle concentrations were significantly lower in 1.0-2.5 cm depth than below (Table 2). By contrast, the uppermost centimetre was affected by surface deposition, ripple migration, erosion/redeposition cycles, microphytobenthic colonisation etc., and due to this mixed influence, no significant overall feature of the top layer could be detected (Table 2). Individual profiles, though, could be qualitatively related to short-term weather changes (Table 4). During increases in wind speed - generally related to rougher seas - the top cm of the sediment was poor in fine fraction. With wind and water calming, recently suspended material re-entered the uppermost sediment layers.

Shallow water sediments are often densely populated by macrofauna (McCall & Tevesz, 1982; Wheatcroft et al., 1990; Marinelli & Boudreau, 1996), so bioturbation is expected to contribute to particle transport across the water-sediment interface. For that reason, we chose a study site that belonged to an intertidal habitat type lowest in macrofauna abundance and biomass within Königshafen, except for some sandbars (Reise et al., 1994). Interannual biomass variabilities of North Sea intertidal communities are about 10-30 % (Beukema et al., 1993; Reise et al., 1994), low enough to base our rough estimate of biogenic particle transport on older data from the same location. According to these data, more than 3/4 of the calculated biodiffusion was due to *Arenicola marina*, however, as throughout the study period we observed lower lugworm densities than Reise et al. (1994), the biodiffusive fine particle flux may be overestimated. As commonly found in literature, our worst case calculations were based on bioturbation modelled as a diffusive process acting along concentration gradients. Although deposit feeding moves particles in a rather non-local manner (e. g. conveyor-belt-like), non-diffusive mechanisms of sediment displacement can combine to produce apparently diffusive profiles (Wheatcroft et al., 1990). In most shallow water environments, mixing rates exceed  $0.32 \cdot 10^{-6} \text{ cm}^2 \text{ s}^{-1}$  (Wheatcroft et al., 1990), so our estimate of  $D_B \leq 1.85 \cdot 10^{-6} \text{ cm}^2 \text{ s}^{-1}$  was in a typical range. Notwithstanding this relatively high biodiffusion coefficient, less than half of the net particle flux could be attributed to biogenic transport. We therefore conclude that in our study physical transport processes had a stronger impact than macrozoobenthos.

Compared to the sediment total, the fine fraction was distinguished as markedly richer in  $C_{\text{org}}$  and N and having smaller C:N ratios. Fresh organic matter preferentially associated with the silt and even more with the clay fraction has been reported of various marine sediments (Bordovskiy, 1965; Tanoue & Handa, 1979; de Flaun & Mayer, 1983; Wiesner et al., 1990; Anton et al., 1993; Mayer, 1994; Lohse et al., 1995). In sandy sediments, fine particles are subject to intense dynamics, because they represent not only the biogeochemically labile fraction, but at the same time also the most mobile part of the sediment. At our study site, 28% of the organic carbon and 12 % of the sedimentary nitrogen were associated with the easily moveable fine particles, that comprised ca. 1% (v/v) of the sediment. The remaining organic material was adsorbed to the coarse sand matrix and therefore moved much less.

Moreover, it could be partly sheltered from microbial degradation by the microtopography of the sand grains (Mayer, 1994). Considering mobility and bioavailability, the adsorbed fraction of organic matter contributed less to the spatial and temporal dynamics we observed than the fine particles. In winter and spring, relatively strong currents caused advective flow through the permeable, rippled sediment, carrying labile POM from the water column down to 5 - 9 cm depth (Figure 2), where retention and adsorption (Huettel et al., 1996) trapped the fine particles. As temperatures and benthic activity were still low at that time of the year, the freshly entered material was decomposed relatively slowly. During summer and early autumn, though, increased degradation activity and moderate current velocities reduced the net penetration of labile POM (Figure 2).

The spatial and temporal variability observed in the POC contents and DIC concentrations (Figure 3 a/b) reflected carbon mineralisation that depended on seasons and sediment depth. In summer, POC contents decreased with depth by the combined effects of organic-rich particle input from the surface and intense degradation in deeper layers. In winter, with particle supply poorer in organics and sedimentary decomposition slowed down, POC contents stayed constant with depth. Gradients in the DIC profiles were influenced by diffusive and advective export counteracting production by fermenting and mineralising bacteria. A balanced situation in summer 1997, with gradients almost vertical, gave way to a gradually increasing dominance of DIC removal, indicated by a marked decrease of concentrations towards the sediment surface. During spring and summer 1998, the transport/production steady state equilibrium gradually re-established. The most variable part of our sediment column were the uppermost 2-3 cm, characterised by a POC minimum and DIC maximum (Figure 3 a/b) as well as a PN minimum (Figure 4). Benthic microbial activity appeared especially high in this horizon as fuelled by recurrent supply of both labile organic matter and oxidants from the water column. Moreover, possible inhibition by metabolic end products could be minimised by advective removal. Remarkably, bacterial counts from the same site (unpubl. data) supported that the microbiologically most active zone was not at the very surface. Bacteria living close to the water-sediment interface experience strong mechanical stress due to harsh hydrodynamic conditions and grazing by meiofauna, making the top centimetre unfavourable to dwell in in spite of optimal food supply.

The narrow  $\text{NO}_x^-$  peaks close to the water-sediment interface, occasionally occurring in the summer and autumn profiles (Figure 4), were probably related to single ragworms (*Nereis* spec.). These polychaetes stimulate subsurface nitrification in their burrow walls (Kristensen & Blackburn, 1987; Huettel, 1988). Apart from the *Nereis*-caused peaks, the summer and winter DIN profiles (Figure 4) were basically similar to those obtained by Lohse et al. (1993) at a North Sea coastal station with a fine sandy bottom as organic-poor as our study site. In summer, subsurface nitrification rates and interfacial DIN fluxes were high (Lohse et al., 1993), providing nutrients for primary production and electron donors for OM mineralisation. As nitrification appears more strictly limited by ammonium availability than by oxygen penetration, lower nitrification rates were measured in winter (Lohse et al., 1993). Neither primary production (Table 4) nor OM mineralisation were major nitrate sinks during winter and early spring, so  $\text{NO}_x^-$  could accumulate in spite of relatively slow production. Deep-reaching exchange of oxygen and DIN with the water column, in the cold season favoured by particularly strong currents and high permeabilities, closely linked benthic and pelagic nitrogen turnover.

Seasonally varying extents of hydrodynamic and biogeochemical influences became obvious in the effects on the labile fine fraction (Figure 2), POC/DIC (Figure 3 a/b) and PN/DIN profiles (Figure 4), with a rather physically dominated winter situation and a microbiologically dominated summer situation. Direct and indirect impacts of medium-term weather changes (Table 4) affected mainly the top 5 cm, whereas below the sediment approached steady-state conditions, indicated by small seasonal amplitudes (Figure 5). Relative amplitudes of concentrations decreased in the order Chl > PN > POC > fine fraction in accordance with the order of biochemical lability. A higher temporal resolution applied to the areal inventories of Chl, PN and POC (Table 5) revealed the net potential of OM mineralisation. These 3 time series coherently showed a continuous net removal of POM from the sedimentary pool throughout the second half of 1997, as well as the net accumulation of freshly entered POM during spring and summer 1998. Early diagenesis could remove labile POC/PN/Chl until only the refractory background was left, corresponding to a labile matter inventory of zero. Negative areal inventories (Table 5), however, cannot be due to degradation alone, but require an additional explanation for the removal of POM from the sediment. We suggest particle efflux by resuspension and/or advective processes.

Interannual variation, roughly estimated from the differences in pool size between Jul 97 and Jul 98, was small compared to the seasonal variation (Table 5), thus making the results of our one-year study to some extent transferable to other years. Model simulations of the North Sea, significantly and reliably supported by field data, have clearly shown annual cycles with strong seasonal variation, both in the water column (Pätsch & Radach, 1997) and in pore water profiles and interfacial fluxes (Ruardij & van Raaphorst, 1995). Interannual variation in the past decades has been mainly related to long-term developments like climate changes (Kröncke et al., 1998) or anthropogenic eutrophication of the coastal region (Pätsch & Radach, 1997). Thus, pronounced seasonality with medium-term steady-state is not an exclusively intertidal feature, but also holds for the subtidal part of the North Sea as a shelf sea of the temperate climate zone.

Life in our sandflat had to cope with an environment variable both in time and in space. Below 5 cm depth, conditions changed only slightly and slowly, and a constantly small bacterial population fed on rather refractory POM or depended on occasional DOM supply from above. The zone between 1 and 5 cm depth was characterised by steep gradients (Table 1) and strong seasonal variation (Figure 5), and tight coupling to the water column made an affluent living for many microbes. They may have spent the winter in a relatively inactive stage and could quickly adapt to changing conditions. The most unsteady part of the sedimentary ecosystem was the uppermost centimetre, directly affected by all consequences of exposure and flooding of the intertidal flat. Free-living bacteria oscillated between benthic and pelagic life, and those attached to sand grains were constantly moved by resuspension/redeposition and ripple migration. Permanent mechanical stress marred a life of optimal food supply and dispersal. Borrowing terms from microbial ecology, *r* strategists may inhabit the top layer, whereas below 5 cm depth *K* strategists may dominate. With increasing water depth, these ecological implications decreasingly apply to subtidal and non-shelf regions due to decreasing tidal, seasonal and hydrodynamic influence on the sea floor.

Since advective transport enhances the oxygen utilisation of permeable sediments, particularly when easily degradable organic carbon is available (Forster et al., 1996), it may as well provide a mechanism to enhance carbon mineralisation (Ziebis et al., 1996b). The sediment we studied met all requirements for advective particle and solute exchange, like surface roughness, high permeability and relatively strong near-bottom currents, and in this paper we have presented

several clear signs of advective influence on the organic matter budget of the uppermost 5 cm. The determination of mineralisation rates by core incubations or in situ measurements using benthic chambers is not appropriate for sands exposed to waves and currents, as these methods cannot include hydrodynamic effects and therefore underestimate turnover rates. Our approach A is an underestimation as well for the reason that POC inputs during autumn, e. g. from the *Rhizosolenia* and *Chaetoceros* blooms (Table 4), were ignored. On the other hand, POC loss was not purely diagenetic, leading to an overestimation of carbon mineralisation. The problem of overestimation is by-passed by considering and treating the tightly coupled benthic and near-bottom pelagic environment as a unit. From the DIC approaches, D agreed best with the result of the POC approach A. D could be taken as a rough estimate for oxic and suboxic mineralisation, but by deduction of the upward diffusing DIC it disregards sulphate reduction as an important degradation process in deeper layers and therefore underestimates the total sedimentary mineralisation. B and C were nearly equal with respect to both the approaches themselves and the results on an annual basis. They would only be prone to slight overestimation, if pore water exchange were incomplete during the preceding flood cycle. We consider a turnover rate of  $120 \text{ g C m}^{-2} \text{ a}^{-1}$  to serve well as a first, preliminary estimate for intertidal sandflats. Further studies should focus on more detailed carbon budgets, including DOC fluxes and benthic primary production, and quantify the degree of coupling between bottom water and permeable sediments at various sandy shelf sites.

Annual carbon turnover rates have been measured in different North Sea sediments, and results ranged between 24 and  $131 \text{ g C m}^{-2} \text{ a}^{-1}$  (Upton et al., 1993; Nedwell et al., 1994; Osinga et al., 1996; Boon et al., 1998; Boon & Duineveld, 1998). Median grain sizes were 100-250  $\mu\text{m}$  and TOC contents one order of magnitude higher than in our sediment, which yet proved to be equally active. Our results support, that the high-energy environment on the continental shelf enhances biogeochemical dynamics in permeable sands. With 30 % of the oceanic primary production (Jørgensen, 1996), shallow coastal waters have a high potential of OM mineralisation, in which sandy sediments may take part to a by far higher extent than to be expected from grain size and TOC content. Since permeable sands cover 43.5 % of the world's continental shelves (Riedl et al., 1972), they should be reconsidered with respect to quantitative importance in the marine carbon cycle.

### Acknowledgements

We thank M. Alisch for helpful support in the field and the co-workers of the BAH Wadden Sea Station for providing lab space and detailed information on Königshafen Bay. This study was supported by the Max Planck Society (MPG), and A.R. received a postgraduate scholarship from Deutsche Forschungsgemeinschaft (DFG).

## 2.4. Bacteria, diatoms and detritus in an intertidal sandflat subject to advective transport across the water-sediment interface

Antje Rusch, Stefan Forster & Markus Huettel

This study focused on organic particles with respect to their transport and sedimentary mineralisation in a North Sea intertidal sandflat previously characterised as strongly influenced by advective transport across and below the water-sediment interface. Measured permeabilities of the sandy sediment ranged from 5.5 to  $41 \cdot 10^{-12} \text{ m}^2$ , and permeabilities calculated from granulometric data exceeded the measured values by a factor of  $4.4 \pm 2.8$ . Bacteria (2-9 % of the POC) were highly variable in space and time. They were less mobile than interstitial fine ( $< 70 \text{ }\mu\text{m}$ ) organic and inorganic particles, as part of the population lived attached to large, heavy sand grains. The vertical distribution of bacteria was closely related to the organic carbon content of the fine-grained interstitial material. In winter, bacterial numbers in the uppermost 5 cm amounted to 39-69 % of the summer ones. Carbon mineralisation rates ranged between  $20 \text{ mg C m}^{-2} \text{ d}^{-1}$  in winter and  $580 \text{ mg C m}^{-2} \text{ d}^{-1}$  in summer, keeping step with finer-grained sediments that contained an order of magnitude more organic carbon. Sedimentary carbohydrates were mainly intracellular or tightly bound to particles, and their concentrations were depth-invariant in winter, but exponentially decreasing with depth in summer. Below 5 cm depth, the mean concentration was  $(1590 \pm 830) \text{ }\mu\text{g cm}^{-3}$ , without major downcore or seasonal changes. Phytobenthos and phytodetritus were dominated by diatoms and comprised merely minor amounts of other primary producers. Planktonic diatom depth profiles were related to weather and phytoplankton conditions, and benthic diatoms showed similar depth distributions due to passive and active motion. The penetration of relatively fresh phytodetritus down to at least 5 cm, shown by chloropigment composition, emphasised the close relation between water column and sandy sediment, facilitated by advective interfacial and subsurface flows.

## Introduction

Intertidal zones are part of the highly dynamic nearshore shelf seas, where fluid motions associated with currents and surface waves reach down to the sea floor and interact with the bottom sediments. In such energetic areas, small and light particles are frequently removed from the sediment, and thus permeable sands are the prevalent sediment type (Emery 1968, Riedl et al. 1972). They allow for advective transport of solutes (Huettel & Gust 1992a, Forster et al. 1996, Ziebis et al. 1996b) and particles (Huettel et al. 1996, Pilditch et al. 1998) across the water-sediment interface, when bottom flows cause pressure gradients that force water through the upper sediment layers.

The intensity of advective interfacial flow depends on current velocity (Forster et al. 1996), sediment topography (Huettel et al. 1996) and permeability (Darcy 1856). The permeability of sands ranges between  $10^{-12} \text{ m}^2$  and  $10^{-10} \text{ m}^2$  and depends on grain size, sorting and compaction (Hsü 1989) as well as on viscosity and density of the pore fluid (Klute & Dirksen 1986). The present study was conducted in an intertidal sandflat with permeabilities in the upper 15 cm permitting advective exchange across the sediment surface under natural hydrodynamic conditions.

We conducted a one-year field study with the objective to demonstrate and understand the mechanisms that cause the spatial and temporal dynamics of particulate organic matter (POM) in the upper 10 cm of the sediment. We set out to prove our working hypothesis that in this sandflat permeability is a key factor for sedimentary POM dynamics by controlling advective transport of suspended matter between water column and sediment. Depth profiles of various pore water solutes strongly indicated advective interfacial transport (Rusch et al. 1999 submitted). We focused on benthic microbes, that not only mineralise organic matter, but also are mobile POM themselves, as are planktonic and benthic diatoms. Photosynthetic pigment analyses provided additional information on POM provenance and state of degradation. Quantities and distribution of extracellular mucopolysaccharides were measured, because they facilitate cell attachment and locomotion and reduce sediment permeability and erosion (Grant & Gust 1987, Decho & Lopez 1993, Yallop et al. 1994, Underwood et al. 1995). Finally we discuss interactions and correlations between the observed particle and sediment characteristics as well as biogeochemical and ecological implications of advective POM transport across the water-sediment interface.

## Methods

### *Study site and sampling*

Our study site was located in Königshafen Bay ( $55^{\circ}02' \text{ N}$ ,  $008^{\circ}26' \text{ E}$ ) near Sylt island in the southern North Sea. At the sampling dates (17 Jul 97, 17 Sep 97, 18 Nov 97, 13 Jan 98, 15/17/19/23/25/27 Mar 98, 12 May 98 and 7 Jul 98), the intertidal sandflat was exposed to waves of less than 0.2 m amplitude and to currents of  $0 - 0.32 \text{ m s}^{-1}$ , measured 2 cm above the bottom.

At each sampling date we took 8 sediment cores of 6.0 cm i.d. and 1 core of 3.6 cm i.d., 20-40 cm long. Throughout the study, the respective sampling spots (0.5 m diameter) were chosen within the same selected circular area of 4 m radius. All time-sensitive procedures were performed in the nearby (500 m) lab immediately after sampling.

### *Sediment permeability and porosity*

Of each core set, one core of 6.0 cm i.d. was cut at ca. 15 cm depth, and the lower, muddy part of the sediment column was discarded. The permeability  $k$  of the upper, sandy part was then determined by the constant head method (Klute & Dirksen 1986) and normalised to 10 cm sediment column length.

We compared these measurements with the permeabilities calculated according to three different empirical relationships suggested by Krumbein/Monk (Eq. 1, Hsü 1989), Carman/Kozeny (Eq. 2, Nield & Bejau 1992) and Hazen (Eq. 3, Eggleston & Rojstaczer 1998). To assess water content, grain size distribution and porosity, the core of 3.6 cm i.d. was sectioned in depth intervals of 0.25 cm (down to 1 cm), 0.5 cm (down to 2 or 4 cm) and 1.0 cm (down to 15 cm), and the slices were oven-dried at 70 °C for 48 h. We determined the water content  $W$  (in % w/w) from the weight loss upon drying and the grain size distribution by dry sieving. The porosity  $p_0$  was calculated from the density of the sand, determined by Archimedes' method, the density of sea water, and  $W$ . The permeabilities  $k_{KM}$ ,  $k_{CK}$  and  $k_H$  of the uppermost 10 cm were then calculated according to Equations 1, 2 and 3, respectively.

$$\text{Equation 1: } k_{KM} = 7.50 \cdot 10^{-4} \cdot d_{50}^2 \cdot e^{-1.31 \cdot \sigma(\phi)}$$

$$\text{Equation 2: } k_{CK} = p_0^3 \cdot d_{50}^2 / (180 \cdot (1-p_0)^2)$$

$$\text{Equation 3: } k_H = 1.019 \cdot 10^{-3} \text{ m}^{-2} \text{ s} \cdot d_{50}^2 \cdot \nu$$

(with  $d_{50}$ : grain size median,  $d_{10}$ : first decile of the grain size distribution,  $\sigma(\phi)$ : standard deviation of grain sizes given in logarithmic  $\phi$  units,  $\nu$ : kinematic viscosity)

### *Bacteria, diatoms and carbohydrates*

Of each core set, one core of 6.0 cm i.d. was sectioned in depth intervals of 0.5 cm (down to 2 or 4 cm) and 1.0 cm (down to 15 cm). From these slices we took aliquots of 1.0 cm<sup>3</sup>, 1.5 cm<sup>3</sup>, 0.2 cm<sup>3</sup> and twice 0.4 cm<sup>3</sup> for analysing bacteria, diatoms, total carbohydrates, water-soluble and EDTA-soluble carbohydrates, respectively.

**Bacteria.** 1 cm<sup>3</sup> of fresh sediment was added to 8 ml of NaCl solution (32 g l<sup>-1</sup>) containing formalin (final concentration: 4 %) and stored in the dark at 4 °C until analysis. Bacterial cells were dislodged from the sand grains by ultrasonic treatment, stained with DAPI, concentrated on polycarbonate membrane filters (0.2 µm pore size) and counted under epifluorescent illumination (Zeiss Axioskop), in all steps following the protocol suggested by Epstein & Rossel (1995). Using a magnification of 1300x, cell numbers were determined from two parallel filters per sample, in 5 randomly chosen counting grids each.

**Diatoms.** 1.5 cm<sup>3</sup> of fresh sediment was added to 6 ml of isohaline NaCl solution containing glutaraldehyde (final concentration: 1.6 %) and stored in the dark at 4 °C until analysis. For the latter, the samples were suspended and the coarse particles (>70 µm) allowed to settle for 20 s, before the supernatant was decanted. After adding 4 ml of NaCl solution to the settled particles, they were once more treated alike. In a pre-test, the efficiency of extracting fine SiC particles from an artificial sand was 80-90 % using this method. We examined the combined supernatant suspensions by light microscopy using a Fuchs/Rosenthal chamber and a magnification of 400x. Diatom frustules were counted separately as planktonic and benthic forms (Pankow 1990) and grouped into 5 length classes each: 10-15 µm, 15-20 µm, 20-25 µm, 25-30 µm and >30 µm.

**Carbohydrates.** Concentrations of total, water-soluble, and EDTA-soluble carbohydrates were assayed by the phenol/sulphuric acid method (Underwood et al. 1995).

### *Pigments*

Of each core set, three cores of 6.0 cm i.d. were sectioned in depth intervals of 0.25 cm (down to 1 cm), 0.5 cm (down to 2 or 4 cm) and 1.0 cm (down to 15 cm). Parallel slices were pooled, gently suspended in isohaline NaCl solution, and allowed to settle. After 20 s, the supernatant was decanted and the remaining sediment once more retreated alike. The decanted suspensions, containing the particulate matter of an effective diameter less than 70  $\mu\text{m}$  (hereafter referred to as "fine fraction"), were centrifuged (15 °C, 5 min, 1200·g). The pellet was freeze-dried, weighed and stored at 4 °C in the dark.

For pigment analysis, we prepared extracts from the fine fraction by dark incubation with 90% acetone at 4 °C for 16 h and subsequent centrifugation (4 °C, 7 min, 1620·g). The supernatant was syringe-filtered through 0.45  $\mu\text{m}$  pores (Nalgene 199-2045 PTFE) and concentrated using a Savant SC 110A vacuum centrifuge.

20  $\mu\text{l}$  of concentrated extract were separated on a Hypersil ODS C18 column using an HPLC system (Waters 600E gradient module, Waters 991 photodiode array detector/integrator). Solvents, gradients, flow rates and a detailed description of the method are given by Karsten & Garcia-Pichel (1996). Pigments were identified by their absorption spectra (350-800 nm) and retention times. The quantification of chloropigments and carotenoids was based on the peak areas at 410 nm and 440 nm, respectively. As calibration standards we used solutions of Chl a (Sigma), porphyrin (Sigma), canthaxanthin (Fluka) and the following carotenoids (<sup>14</sup>C Agency Denmark):  $\alpha$ -carotene, fucoxanthin, 19'-hexanoyloxyfucoxanthin, 19-butylfucoxanthin, lutein, and peridinin. Qualitative standard solutions of unknown concentration were prepared of  $\beta$ -carotene, BChl a (*Rhodospirillum rubrum*), BChl c (*Prosthecochloris* spec.), chlorobactene (*Chlorobium vibrioforme*), and isorenieratene (*Chlorobium phaeovibroides*). Other pigments were named operationally in the order of their retention times: chloropigments XA - XF and carotenoids YA - YF. The detection limit was an absorbance of 0.005 AU (absorbance units), corresponding to 110-330 ng pigment per  $\text{cm}^3$  of sediment.

## Results

### *Sediment permeability*

The measured permeabilities  $k$  and the calculated permeabilities  $k_{\text{KM}}$ ,  $k_{\text{CK}}$  and  $k_{\text{H}}$  are listed in Table 1. There was a significant positive correlation between  $k$  and  $k_{\text{KM}}$  ( $\alpha = 1\%$ ) and between  $k$  and  $k_{\text{H}}$  ( $\alpha = 5\%$ ) with a slope of the regression line of 1.19 and 0.88, respectively. The slope of the regression line between  $k$  and  $k_{\text{CK}}$  was 0.88, the correlation lacking significance, though. There was no seasonal trend in the measured or calculated permeabilities.

Porosities and grain size distributions depended on sediment depth ( $\alpha = 5\%$ , Wilcoxon matched pairs signed rank test, Sachs 1997):

$$d_{50}(0-2 \text{ cm}) \approx d_{50}(10-15 \text{ cm}) > d_{50}(2-5 \text{ cm}) \approx d_{50}(5-10 \text{ cm})$$

$$\text{and } p_0(0-2 \text{ cm}) > p_0(2-5 \text{ cm}) \approx p_0(5-10 \text{ cm}) \approx p_0(10-15 \text{ cm}).$$

Mean values, averaged over all sampling dates, were  $d_{50}(0-2 \text{ cm}, 10-15 \text{ cm}) = 571 \mu\text{m} \pm 101 \mu\text{m}$ ,  $d_{50}(2-10 \text{ cm}) = 481 \mu\text{m} \pm 83 \mu\text{m}$ ,  $p_0(0-2 \text{ cm}) = 0.374 \pm 0.057$ , and  $p_0(2-15 \text{ cm}) = 0.322 \pm 0.020$ .

	k (0-10 cm) in $10^{-12} \text{ m}^2$	$k_{KM}/k$	$k_{CK}/k$	$k_H/k$
17 Jul 97	15.0	2.94		2.09
17 Sep 97	40.7	2.35	1.92	2.09
18 Nov 97	18.7   6.7	2.37   6.60	4.90   13.7	2.73   7.61
13 Jan 98	10.8	3.60	4.94	3.93
13 Jan 98	12.4	3.20	4.26	3.24
17 Mar 98	23.0	1.66	1.56	1.98
19 Mar 98	9.4	4.08	4.90	4.11
23 Mar 98	13.6	2.81	1.84	3.64
25 Mar 98	5.5	9.53	6.44	11.9
27 Mar 98	6.7	5.53	6.84	5.30
12 May 98	10.3	3.77	7.54	3.77
7 Jul 98	34.2	1.82	2.78	1.78
mean		$3.87 \pm 2.21$	$5.13 \pm 3.35$	$4.17 \pm 2.82$
median		3.20	4.90	3.64

Table 1: Permeability of the upper 10 cm of the sediment. k: measured and normalized,  $k_{KM}$ : calculated according to Krumbein/Monk (Eq. 1),  $k_{CK}$ : calculated according to Carman/Kozeny (Eq. 2),  $k_H$ : calculated according to Hazen (Eq. 3).

#### *Bacteria and POC mineralisation*

Bacterial cell numbers and depth distributions showed distinct seasonal changes (Figure 1). There was a subsurface maximum in 1.5 - 2.5 cm depth during summer (May, Jul, Sep) and in 3.0 - 4.5 cm depth during winter (Nov, Jan, Mar). Above it, bacterial numbers steeply decreased towards the sediment surface (except for Nov 97), with minimum numbers attained in 0 - 2.5 cm depth. The gradient between this minimum and the subsurface maximum as well as the relative bandwidth,  $(\text{max}-\text{min})/\text{max}$ , of cell numbers within a profile (Table 2) decreased in autumn and winter (Sep 97 - Mar 98) and increased in spring and summer (Mar 98 - Jul 98).

With an estimated mean cell diameter of  $1 \mu\text{m}$  and a cellular organic carbon concentration of  $1.1 \cdot 10^{-13} \text{ g } \mu\text{m}^{-3}$  (Ritzrau & Graf 1992, Harvey et al. 1995), bacterial POC amounted to 3 - 22  $\mu\text{g } (\text{cm}^3 \text{ sediment})^{-1}$ . By comparison, total sedimentary POC was between 32 and 2030  $\mu\text{g } \text{cm}^{-3}$ , and median values of bacterial contribution to the sedimentary carbon pool ranged between 2.2% in July and 8.6% in January. In spite of this relatively small share, bacteria and POC appeared related to each other in various aspects. Throughout the year, the depth of maximum bacterial cell numbers was close to, i.e. between 1 cm above and 2 cm below, the depth of fine particles richest in POC (Figure 1). Maximum bacterial numbers (Table 2) and maximum POC contents (Table 3) tended to be positively correlated, however not significantly. The same holds for the inventories (0-5 cm depth) of bacteria and POC.

Carbon mineralisation rates (Table 3) showed seasonal changes parallel to that of maximum bacterial cell numbers and numbers in 1-2 cm depth and 0-5 cm depth (Figure 2). However, the correlation between rates and these bacterial numbers was statistically not significant (Sachs 1997).

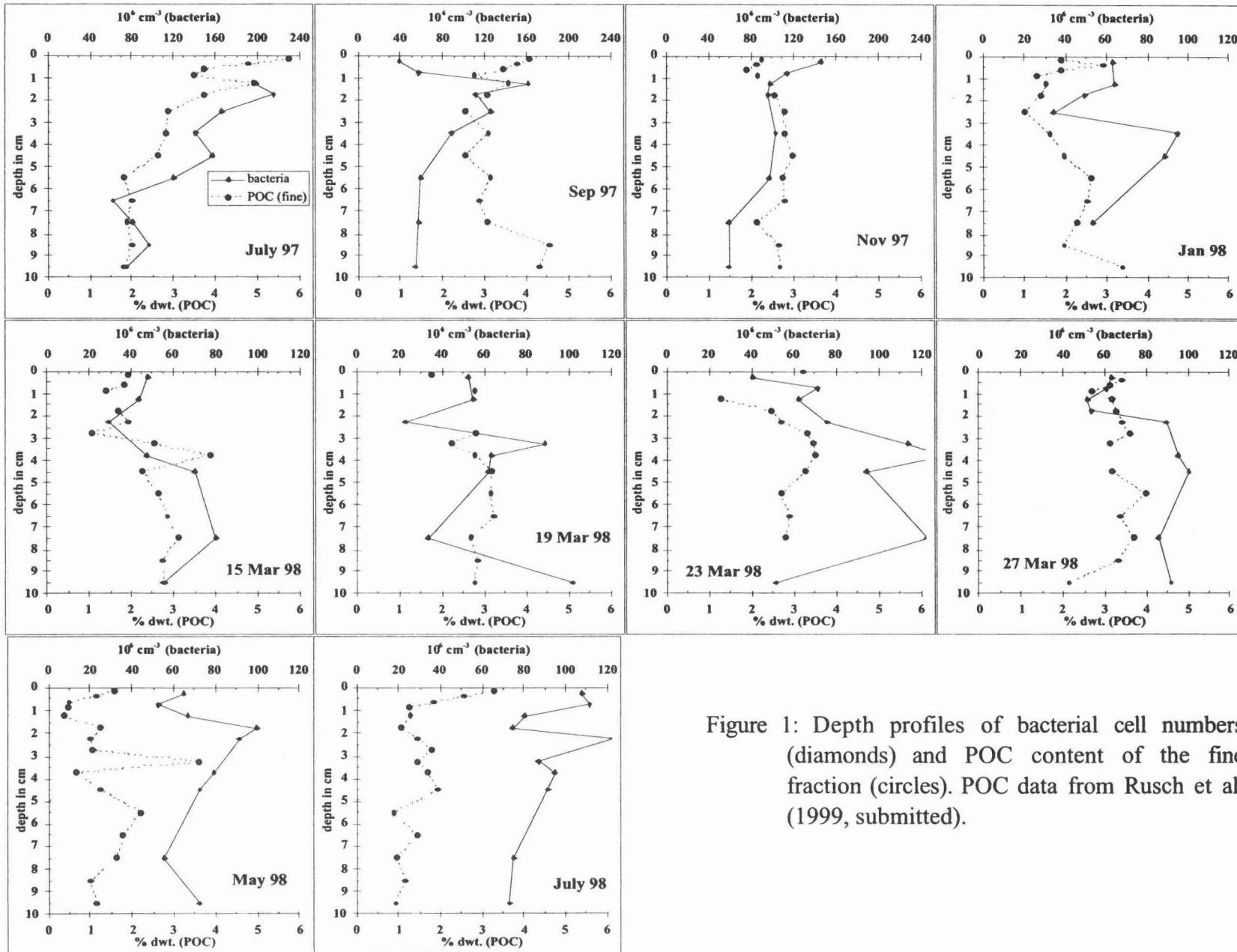


Figure 1: Depth profiles of bacterial cell numbers (diamonds) and POC content of the fine fraction (circles). POC data from Rusch et al. (1999, submitted).

	maximum number $10^6 \text{ cm}^{-3}$	gradient $10^6 \text{ cm}^{-4}$	(max-min)/max
Jul 97	215		
Sep 97	162	123	0.760
Nov 97	147		
Jan 98	95.0	60.8	0.640
Mar 98	97.5	36.9	0.405
May 98	99.7	54.3	0.545
Jul 98	112	96.6	0.785

Table 2: Sedimentary bacteria. Gradient: between minimum and subsurface maximum.

	maximum POC content % dwt.	inventory (0-5 cm) $\text{g m}^{-2}$	mineralisation rate $\text{mg C m}^{-2} \text{ d}^{-1}$		
			B	C	D
Jul 97	4.90	31.7	201	519	
Sep 97	3.56	15.1	256	365	311
Nov 97	2.96	13.1	141		204
Jan 98	2.63	4.05	217	101	20
Mar 98	3.64	6.14	265	244	42
May 98	3.61	26.9	565	418	190
Jul 98	1.77	35.9	579	550	464
correlation to inventory			n. s.	**	*

Table 3: Particulate organic carbon (POC). Maximum content in the fine fraction, total amount in the upper 5 cm, and carbon mineralisation rates calculated from depth profiles of dissolved inorganic carbon (DIC). POC contents, DIC concentrations and computation approaches from Rusch et al. (1999, submitted). Carbon mineralisation rates were calculated from DIC profiles according to three different approaches, B, C and D, by depth integration of DIC concentrations using three different background concentrations. Computations were based on the assumption that DIC accumulated between the time of highest near-bottom tidal current velocity and sampling. Significant correlations: \*:  $\alpha = 5\%$ , \*\*:  $\alpha = 1\%$ .

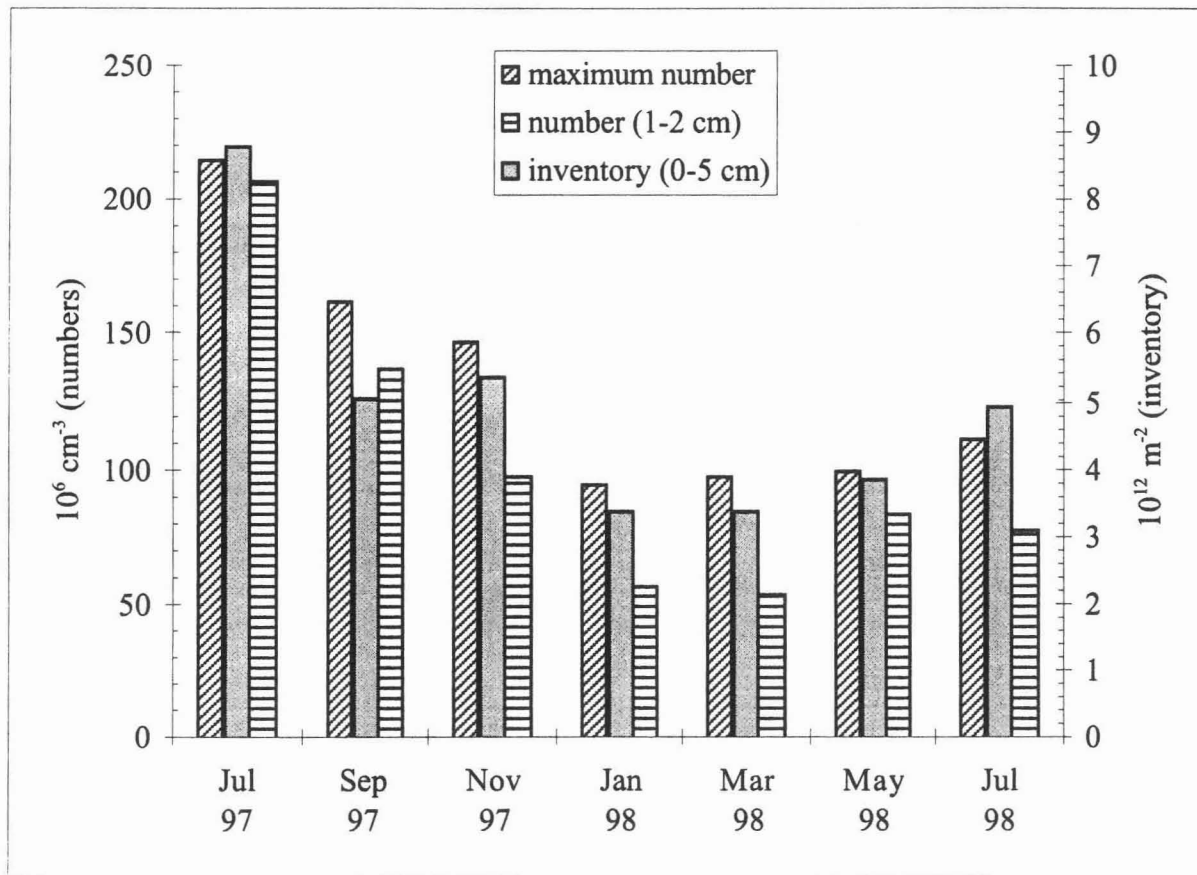


Figure 2: Seasonality of sedimentary bacteria: maximum numbers, numbers in the most active zone (1-2 cm depth), and inventory (0-5 cm).

Figure 3 illustrates that organic-rich fine particles and optimum conditions for sedimentary bacteria were found in steadily deeper layers during autumn and winter and gradually closer to the sediment surface in the following spring and summer. Throughout the year, both maxima were located in the zone influenced by advective exchange across the water-sediment interface. The zone of DIC accumulation due to intense mineralisation narrowed in autumn and winter and expanded during spring and summer. From Nov 97 until Mar 98 it did not cover the depth of maximum bacterial cell numbers.

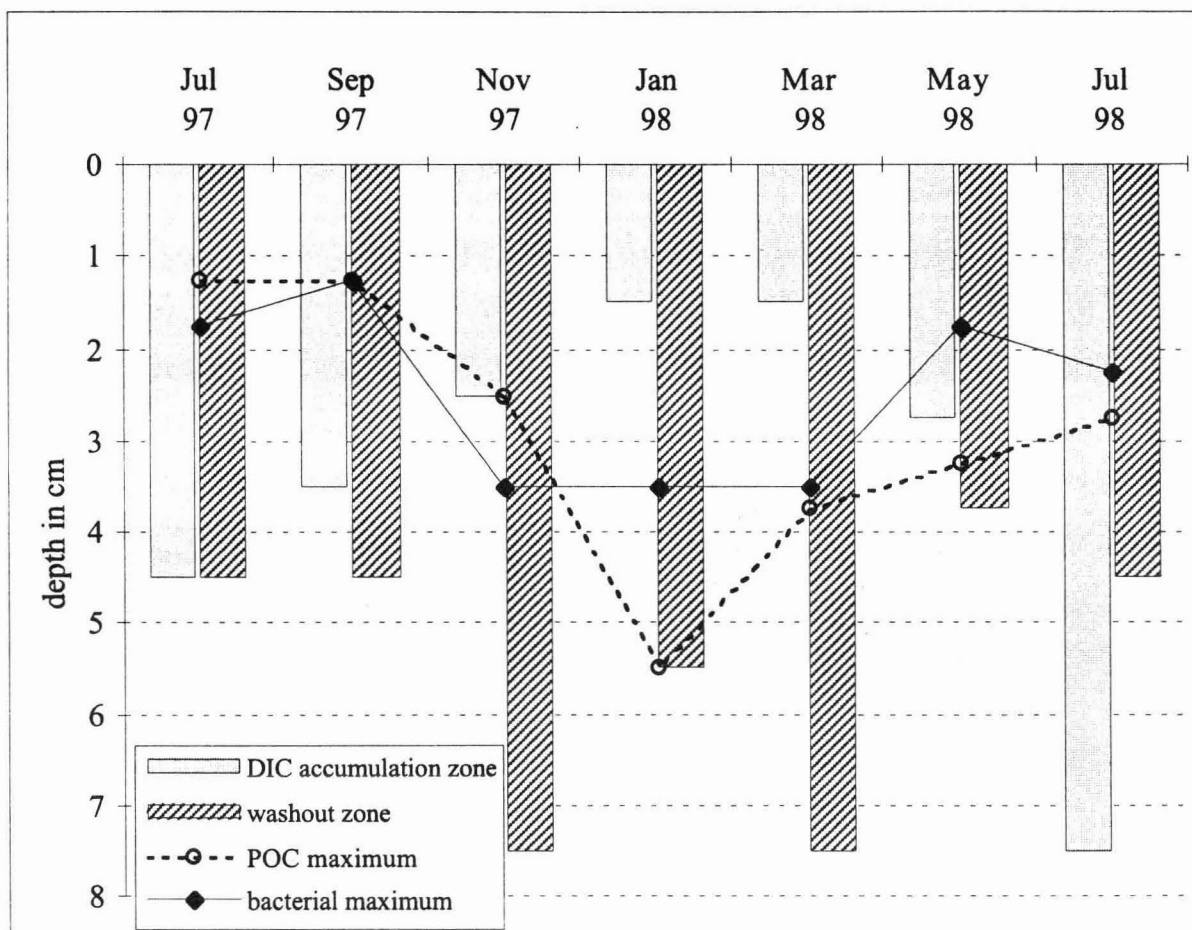


Figure 3: Horizons related to POC degradation. Hatched bars: depth interval from which fine-grained material was partially removed by hydrodynamic processes, with maximum concentrations of fine particles defining the lower end of this "washout" zone (Rusch et al. 1999, submitted). Stippled bars: zone of intense carbon mineralisation, defined as the depth interval of a local, cap-shaped DIC surplus superimposed on the basically linear depth profile. DIC was considered to accumulate during and near slack tide, whereas particle washout was rather associated with stronger ebb and flood currents in the tidal cycle. Circles: depth of maximum POC content of the fine fraction. Diamonds: depth of maximum bacterial cell numbers.

### Carbohydrates

The share of sea water soluble and EDTA soluble carbohydrates was  $0.99\% \pm 1.54\%$  ( $n = 120$ ) and  $5.73\% \pm 4.52\%$  ( $n = 120$ ) of total carbohydrates, respectively. We observed no seasonal trend or characteristic depth profile in these data.

Total carbohydrate concentrations decreased exponentially with depth in summer (Jul 97, Sep 97, May 98, Jul 98), whereas the winter (Jan 98, Mar 98) profiles showed little variation (Figure 4). Below 5 cm depth, only minor downcore or temporal changes occurred, and the mean concentration amounted to  $(1589 \pm 830) \mu\text{g cm}^{-3}$  ( $n = 63$ ). Carbohydrates in the upper 5 cm exceeding this background concentration were integrated for each sampling date (March: mean). The resulting areal inventories (in  $\text{g m}^{-2}$ ) steadily decreased from 130.7 in Jul 97 to 80.9 in Sep 97 and 66.2 in Jan 98, attained the minimum of -6.7 in Mar 98 and afterwards gradually increased to 18.0 in May 98 and 31.4 in Jul 98.

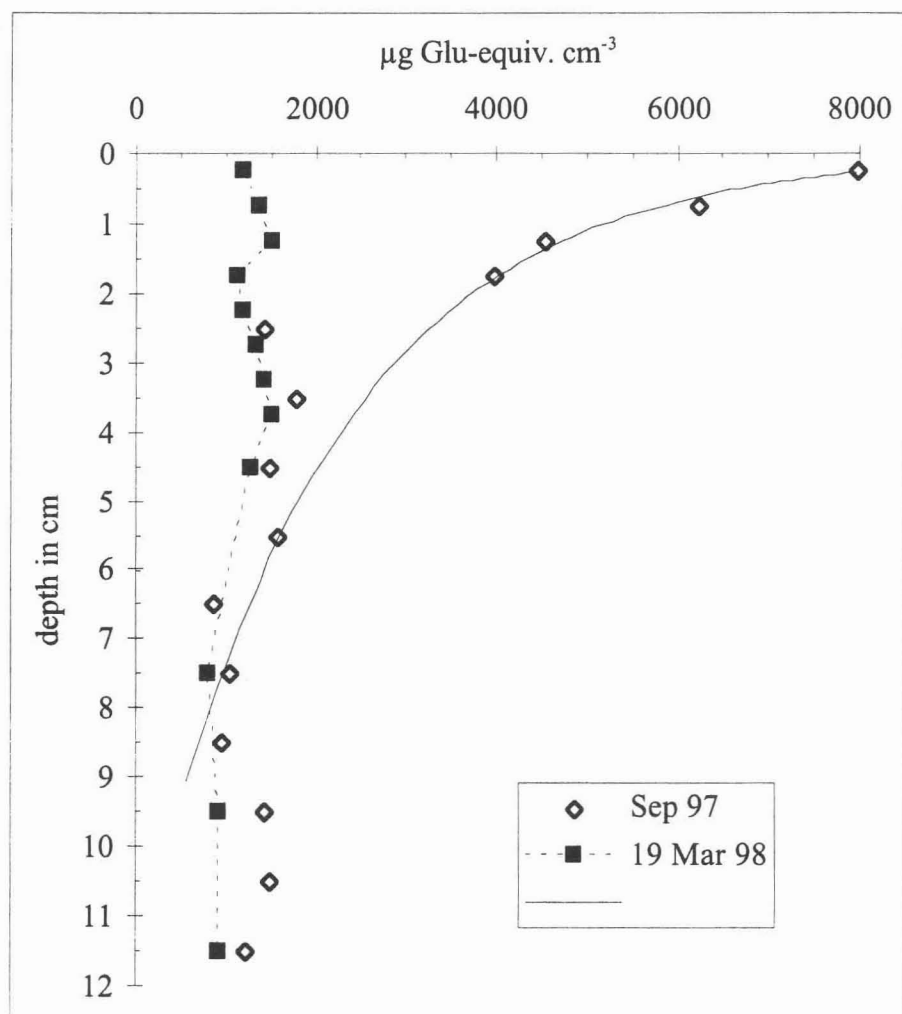


Figure 4: Depth profiles of total carbohydrate (given as glucose equivalent) concentrations. Diamonds: Sep 97 representing summer, with exponential data fit (solid line). Squares: 19 Mar 98 representing winter. The complete data set of all profiles is available from the authors.

Carbohydrate inventories were significantly correlated neither to sediment permeabilities (Table 1) nor to the corresponding inventories of POC, PN or Chl (data from Rusch et al. 1999, submitted). In several cores, however, total carbohydrate concentrations were significantly correlated to the concentrations of POC, Chl or bacteria (Table 4).

The difference between carbohydrate organic carbon (chOC) and POC(fine) can be used as a measure of the minimum amount of carbohydrates associated with the coarse fraction, if  $chOC - POC(fine) > 0$ . In our profiles, this difference was positive throughout the top 10 cm (except for 4 data points in May 98), revealing that there was more carbohydrate  $C_{org}$  in the coarse fraction than non-carbohydrate  $C_{org}$  in the fine fraction. With increasing sediment depth,  $chOC - POC(fine)$  tended to decrease. That means, adsorption of carbohydrates to the sand grains was less in deeper strata compared to above, or carbohydrate occurrence was selectively restricted to near-surface sediment, or both.

	POC	Chl	bacteria
carbohydrates	Jul 97 (*)  Jul 98 (*)	Jul 97 (**) Sep 97 (***) 15 Mar 98 (*) Jul 98 (**)	Jul 97 (***)  Jul 98 (*)
Chl	Jul 97 (*) Jul 98 (*)		
bacteria	Jul 97 (**)	Jul 97 (***) 15 Mar 98 (*)	

Table 4: Significant correlations between the concentrations of carbohydrates, POC, chlorophyll and bacteria. \*:  $\alpha = 5\%$ , \*\*:  $\alpha = 1\%$ , \*\*\*:  $\alpha = 0.1\%$ .

### Diatoms

In our samples, most benthic diatoms were naviculoid. Planktonic diatoms were mainly centric, except for rod-shaped *Rhizosolenia spec.* and the almost brick-shaped, occasionally chain-forming *Brockmanniella brockmannii* (Hasle et al. 1983). The size class 15-20  $\mu\text{m}$  was dominated by *B. brockmannii*, whereas no prominence of a certain family was observed in any other size class.

To improve the comparability of algal cell depth distributions, we present our data in terms of "relative particle numbers", i.e. diatom numbers in a certain depth interval divided by the total number of diatoms found in the core. Depth profiles could be classified into 3 major types, and a representative of each is shown in Figure 5. The dominant one was an exponential or linear decrease of relative particle numbers with depth (Figure 5a), a more or less even depth distribution of frustules (Figure 5b) occurred several times, and some profiles exhibited a subsurface maximum (Figure 5c). There was no general difference between the depth distributions of planktonic and benthic diatoms ( $\alpha = 10\%$ , Wilcoxon matched pairs signed rank test, Sachs 1997), nor did depth distributions depend on cell size (Kruskal/Wallis test). However, a significant difference between the sampling dates was detected in the depth distributions of benthic ( $\alpha = 1\%$ ) and planktonic ( $\alpha = 0.1\%$ ) diatoms (Kruskal/Wallis test). In Jul 97, Nov 97, Jan 98 and 15 Mar 98, profiles were predominantly of the type shown in Figure 5a. Approximately even depth distributions (Figure 5b) were observed in Sep 97, 19 Mar 98 and 23 Mar 98, whereas a subsurface maximum (Figure 5c) occurred on 27 Mar 98 as well as in most profiles of May 98 and Jul 98.

The biovolume of benthic and planktonic diatoms was calculated from the numbers in each size class, approaching cell shapes in pervalvar view as rectangular (*B. brockmannii*), circular (other planktonic forms) or elliptic (benthic forms). The height of the frustule was estimated a quarter of its length. Diatom biovolumes were significantly correlated to POC concentrations in Sep 97 ( $\alpha = 0.1\%$ ) and Jan 98 ( $\alpha = 5\%$ ) as well as to Chl concentrations and bacterial numbers in Sep 97 ( $\alpha = 5\%$ ). The inventories (0-5 cm) of diatom biovolume and carbohydrates were significantly ( $\alpha = 5\%$ ) correlated with exception of Jan 98 and Mar 98.

In each size class following the computation approaches given by Smayda (1978), diatom POC amounted to 10-170  $\mu\text{g (cm}^3 \text{ sediment)}^{-1}$ . Accordingly diatoms constituted 8-18 %, in Mar 98 even 28 %, of total sedimentary POC.

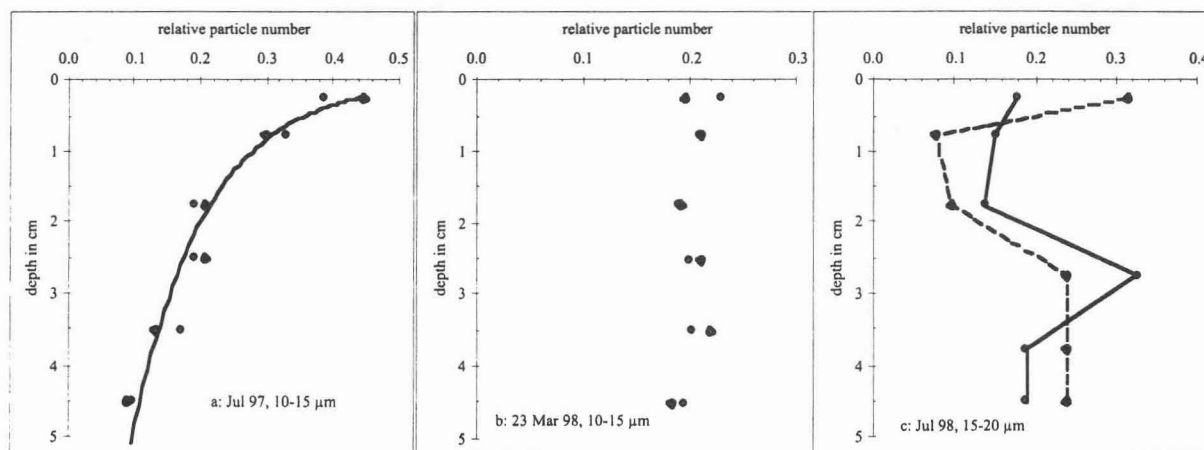


Figure 5: Depth profiles of relative particle numbers. Circles: planktonic diatoms, diamonds: benthic diatoms. a: exponential decrease, represented by Jul 97, 10-15  $\mu\text{m}$ . b: even depth distribution, represented by 23 Mar 98, 10-15  $\mu\text{m}$ . c: subsurface maximum, represented by Jul 98, 15-20  $\mu\text{m}$ . The complete data set of all profiles is available from the authors.

#### *Photosynthetic pigments*

**Bacteriochlorophyll.** HPLC analysis of our samples was unable to detect any BChl. Due to relatively small total bacterial numbers compared to a relatively high detection limit, no conclusion on the presence or absence of phototrophic microbes could be drawn.

**Carotenoids.** Detectable amounts of carotenoids were found in the samples of Jul 97, Sep 97 and Nov 97. They consisted of 40-100 % fucoxanthin, 0-30 % YA, 0-20 % YC, and 0-20 % others. Canthaxanthin, lutein and peridinin were below the detection limit. The share of hydrophobic carotenoids with long retention times tended to increase with sediment depth.

**Chloropigments.** Concentrations determined by fluorometry (Rusch et al. 1999, submitted) and by HPLC were significantly ( $\alpha = 0.1$  %) correlated, with the slope of the regression line near unity.

For the following, the chloropigments were grouped into 3 sets. The hydrophobic set comprises chlorophyll and its early degradation products, pheophytin and XF (probably pheophorbide). XA and XB constitute the hydrophilic set, and the intermediate set consists of XC - XE. Figure 6 shows depth profiles of chloropigments based on fluorometric measurements, supplemented by HPLC data on the pigment composition. The share of hydrophobic chloropigments, indicating barely degraded material, tended to decrease from the surface downwards. Especially high shares in the uppermost layers and in the seston were observed in Jul 97, Sep 97, Mar 98 and Jul 98 (Figure 6) concurrent with phytoplankton blooms of *Phaeocystis globosa*, *Chaetoceros spec.*, *Brockmanniella brockmannii*/*Skeletonema costatum* and *Phaeocystis globosa*, respectively. By contrast, suspended and sedimentary fine particles were dominated by intermediate and hydrophilic chloropigments in Nov 97, Jan 98 and May 98, indicating advanced degradation of phytodetritus.

Correlations. Except for the carotenoid YA, concentrations of none of the pigments or pigment groups were significantly ( $\alpha = 5\%$ ) correlated to the diatom biovolume. Carbohydrate concentrations were significantly correlated to the hydrophilic ( $\alpha = 5\%$ ) and the hydrophobic ( $\alpha = 0.1\%$ ) chloropigments, but not to the intermediate ones. There was a highly significant ( $\alpha = 0.1\%$ ) correlation between POC concentrations and each of the chloropigment sets.

## Discussion

Besides catalysing a matchless variety of biogeochemical reactions, bacteria are part of the sedimentary POM pool and food web. Moreover, microbial exopolymers can alter the cohesivity of sediments (Grant & Gust 1987, Dade et al. 1990) and the adsorption of DOM and cells to the matrix (Decho & Lopez 1993). Both affect advective fluxes, that depend on sediment permeability as well as on size and mobility of the transported particles, e.g. bacterial cells. In intertidal areas, the pronounced influences of seasons and water movements add to the interactions between sedimentary bacteria and their dynamic environment.

### *Microbial particles subject to hydrodynamic forces*

Unlike most depth distributions of bacteria reported in literature, with maximum cell numbers at the sediment surface (e.g. Sahm et al. 1999, Sievert et al. 1999), our profiles exhibited a subsurface maximum below a minimum (Figure 1). This characteristic feature was also found in the depth profiles of the fine fraction ( $< 70 \mu\text{m}$ ) and can be attributed to advective washout and subsequent re-entry from the surface. Maximum bacterial numbers were observed 2-4 cm closer to the sediment-water interface than maximum concentrations of fine particulates (Figure 3), indicating somewhat lower susceptibility to hydrodynamic forces. Free-living single cells are most easily moved through the pore space and across the sediment surface. Bacteria attached to particles, however, benefit nutritionally over free-living forms by close association with an organic substrate and by increased solute flux due to fluid turbulence around the host particle (Logan & Kirchman 1991). In our permeable sand, advective pore water flows could provide solutes and turbulence, and bacteria are likely to adhere to organic-rich fine particles or to the more protected habitat of microtopographic structures on coarse sand grains. With part of the microbial population attached to the coarse fraction ( $> 70 \mu\text{m}$ ), the bulk hydrodynamic mobility of sedimentary bacteria could fall short of that of the fine fraction. So maximum numbers of bacteria thrive in a zone, where the bulk of small particles could not resist being carried out of the sediment (Figure 3).

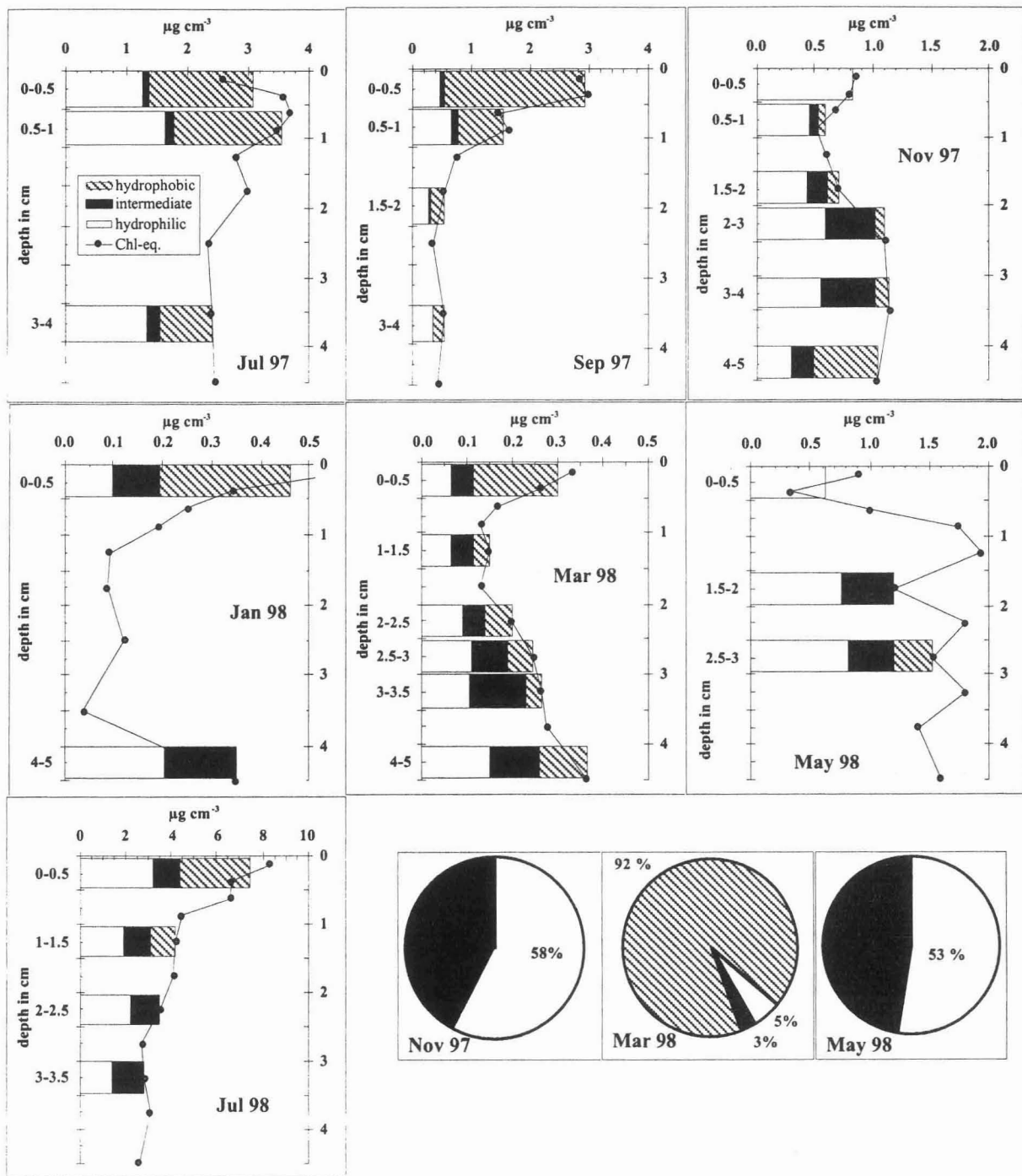


Figure 6: Depth profiles of chloropigment concentrations, given as chlorophyll equivalents per sediment volume. Circles: total, hatched: hydrophobic, dark grey: intermediate, stippled: hydrophilic. Lower right panel: chloropigment composition of suspended particulate material in Nov 97, Mar 98 and May 98.

The microbial population of our sandflat was highly dynamic in space and time, as shown by steep gradients and broad range within the profiles (Table 2) and by marked seasonal variation in the maximum number, the number in the most active zone and the inventory (Figure 2). Gradients and bandwidths gradually decreased from autumn till late winter (Mar 98) and increased in spring and summer, as location and size of the maximum varied seasonally. Due to decreasing food supply from above and hydrodynamic washout reaching deeper into the sediment, maximum bacterial numbers were found deeper in winter than in summer (Figure 3), thus making the gradient shallower. Lower maximum cell numbers (Table 2) added to this decrease of the gradient and furthermore narrowed the bandwidth. Reversely in summer calmer hydrodynamic conditions, affluent food supply and higher maximum bacterial numbers increased both bandwidths and gradients. Apart from selection by interstitial water flows and availability of organic-rich particles acting on microbial life in a given sediment depth, bacteria may also actively respond to seasonally changing conditions by vertical migration towards their current optimum depth.

#### *Microbial organic matter*

Strong correlations between bacteria and organic-rich fine particles may arise, when microbial cells themselves are major part of the sedimentary POC. This was not the case in our sandflat, with bacteria contributing less than 9% to the POC pool. Nor were POC compounds likely to be products of microbial primary production. Due to the HPLC detection limit and relatively small overall numbers of bacteria, our analyses failed to give clear evidence of the presence or absence of phototrophs. As the microbial contribution to photosynthetic pigments was undetectable, the microbial contribution to primary production was probably insignificant, too. Hence the main ecological role of our sandflat bacteria in organic matter turnover was degradation.

#### *Microbial decomposition of organic matter*

Although the standing stock of bacteria contributed only minor part to sedimentary POC, cell numbers and POC were closely related. Maxima neighboured each other (Figure 3) and seasonally developed parallel, with bacteria slightly delayed (Table 2, Table 3) due to the dependence of heterotrophic microbial communities on organic matter supply. The close spatial coherence between bacteria and fine particles richest in POC might also imply that the major part of the microbes in our sandy sediment were attached to the interstitial fine fraction rather than to the organic-poor matrix. On the other hand, we favour the view that a bacterial population largely attached to sand grains, as suggested by their hydrodynamic mobility, profits from pore water DOC and prospers where organic-rich material is abundant, without necessarily direct contact to the fine-grained POM. Optimum growth conditions could also contribute to make up for hydrodynamic losses and may serve as an additional explanation for the maintenance of high bacterial numbers within the reach of advective flushing (Figure 3).

Carbon turnover rates generally decreased from Jul 97 until Jan 98 and afterwards increased again, corresponding to the seasonal changes of the POC inventory (Table 3). The significant correlation between the potential of mineralisation and the actual rates emphasises tight coupling and a high degree of using the POC potential available. As both POC concentrations and temperatures were lower in winter, less bacteria could make their living (Figure 2) and mineralisation weakened (Table 3) compared to summer. The number of DAPI-stained cells, irrespective of their being dead or alive, decreased not as strongly as carbon turnover rates, indicating that the surviving winter population consisted either of relatively many cells in

reduced metabolic activity or of few cells in a fully active stage, probably something in between. The depths of highest numbers of bacteria and organic-rich fine particles increased towards the cold season and decreased in the following spring and summer (Figure 3). Optimum living conditions, as determined by hydrodynamically induced mechanical stress and by POC penetration, amount and quality, established in deeper sediment layers throughout winter and closer to the surface in summer. The seasonality of organic matter degradation was revealed not only in rates (Table 3), but also in the depth range of intense DIC production (Figure 3). Remarkably, this DIC accumulation zone did not cover the depth of maximum cell numbers from Nov 97 till Jan 98, thus affirming the hypothesis of microbial dormancy in winter.

Organic matter mineralisation was assessed by means of DIC depth profiles, and the approaches to calculate DIC production rates as well as the results on an annual basis have been discussed elsewhere (Rusch et al. 1999, submitted). In the following we focus on the seasonality of mineralisation rates (Table 3) and the DIC accumulation zone (Figure 3). Carbon mineralisation rates in our coarse, organic-poor sand ranged between 20 and 579 mg C m<sup>-2</sup> d<sup>-1</sup>, whereas rates in a similar North Sea sediment were 60 - 192 mg C m<sup>-2</sup> d<sup>-1</sup> (Upton et al. 1993). We attribute these lower rates to the measurement by core incubations that exclude advective oxidant supply and therefore may severely underestimate mineralisation rates in permeable sediments. Rates measured in fine sandy sediments of the North Sea and the Baltic Sea, that were an order of magnitude richer in organic carbon than ours, ranged between 4 and 555 mg C m<sup>-2</sup> d<sup>-1</sup>, depending on season and location (Canfield et al. 1993, Upton et al. 1993, Kristensen & Hansen 1995, Osinga et al. 1996, Boon & Duineveld 1998, Boon et al. 1998). In these finer-grained sediments, permeability may have limited advective interfacial flows that both remove reduced metabolites and supply oxidants. By contrast, coarser sands like ours facilitated more intense and deeper-reaching exchange across the water-sediment interface, thereby enhancing turnover (Forster et al. 1996, Reimers et al. 1996, Huettel et al. 1998). The relatively low organic carbon contents of non-accumulating permeable sediments are therefore considered a consequence of rapid mineralisation.

#### *Diatoms as sedimentary organic matter*

In marine ecosystems diatoms act as primary producers, may run a heterotrophic metabolism for several days (Harvey et al. 1995, Nelson et al. 1999) and can constitute a major part of the POM in the water column and the sediment. Total POC concentrations in our sandflat ranged between 32 and 2030 µg cm<sup>-3</sup>, with bacteria contributing up to 22 µg cm<sup>-3</sup> and diatoms up to 170 µg cm<sup>-3</sup>. Thus, diatom carbon was not negligible, though the main part of sedimentary POC was detritus or adsorbed extracellular substances, both possibly derived from diatoms.

The depth distribution of diatom frustules did not significantly differ between planktonic and benthic forms, suggesting similar mobility on the scale of our depth resolution. In sandy sediments moderately exposed to waves and currents, attached benthic diatoms generally dominate over motile ones (Asmus & Bauerfeind 1994). On the other hand, sandflat diatoms can actively move vertically with an amplitude of several cm, controlled by wave energy, light and chemical gradients (Kingston 1999). We detected no significant difference between the depth distributions of differently sized diatoms, as given the studied size range of diatoms, the spatial resolution of the depth profiles was insufficient.

Depth distributions depended on the sampling date, forming 3 profile types (Figure 5). Relative particle numbers decreasing exponentially with depth were observed, when supply from above exceeded degradation, either due to diatom blooms (Jul 97, *Rhizosolenia imbricata*)

or because of low temperatures slowing down degradation (Jan 98, 15 Mar 98). When supply and removal were balanced, profiles were vertical. The 1998 diatom spring bloom was followed by a summer poor in diatom phytoplankton and favouring decomposition and hydrodynamic removal, causing a subsurface maximum of relative particle numbers (Figure 5c). Phytoplankton blooms generally provide large numbers of monospecific, almost equally sized cells, and thus, *B. brockmannii* frustules from the 1997 and 1998 spring blooms dominated the 15-20  $\mu\text{m}$  size class in our samples. The 1997 summer and autumn blooms, however, failed to become likewise evident, as they were far less pronounced and apparently insufficient to prevail among the older frustules accumulated in the sediment.

Shortly after a diatom bloom in Sep 97, diatom biovolumes were significantly correlated to POC and Chl concentrations, supporting that diatoms were a major source of sedimentary organic carbon. During the rest of the year this relation was less prominent, as different degrees of hydrodynamic mobility and biogeochemical lability of diatoms, organic carbon and Chl interfered. The significant correlation between diatom and carbohydrate inventories emphasises diatoms as the main provenance of intra- and extracellular carbohydrates.

#### *Sedimentary organic matter*

Phytopigments are widely used as biomarkers to trace transport or degradation pathways of algal material or to reveal the origin of phytodetritus, the major food source of heterotrophic microbenthos. In this study, chloropigment concentrations served as a measure of the amounts of relatively fresh algal material, chloropigment composition to assess its state of degradation, carotenoid composition to reveal its provenance from certain algal classes, and bacteriochlorophyll to estimate the number of phototrophic bacteria.

Generally canthaxanthin serves as a biomarker for cyanobacteria, peridinin for Dinophyceae, and lutein for Rhodophyceae and Chlorophyceae (Goodwin 1980, Bianchi et al. 1988, Rowan 1989, Abele-Oeschger 1991, Steenbergen et al. 1994). As none of these carotenoids was detected, we conclude that cyanobacteria, dinoflagellates and macroalgae constituted a trifling part of the phytodetritus and phytobenthos in our sandflat. Fucoxanthin or close derivatives are the major carotenoid of Bacillariophyceae, Haptophyceae and Phaeophyceae (Goodwin 1980, Rowan 1989, Abele-Oeschger 1991). They were prevalent in our samples, corresponding to the dominance of diatoms in Königshafen phytoplankton and phytobenthos at sandy sites (Asmus & Bauerfeind 1994) or to detrital *Fucus* spec. growing in other parts of the bay (Schories et al. 1997). The apparent absence of carotenoids in the second summer of our study may be explained by a combination of low algal cell numbers (see above) with the relatively high detection limit.

Chloropigments, especially the most hydrophobic ones, proved to be good indicators of sedimentary organic matter, as they were significantly correlated to POC and carbohydrates. However, there was no correlation to the diatom biovolume, probably because the decomposition of frustules was much slower than that of pigments.

The set of hydrophobic chloropigments (chlorophyll, pheophytin, pheophorbide) was used as a marker for barely degraded material. In most profiles, its share tended to decrease downcore, but was often present even in 4-5 cm depth (Figure 6). This deep penetration of fresh phytodetritus demonstrated the close link between the water column and at least the uppermost 5 cm of our permeable sediment. Likewise temporally, seston composition and phytoplankton blooms were closely related to the sedimentary chloropigment composition. Chlorophyll, albeit the most labile fraction of organic matter (Henrichs & Doyle 1986), was more quickly entered and transported through the upper sediment strata than decomposed.

This emphasises the efficiency of interfacial and subsurface particle transport by advection, considered a major mechanism in our sandflat, whereas bioturbation and ripple migration were less important (Rusch et al. 1999, submitted).

Several depth profiles of Chl concentrations had a subsurface maximum (Figure 6), that can be attributed to the same hydrodynamic processes that caused subsurface maxima in bacterial cell numbers (Figure 1) and the concentration of fine particulate material. Subsurface Chl maxima were occasionally detected in the finer-grained sediments of Long Island Sound, USA (Sun et al. 1991, Sun et al. 1994), and at two North Sea sites exposed to near-bottom water currents of up to  $0.25 \text{ m s}^{-1}$  (Frisian Front) and up to  $0.45 \text{ m s}^{-1}$  (Broad Fourteens) over a fine sandy bottom and over medium coarse sand, respectively (Boon & Duineveld 1998). In Long Island Sound they were explained as a consequence of rates and mechanisms of decay varying with depth, seasonally changing input, and non-diffusive vertical transport by conveyor-belt feeders (Sun et al. 1991, Sun et al. 1994). Non-local mixing was considered a major cause at the North Sea locations, particularly at the Frisian Front station abundant in macrozoobenthos, and advective transport possibly enhanced interfacial particle fluxes at station Broad Fourteens (Boon & Duineveld 1998). We suggest that generally the deep penetration of fine-grained POM is advectively enhanced in sandy shelf sediments subject to moderate near-bottom currents. Furthermore, resuspension and depth-dependent decomposition, both enhanced advectively as well, may partially remove near-surface POM and thereby cause a subsurface maximum.

#### *Carbohydrates produced and consumed by bacteria*

Besides intracellular storage polysaccharides, copious amounts of exopolymeric substances (EPS) are produced by aquatic micro-organisms, benthic diatoms, benthic fauna and colony-forming planktonic algae. Capsule EPS high in glycoproteins are primarily produced during the log phase of growth, whereas mucus EPS are largely polysaccharide and mainly secreted in the stationary phase or during nutrient limitation (Decho & Lopez 1993). Their various ecological functions include cell attachment, locomotion, protection from desiccation or digestion, and sorption of solutes and colloidal compounds (Decho & Lopez 1993, Underwood et al. 1995, Smith & Underwood 1998).

Mainly dealing with microbial or diatom mats, former studies on sedimentary polysaccharides have focused on the uppermost centimetre. We show profiles of carbohydrates in a sandy marine sediment down to 12 cm depth (Figure 4).

The sea water soluble fraction, containing diatom motility polysaccharides (Underwood et al. 1995), comprised only 1 % of the carbohydrates in our Sylt sediment. We sampled before complete exposure of the study site, and water soluble carbohydrates could not accumulate during submergence, or this labile DOC was rapidly degraded. The EDTA extractable fraction, containing more tightly bound EPS, bacterial capsular EPS and some intracellular carbohydrates due to cell leakage (Underwood et al. 1995), amounted to 5.7 % of the carbohydrates in our sandflat. Accordingly, the vast majority of sedimentary polysaccharides was intracellular or very tightly bound to particles. With increasing proximity to the sediment surface, i.e. increasing hydrodynamic impact, carbohydrates tended to be increasingly adsorbed to the coarse sand grains and decreasingly to the fine fraction, that was more susceptible to resuspension and advective removal from the sediment.

In summer total carbohydrate concentrations decreased exponentially with depth, whereas winter profiles were almost vertical (Figure 4). The concentrations in winter or below 5 cm depth represented the refractory part, and planktonic and benthic primary production in

summer added more easily degradable material to the upper 5 cm of the sediment. In summer 1998, there were less carbohydrates than in summer 1997, with a corresponding interannual difference in bacterial inventories (Figure 2). The second summer of our study was characterised by stronger winds, less sunshine and lower temperatures than the first one (Deutscher Wetterdienst 1998, unpubl. data), so polysaccharide production in the course of overflow metabolism (Staats 1999) was less pronounced. Throughout the year, significantly correlated concentrations were detected most often between carbohydrates and Chl (Table 4), indicating their similarly high lability. The concentrations of the more refractory bulk POC were correlated to the other OM indicators only in Jul 97 and Jul 98 (Table 4), when labile components dominated sedimentary POC.

#### *Permeable sediments as microbial habitat*

Maximum numbers of bacteria were found neither at the sediment surface nor associated with largest amounts of sedimentary POM, but with the organic-richest fine particles (Figure 3). Intense carbon turnover (Table 3) catalysed by the relatively small microbial population of an organic-poor sand was facilitated by the deep penetration of POM and oxidants into the sediment. In permeable, non-accumulating sands, solute and particle fluxes across the water-sediment interface are enhanced by advection, with sediment permeability among the main factors controlling transport rates and penetration depths (Forster et al. 1996, Huettel et al. 1996, Shum & Sundby 1996).

Sediment permeabilities may be modified by exopolysaccharides, but in our sandflat, carbohydrate concentrations were relatively low and apparently insufficient to cause measurable changes in permeability, as evident in the lack of significant correlation. Although sediment permeability varied temporally, it appeared unrelated to the seasons. Throughout the year only minor changes occurred in the fine particle concentration below 5 cm depth, so seasonal changes in the grain size distribution of the top 5 cm had no clearly measurable effect on the permeability of a 15-20 cm long core. To assess temporal and spatial variations of sediment permeability and relate them to advective flow and its consequences, in situ measurements with sufficient depth resolution are needed. Our sediment exhibited significant vertical variation of median grain size and porosity, that may serve as a crutch to roughly estimate the corresponding variation of permeability but cannot substitute direct measuring.

Mostly, marine sediments are characterised by grain size and porosity, and there are several empirical approaches to estimate permeability from granulometric data. We compared measured permeabilities to calculated ones (Table 1) and found no satisfactory conformity. Although both  $k_{KM}$  and  $k_H$  were significantly correlated to  $k$  with a slope near unity, there was a considerable offset, so that calculated values were about 4 times the measured ones. The Carman/Kozeny approach, applicable to almost spherical, well-sorted grains (Nield & Bejau 1992), even resulted in 5 times the measured permeabilities. Equations predicting aquifer permeabilities from grain size generally give poor estimates (Eggleston & Rojstaczer 1998), with errors often more than an order of magnitude (Shepherd 1989). Logarithmic scaling and interpolation to determine  $d_{10}$ ,  $d_{50}$  and  $\sigma(\phi)$  may have introduced a relative error of 0.1 each, and with an estimated relative error of 0.05 in the determination of  $p_0$ , these errors added up to 0.68, 0.45 and 0.20 for  $k_{KM}$ ,  $k_{CK}$  and  $k_H$ , respectively. Moreover, the sediment cores had possibly been compacted by sampling, and some experimental error was added by the measuring system. But still these errors fail to explain the full discrepancy. We prefer to rely on direct measurements rather than on the estimation approaches.

### *Conclusions*

Shallow water sediments like the sandflat we studied are often exposed to strong near-bottom water currents and are well-supplied with POM from the euphotic zone. Their high permeability facilitates deep-reaching advective transport of POM, oxidants, bacteria and degradation products into and out of the sediment, so that sandy continental shelf sediments may play an important role in marine organic matter turnover in spite of their low organic content. In an intertidal sandflat previously characterised as strongly influenced by advective interfacial and subsurface flows, we have used phytopigments to show the close link between water column and the uppermost 5 cm of the sediment. The microbial population was spatially and temporally highly dynamic and rapidly mineralised organic matter, attributable to advectively enhanced interfacial fluxes of solutes and particles. The hydrodynamic influence was also revealed in the adsorption of carbohydrates to the coarse sand matrix increasing towards the sediment surface. Together with earlier data from the same study (Rusch et al. 1999, submitted) and various significant intercorrelations, our investigations have sketched a coherent picture of the circumstances, organisms, substances and processes involved in the ecologically significant biogeochemistry of sandy intertidal sediments.

### Acknowledgements

We thank M. Alisch for her help during field work and the BAH Wadden Sea Station for providing lab space and detailed information on Königshafen. Deutscher Wetterdienst (DWD) kindly placed local weather data throughout the study period at our disposal. We acknowledge F. Garcia-Pichel and J. Zopfi for providing pigment standards and advice in HPLC analysis and appreciate valuable discussions with B. B. Jørgensen. This study was supported by the Max Planck Society (MPG), and A. R. received a postgraduate scholarship from Deutsche Forschungsgemeinschaft (DFG).

### 3. SUMMARY

#### 3.1. Summary and outlook

This thesis presents new findings on the dynamics of fine-grained organic material in permeable shelf sediments, founded on in situ experiments and a one-year field study in an intertidal sandflat. The main results of these investigations are:

In shallow shelf regions, advective exchange of solutes and particles between the bottom water and permeable sandy sediments can be a fast and efficient transport process. Within 13 h, tracer particles (1-30  $\mu\text{m}$ ) were carried ca. 5 cm into coarse-grained (500-1000  $\mu\text{m}$ ) sediment. The net rate of bottom water "filtration" by this sediment averaged 14  $\text{l m}^{-2} \text{h}^{-1}$ .

The depth distributions of natural and artificial particles depended on sediment permeability and particle size. Thus, the corresponding results of earlier laboratory studies are confirmed in a natural marine environment.

The depth distributions of fine-grained (< 70  $\mu\text{m}$ ) material and pore water characteristics in natural sandy sediment indicated hydrodynamic influence down to 4-8 cm below the sediment surface. Worst case estimates of biodiffusion coefficients at the study site imply only minor macrofaunal contribution to particle transport.

Bacteria (2-9 % of the POC) were less susceptible to water flows through the sediment than the interstitial fine-grained material, as part of the population lived attached to large, heavy sand grains. The vertical distribution of bacteria was closely related to the organic carbon content of the fine-grained particulate matter.

The hydrodynamic influence on the studied shelf sediment was also revealed in the adsorption of carbohydrates to the coarse sand matrix increasing towards the sediment surface.

Advective interfacial and subsurface flows can be responsible for a tight coupling between the water column and sandy sediments. The depth distribution of planktonic diatoms found in the sediment was related to weather and phytoplankton conditions, and relatively fresh phytodetritus penetrated at least 5 cm into the permeable bottom.

Areal inventories of POC, PN and Chl as well as depth profiles of POC and Chl contents, DIN concentrations and bacterial cell numbers showed strong seasonal variation affecting the uppermost 5 cm of the sediment. Advective transport appeared most important in winter and spring, whereas early diagenetic processes rather dominated in summer and autumn.

Advectively enhanced penetration of POM and dissolved oxidants can increase the sedimentary capacity and rates of organic matter decomposition. Carbon mineralisation rates at the study site ranged between 20  $\text{mg C m}^{-2} \text{d}^{-1}$  in winter and 580  $\text{mg C m}^{-2} \text{d}^{-1}$  in summer, keeping step with rates reported of finer-grained sediments that contained an order of magnitude more organic carbon.

These results support that the hydrodynamic regime of shelf seas enhances biogeochemical dynamics in permeable sands. Well-supplied with organic matter from the highly productive euphotic zone and efficiently trapping POM, sandy shelf sediments nevertheless maintain their non-accumulating character due to high turnover and flushing rates. As permeable sediments cover extensive areas of the continental shelves, they should be reconsidered with respect to quantitative importance in the marine carbon cycle.

Besides various implications on organic matter turnover, advective solute and particle transport undoubtedly also influences the benthic ecology of sandy shallow water sediments. Further studies could provide interesting insights in microbial communities that are exposed to and adapted to different degrees of seasonal and hydrodynamic influence and environmental variability.

This study has shown features and effects of advective interfacial and interstitial water flows in a particular marine environment. However, the importance and implications of advective transport processes remain to be investigated in a variety of other marine and limnic ecosystems.

Sediment permeability has been revealed a key factor for advective fluxes, but closer investigations are hampered by the lack of sensitive and precise methods to measure hydraulic conductivities in situ with sufficient depth resolution. Methodical developments, like a suitable in situ permeameter or shipboard techniques for taking undisturbed cores from permeable subtidal sediments, could largely improve future research on sandy sediments.

### 3.2. Zusammenfassung und Ausblick

Die vorliegende Arbeit stellt neue Erkenntnisse über die Dynamik feinkörnigen organischen Materials in permeablen Schelfsedimenten vor. Sie gründen auf in-situ-Experimenten und einer einjährigen Feldstudie an einem Sandwatt-Standort. Die wichtigsten Ergebnisse dieser Untersuchungen sind:

In flachen Schelfgebieten kann der advective Austausch gelöster und partikulärer Stoffe zwischen dem bodennahen Wasser und permeablen sandigen Sedimenten ein schneller und wirkungsvoller Transportprozeß sein. Tracerpartikel (1-30  $\mu\text{m}$ ) wurden innerhalb von 13 h etwa 5 cm tief in grobkörniges (500-1000  $\mu\text{m}$ ) Sediment eingetragen. Dieses Sediment "filtrierte" Bodenwasser mit einer mittleren Nettorate von  $14 \text{ l m}^{-2} \text{ h}^{-1}$ .

Die Tiefenverteilung natürlicher und künstlicher Partikel hing von der Permeabilität des Sedimentes und der Größe der Partikel ab. Damit werden entsprechende Ergebnisse früherer Laborversuche in einem natürlichen marinen Umfeld bestätigt.

Die Tiefenverteilung feinkörnigen ( $< 70 \mu\text{m}$ ) Materials und die Beschaffenheit des Porenwassers in natürlichem sandigem Sediment geben zu erkennen, daß der Einfluß hydrodynamischer Prozesse bis in 4-8 cm Tiefe reichte. Eine Abschätzung des größtmöglichen Biodiffusionskoeffizienten am Probenahmeort läßt darauf schließen, daß Makrofauna dort nur wenig zum Partikeltransport beiträgt.

Bakterien (2-9 % des POC) wurden von Wasserströmen durch das Sediment weniger mitbewegt als das feinkörnige Material im Porenraum. Ein Teil der Population war demnach relativ fest mit großen, schweren Sandkörnern verbunden. Die vertikale Verteilung der Bakterien stand in engem Zusammenhang mit dem Gehalt der Feinfraktion an organischem Kohlenstoff.

Der hydrodynamische Einfluß auf das untersuchte Schelfsediment äußerte sich auch in einer Zunahme der Adsorption von Kohlehydraten an die grobe Sandmatrix zur Sedimentoberfläche hin.

Advektive Flüsse durch und unterhalb der Grenzfläche zwischen Wassersäule und sandigen Sedimenten können diese Kompartimente eng aneinander koppeln. Die Tiefenverteilung planktischer Diatomeen im Sediment hing mit den Wetterverhältnissen und der Phytoplanktonsituation zusammen, und relativ frischer Phytodetritus gelangte mindestens 5 cm tief in den permeablen Meeresboden.

Flächenbezogene Mengen von POC, PN und Chl sowie Tiefenprofile der POC- und Chl-Gehalte, der DIN-Konzentrationen und Bakterienzahlen zeigten starke jahreszeitliche Veränderungen in den obersten 5 cm des Sedimentes. Advektiver Transport schien im Winter und Frühjahr von größter Bedeutung zu sein, während Frühdiagenese eher im Sommer und Herbst dominierte.

Advektiv verstärkter und vertiefter Eintrag von POM und gelösten Oxidationsmitteln kann die Abbaukapazität des Sedimentes und die Umsatzraten organischen Materials erhöhen. Im untersuchten Sandwatt reichten die Raten der Kohlenstoffmineralisation von  $20 \text{ mg C m}^{-2} \text{ d}^{-1}$  im Winter bis zu  $580 \text{ mg C m}^{-2} \text{ d}^{-1}$  im Sommer. Sie liegen damit im gleichen Bereich wie (Literatur-)Raten in feinerkörnigen Sedimenten mit erheblich höherem Gehalt an organischem Kohlenstoff.

Diese Ergebnisse belegen, daß die Hydrodynamik in Schelfmeeren die biogeochemische Dynamik permeabler Sande verstärkt. Obwohl viel organisches Material aus der hochproduktiven euphotischen Zone an sandige Schelfböden gelangt und dort effizient eingefangen wird, bleibt der nichtaccumulierende Charakter dieser Sedimente durch intensiven Umsatz und Durchspülung erhalten. Permeable Sedimente bedecken weite Teile des Kontinentalschelfs und verdienen daher auch im Hinblick auf ihre quantitative Bedeutung im marinen Kohlenstoffkreislauf weitere Betrachtungen.

Neben verschiedenen Auswirkungen auf den Umsatz organischen Materials beeinflußt der advektive Transport von Partikeln und gelösten Stoffen zweifellos auch die benthische Ökologie sandiger Flachwassersedimente. Zukünftige Forschung könnte interessante Einblicke in mikrobielle Gemeinschaften vermitteln, die saisonalen und hydrodynamischen Einflüssen sowie schwankenden Umweltbedingungen in unterschiedlichem Maße ausgesetzt und daran angepaßt sind.

Die Eigenschaften und Wirkungen advektiver Flüsse an der Wasser-Sediment-Grenzschicht und durch den Porenraum sind hier für ein bestimmtes marines Umfeld untersucht worden. Die Bedeutung und Auswirkungen advektiver Transportprozesse in diversen anderen marinen und limnischen Ökosystemen ist jedoch bisher nicht erforscht.

Die Permeabilität des Sedimentes hat sich als Schlüsselfaktor für advective Flüsse erwiesen, aber genauere Untersuchungen scheitern daran, daß empfindliche und genaue Methoden fehlen, um hydraulische Leitfähigkeiten in situ mit ausreichender Tiefenauflösung zu messen. Methodische Fortschritte wie ein geeignetes in-situ-Permeameter oder schiffstaugliche Verfahren, ungestörte Kerne auch aus permeablen subtidalen Sedimenten zu erhalten, könnten die zukünftige Forschung an sandigen Sedimenten erheblich fördern.

## 4. REFERENCES

Abele-Oeschger, D, 1991. Potential of some carotenoids in two recent sediments of Kiel Bight as biogenic indicators of phytodetritus.

*Marine Ecology Progress Series* **70**, 83-92.

Aleev, MY, 1991. A new method for determining the swimming velocity of plankton organisms.

*Gidrobioloicheskii Zhurnal* **27**, 70-74.

Aller, RC, 1978. The effects of animal-sediment interactions on geochemical processes near the sediment-water interface.

In: Wiley, ML (ed.). *Estuarine Interactions*. Academic Press.

Andersen, FØ & Helder, W, 1987. Comparison of oxygen microgradients, oxygen flux rates and electron transport system activity in coastal marine sediments.

*Marine Ecology Progress Series* **37**, 59-264.

Anderson, RF, Rowe, GT, Kemp, PF, Trumbore, S & Biscaye, PE, 1994. Carbon budget for the mid-slope depocenter of the Middle Atlantic Bight.

*Deep Sea Research II (Topical Studies in Oceanography)* **41**, 669-703.

Anton, KK, Liebezeit, G, Rudolph, C & Wirth, H, 1993. Origin, distribution and accumulation of organic carbon in the Skagerrak.

*Marine Geology* **111**, 287-297.

Asmus, RM & Bauerfeind, E, 1994. The microphytobenthos of Königshafen - spatial and seasonal distribution on a sandy tidal flat.

*Helgoländer Meeresuntersuchungen* **48**, 257-276.

Austen, G, 1994. Hydrodynamics and particulate matter budget of Königshafen, southeastern North Sea.

*Helgoländer Meeresuntersuchungen* **48**, 183-200.

Austen, I, 1997. Temporal and spatial variations of biodeposits - a preliminary investigation of the role of fecal pellets in the Sylt-Rømø tidal area.

*Helgoländer Meeresuntersuchungen* **51**, 281-294.

Bacon, MP, Belastock, RA & Bothner, MH, 1994.  $^{210}\text{Pb}$  balance and implications for particle transport on the continental shelf, U.S. Middle Atlantic Bight.

*Deep Sea Research II (Topical Studies in Oceanography)* **41**, 511-535.

Basu, AJ & Khalili, A, 1999. Computation of flow through a fluid-sediment interface in a benthic chamber.

*Physics of Fluids* **11**, 1395-1405.

- Beavers, GJ & Joseph, DD, 1967. Boundary conditions at a naturally permeable wall. *Journal of Fluid Mechanics* **30**, 197-207.
- Beukema, JJ, Essink, K, Michaelis, H & Zwarts, L, 1993. Year-to-year variability in the biomass of macrobenthic animals on tidal flats of the Wadden Sea: How predictable is this food source for birds? *Netherlands Journal of Sea Research* **31**, 319-330.
- Bianchi, TS, Dawson, R & Sawangwong, P, 1988. The effects of macrobenthic deposit-feeding on the degradation of chloropigments in sandy sediments. *Journal of Experimental Marine Biology and Ecology* **122**, 243-255.
- Boon, AR & Duineveld, GCA, 1998. Chlorophyll a as a marker for bioturbation and carbon flux in southern and central North Sea sediments. *Marine Ecology Progress Series* **162**, 33-43.
- Boon, AR, Duineveld, GCA, Berghuis, EM & van der Weele, JA, 1998. Relationships between benthic activity and the annual phytopigment cycle in near-bottom water and sediments in the Southern North Sea. *Estuarine, Coastal and Shelf Science* **46**, 1-13.
- Bordovskiy, OK, 1965. Accumulation and transformation of organic substances in marine sediments. 3. Accumulation of organic matter in bottom sediments. *Marine Geology* **3**, 33-82.
- Boudreau, BP, 1997. Diagenetic models and their implementation: modelling transport and reactions in aquatic sediments. Springer-Verlag.
- Boudreau, BP, 1998. Mean mixed depth of sediments: The wherefore and the why. *Limnology and Oceanography* **43**, 524-526.
- Braman, RS & Hendrix, SA, 1989. Nanogram nitrite and nitrate determination in environmental and biological materials by vanadium(III) reduction with chemiluminescence detection. *Analytical Chemistry* **61**, 2715-2718.
- Brinkman, HC, 1947. On the permeability of media consisting of closely packed porous particles. *Applied Sciences Research* **A1**, 81-86.
- Burford, MA, Long, BG & Rothlisberg, PC, 1994. Sedimentary pigments and organic carbon in relation to microalgal and benthic faunal abundance in the Gulf of Carpentaria. *Marine Ecology Progress Series* **103**, 111-117.
- Buscail, R, Pocklington, R & Germain, C, 1995. Seasonal variability of the organic matter in a sedimentary coastal environment: Sources, degradation and accumulation (continental shelf of the Gulf of Lions, northwestern Mediterranean Sea). *Continental Shelf Research* **15**, 843-869.

Canfield, DE, Thamdrup, B & Hansen, JW, 1993. The anaerobic degradation of organic matter in Danish coastal sediments: Iron reduction, manganese reduction, and sulfate reduction. *Geochimica et Cosmochimica Acta* **57**, 3867-3883.

Churchill, JH, Wirick, CD, Flagg, CN & Pietrafesa, LJ, 1994. Sediment resuspension over the continental shelf east of the Delmarva Peninsula. *Deep Sea Research II* **41**, 341-363.

Clement, TP, Peyton, BM, Skeen, RS, Jennings, DA & Petersen, JN, 1997. Microbial growth and transport in porous media under denitrification conditions: Experiments and simulations. *Journal of Contaminant Hydrology* **24**, 269-285.

Dade, WB, Davis, JD, Nichols, PD, Nowell, ARM, Thistle, D, Trexler, MB & White, DC, 1990. Effects of bacterial exopolymer adhesion on the entrainment of sand. *Geomicrobiology Journal* **8**, 1-16.

Darcy, HPG, 1856. Les Fontaines Publiques de la Ville de Dijon. Victor-Dalmont.

Decho, AW & Lopez, GR, 1993. Exopolymer microenvironments of microbial flora: Multiple and interactive effects on trophic relationships. *Limnology and Oceanography* **38**, 1633-1645.

DeFlaun, MF & Mayer, LM, 1983. Relationships between bacteria and grain surfaces in intertidal sediments. *Limnology and Oceanography* **28**, 873-881.

Dyer, KR, 1986. Coastal and estuarine sediment dynamics. John Wiley & Sons.

Eggleston, J & Rojstaczer, S, 1998. Inferring spatial correlation of hydraulic conductivity from sediment cores and outcrops. *Geophysical Research Letters* **25**, 2321-2324.

Eisma, D, 1993. Suspended matter in the aquatic environment. Springer.

Eisma, D & Kalf, J, 1987. Distribution, organic content and particle size of suspended matter in the North Sea. *Netherlands Journal of Sea Research* **21**, 265-285.

Emerson, CW, 1990. Influence of sediment disturbance and water flow on the growth of the soft shell clam *Mya arenaria* L. *Canadian Journal of Fisheries & Aquatic Sciences* **47**, 1655-1663.

Emery, KO, 1968. Relict sediments on continental shelves of world. *American Association of Petroleum Geologists Bulletin* **52**, 445-464.

- Epstein, SS & Rossel, J, 1995. Enumeration of sandy sediment bacteria: search for optimal protocol.  
*Marine Ecology Progress Series* **117**, 289-298.
- Fabregas, J, Abalde, J & Herrero, C, 1989. Biogeochemical composition and growth of the marine microalga *Dunaliella tertiolecta* Butcher with different ammonium nitrogen concentrations and chloride, sulfate, nitrate, and carbonate.  
*Aquaculture* **83**, 289-304.
- Forster, S & Graf, G, 1995. Impact of irrigation on oxygen flux into the sediment: intermittent pumping by *Callianassa subterranea* and "piston pumping" by *Lanice conchilega*.  
*Marine Biology* **123**, 335-346.
- Forster, S, Huettel, M & Ziebis, W, 1996. Impact of boundary layer flow velocity on oxygen utilization in coastal sediments.  
*Marine Ecology Progress Series* **143**, 173-185.
- Galloway, JN, Howarth, RW, Michaels, AF, Nixon, SW, Prospero, JM & Dentener, FJ, 1996. Nitrogen and phosphorus budgets of the North Atlantic Ocean and its watershed.  
*Biogeochemistry* **35**, 3-25.
- Gehlen, M, Malschaert, H & Vanraaphorst, WR, 1995. Spatial and temporal variability of benthic silica fluxes in the southeastern North Sea.  
*Continental Shelf Research* **15**, 1675-1696.
- Glud, RN, Forster, S & Huettel, M, 1996. Influence of radial pressure gradients on solute exchange in stirred benthic chambers.  
*Marine Ecology Progress Series* **141**, 303-311.
- Glud, RN, Gundersen, JK, Revsbech, NP, Jørgensen, BB & Huettel, M, 1995. Calibration and performance of the stirred flux chamber from the benthic lander Elinor.  
*Deep-Sea Research I* **42**, 1029-1042.
- Goodwin, TW, 1980. The biochemistry of the carotenoids. Chapman & Hall.
- Graf, G, 1992. Benthic-pelagic coupling: a benthic view.  
*Oceanography and Marine Biology Annual Review* **30**, 149-190.
- Grant, J, Cranford, P & Emerson, C, 1997. Sediment resuspension rates, organic matter quality and food utilization by sea scallops (*Placopecten magellanicus*) on Georges Bank.  
*Journal of Marine Research* **55**, 965-994.
- Grant, J & Gust, G, 1987. Prediction of coastal sediment stability from photopigment content of mats of purple sulphur bacteria.  
*Nature* **330**, 244-246.

- Hall, POJ & Aller, RC, 1992. Rapid, small-volume, flow injection analysis for  $\Sigma\text{CO}_2$  and  $\text{NH}_4^+$  in marine and freshwaters.  
*Limnology and Oceanography* **37**, 1113-1119.
- Hansen, LS & Blackburn, TH, 1992. Effect of algal bloom deposition on sediment respiration and fluxes.  
*Marine Biology* **112**, 147-152.
- Haq, BU & Boersma, A (ed.), 1978. Introduction to marine micropaleontology. Elsevier Biomedical.
- Hargrave, BT, 1972. Aerobic decomposition of sediment and detritus as a function of particle surface area and organic content.  
*Limnology and Oceanography* **17**, 583-596.
- Harrison, WD, Musgrave, D & Reeburgh, WS, 1983. A wave-induced transport process in marine sediments.  
*Journal of Geophysical Research* **88**, 7617-7622.
- Harvey, HR, Tuttle, JH & Bell, JT, 1995. Kinetics of phytoplankton decay during simulated sedimentation: Changes in biochemical composition and microbial activity under oxic and anoxic conditions.  
*Geochimica et Cosmochimica Acta* **59**, 3367-3377.
- Harvey, JW & Nuttle, WK, 1995. Fluxes of water and solute in a coastal wetland sediment. 2. Effect of macropores on solute exchange with surface water.  
*Journal of Hydrology* **164**, 109-125.
- Hasle, GR, von Stosch, HA & Syvertsen, EE, 1983. Cymatosiraceae, a new diatom family.  
*Bacillaria* **6**, 9-156.
- Henrichs, SM & Doyle, AP, 1986. Decomposition of  $^{14}\text{C}$ -labeled organic substances in marine sediments.  
*Limnology and Oceanography* **31**, 765-778.
- Hsü, KJ, 1989. Physical principles of sedimentology. Springer.
- Huettel, M, 1988. Zur Bedeutung der Macrofauna für die Nährsalzprofile im Wattsediment. PhD thesis, Christian-Albrechts-Universität Kiel.
- Huettel, M & Gust, G, 1992a. Impact of bioroughness on interfacial solute exchange in permeable sediments.  
*Marine Ecology Progress Series* **89**, 253-267.
- Huettel, M & Gust, G, 1992b. Solute release mechanisms from confined sediment cores in stirred benthic chambers and flume flows.  
*Marine Ecology Progress Series* **82**, 187-197.

- Huettel, M, Ziebis, W & Forster, S, 1996. Flow-induced uptake of particulate matter in permeable sediments.  
*Limnology and Oceanography* **41**, 309-322.
- Huettel, M, Ziebis, W, Forster, S & Luther III, GW, 1998. Advective transport affecting metal and nutrient distributions and interfacial fluxes in permeable sediments.  
*Geochimica et Cosmochimica Acta* **62**, 613-631.
- Jago, CF & Jones, SE, 1998. Observation and modelling of the dynamics of benthic fluff resuspended from a sandy bed in the southern North Sea.  
*Continental Shelf Research* **18**, 1255-1265.
- Jahnke, RA, Marinelli, RL, Eckmann, JE & Nelson, JR, 1996. Porewater nutrient distributions in nonaccumulating, sandy sediments of the South Atlantic Bight continental shelf.  
*EOS* **76**, 202.
- Jenness, MI & Duineveld, GCA, 1985. Effects of tidal currents on chlorophyll a content of sandy sediments in the southern North Sea.  
*Marine Ecology Progress Series* **21**, 283-287.
- Jickells, TD, 1998. Nutrient biogeochemistry of the coastal zone.  
*Science* **281**, 217-222.
- Jones, SE, Jago, CF, Bale, AJ, Chapman, D, Howland, RJM & Jackson, J, 1998. Aggregation and resuspension of suspended particulate matter at a seasonally stratified site in the southern North Sea - physical and biological controls.  
*Continental Shelf Research* **18**, 1283-1309.
- Jørgensen, BB, 1996. Material flux in the sediment.  
In: Jørgensen, BB & Richardson, K (ed.). *Eutrophication in Coastal Marine Ecosystems*. American Geophysical Union.
- Karsten, U & Garcia-Pichel, F, 1996. Carotenoids and mycosporine-like amino acid compounds in members of the genus *Microcoleus* (cyanobacteria): a chemosystematic study.  
*Systematic and Applied Microbiology* **19**, 285-294.
- Kennish, MJ (ed.), 1994. *Practical handbook of marine science*. CRC Press.
- Khalili, A, Basu, AJ & Huettel, M, 1997. A non-Darcy model for recirculating flow through a fluid-sediment interface in a cylindrical container.  
*Acta Mechanica* **123**, 75-87.
- Khalili, A, Basu, AJ, Pietrzyk, U & Raffel, M, 1999. An experimental study of recirculating flow through fluid-sediment interfaces.  
*Journal of Fluid Mechanics* **383**, 229-247.

- Kingston, MB, 1999. Wave effects on the vertical migration of two benthic microalgae: *Hantzschia virgata* var. *intermedia* and *Euglena proxima*. *Estuaries* **22**, 81-91.
- Klute, A & Dirksen, C, 1986. Hydraulic conductivity and diffusivity: laboratory methods. In: Klute, A (ed.). *Methods of soil analysis - part 1 - physical and mineralogical methods*. American Society of Agronomy.
- Kristensen, E & Blackburn, TH, 1987. The fate of organic carbon and nitrogen in experimental marine sediment systems: Influence of bioturbation and anoxia. *Journal of Marine Research* **45**, 231-257.
- Kristensen, E & Hansen, K, 1995. Decay of plant detritus in organic-poor marine sediment: production rates and stoichiometry of dissolved C and N compounds. *Journal of Marine Research* **53**, 675-702.
- Kristensen, E, Jensen, MH & Jensen, KM, 1997. Temporal variations in microbenthic metabolism and inorganic nitrogen fluxes in sandy and muddy sediments of a tidally dominated bay in the northern Wadden Sea. *Helgoländer Meeresuntersuchungen* **51**, 295-320.
- Kröncke, I, Dippner, JW, Heyen, H & Zeiss, B, 1998. Long-term changes in macrofaunal communities off Norderney (East Frisia, Germany) in relation to climate variability. *Marine Ecology Progress Series* **167**, 25-36.
- Krumbein, WE, Paterson, DM & Stal, LJ (ed.), 1994. *Biostabilization of sediments*. Bibliotheks- und Informationssystem der Universität Oldenburg.
- Logan, BE & Kirchman, DL, 1991. Uptake of dissolved organics by marine bacteria as a function of fluid motion. *Marine Biology* **111**, 175-181.
- Lohse, L, Epping, EHG, Helder, W & van Raaphorst, W, 1996. Oxygen pore water profiles in continental shelf sediments of the North Sea: turbulent versus molecular diffusion. *Marine Ecology Progress Series* **145**, 63-75.
- Lohse, L, Malschaert, JFP, Slomp, C, Helder, W & van Raaphorst, W, 1995. Sediment-water fluxes of inorganic nitrogen compounds along the transport route of organic matter in the North Sea. *Ophelia* **41**, 173-197.
- Lohse, L, Malschaert, JFP, Slomp, CP, Helder, W & van Raaphorst, W, 1993. Nitrogen cycling in North Sea sediments: interaction of denitrification and nitrification in offshore and coastal areas. *Marine Ecology Progress Series* **101**, 283-296.

- Lustwerk, RL & Burdige, DJ, 1995. Elimination of dissolved sulfide interference in the flow injection determination of  $\Sigma\text{CO}_2$  by addition of molybdate.  
*Limnology and Oceanography* **40**, 1011-1012.
- Malan, DE & McLachlan, A, 1991. In situ benthic oxygen fluxes in a nearshore coastal marine system: a new approach to quantify the effect of wave action.  
*Marine Ecology Progress Series* **73**, 69-81.
- Marano, F, Berrebbah, H, Schovaert, D, Betrencourt, C & Volochine, B, 1989. Ciliary beat and cell motility of *Dunaliella*.  
Seventh International Congress of Biorheology, Nancy, France.
- Marinelli, RL & Boudreau, BP, 1996. An experimental and modeling study of pH and related solutes in an irrigated anoxic coastal sediment.  
*Journal of Marine Research* **54**, 939-966.
- Marinelli, RL, Jahnke, RA, Craven, DB, Nelson, JR & Eckman, JE, 1998. Sediment nutrient dynamics on the South Atlantic Bight continental shelf.  
*Limnology and Oceanography* **43**, 1305-1320.
- Mayer, LM, 1994. Surface area control of organic carbon accumulation in continental shelf sediments.  
*Geochimica et Cosmochimica Acta* **58**, 1271-1284.
- McCall, PL & Tevesz, MJS (ed.), 1982. Animal-sediment relations. Plenum Press.
- McCaulou, DR, Bales, RC & Arnold, RG, 1995. Effect of temperature controlled motility on transport of bacteria and microspheres through saturated sediment.  
*Water Resources Research* **31**, 271-280.
- McLachlan, A, 1996. Physical factors in benthic ecology - effects of changing sand particle size on beach fauna.  
*Marine Ecology Progress Series* **131**, 205-217.
- Miller, DC, 1989. Abrasion effects on microbes in sandy sediments.  
*Marine Ecology Progress Series* **55**, 73-82.
- Nedwell, DB, Parkes, RJ & Assinder, DJ, 1994. Seasonal fluxes across the sediment-water interface, and processes within sediments.  
In: Charnock, H, Dyer, KR, Huthnance, JM, Liss, PS, Simpson, JH & Tett, PB (ed.).  
Understanding the North Sea system. Chapman & Hall.
- Nelson, JR, Eckman, JE, Robertson, CY, Marinelli, RL & Jahnke, RA, 1999. Benthic microalgal biomass and irradiance at the sea floor on the continental shelf of the South Atlantic Bight: Spatial and temporal variability and storm effects.  
*Continental Shelf Research* **19**, 477-505.

- Nield, DA & Bejau, A, 1992. Convection in porous media. Springer.
- Olesen, M & Lundsgaard, C, 1995. Seasonal sedimentation of autochthonous material from the euphotic zone of a coastal system.  
*Estuarine, Coastal and Shelf Science* **41**, 475-490.
- Ong, B & Krishnan, S, 1995. Changes in the macrobenthos community of a sand flat after erosion.  
*Estuarine, Coastal and Shelf Science* **40**, 21-33.
- Osinga, R, Kop, AJ, Duineveld, GCA, Prins, RA & van Duyl, FC, 1996. Benthic mineralization rates at two locations in the southern North Sea.  
*Journal of Sea Research* **36**, 181-191.
- Pankow, H, 1990. Ostsee-Algenflora. Gustav-Fischer-Verlag.
- Pätsch, J & Radach, G, 1997. Long-term simulation of the eutrophication of the North Sea: temporal development of nutrients, chlorophyll and primary production in comparison to observations.  
*Journal of Sea Research* **38**, 275-310.
- Pilditch, CA, Emerson, CW & Grant, J, 1998. Effect of scallop shells and sediment grain size on phytoplankton flux to the bed.  
*Continental Shelf Research* **17**, 1869-1885.
- Reimers, CE, Glenn, SM & Creed, EL, 1996. The dynamics of oxygen uptake by shelf sediments.  
*EOS* **76**, 202.
- Reise, K, 1985. Tidal flat ecology. Springer-Verlag.
- Reise, K, Herre, E & Sturm, M, 1994. Biomass and abundance of macrofauna in intertidal sediments of Königshafen in the northern Wadden Sea.  
*Helgoländer Meeresuntersuchungen* **48**, 201-215.
- Revsbech, NP, 1989. An oxygen microsensor with guard cathode.  
*Limnology and Oceanography* **34**, 474-478.
- Rhoads, DC, 1973. The influence of deposit - feeding benthos on water turbidity and nutrient recycling.  
*American Journal of Science* **273**, 1-22.
- Rhoads, DC & Hecker, B, 1994. Processes on the continental slope off North Carolina with special reference to the Cape Hatteras region.  
*Deep Sea Research II* **41**, 965-980.

- Rice, DL, Bianchi, TS & Roper, EH, 1986. Experimental studies of sediment reworking and growth of Scoloplos spp. (Orbiniidae:Polychaeta).  
*Marine Ecology Progress Series* **30**, 9-19.
- Riedl, RJ, Huang, N & Machan, R, 1972. The subtidal pump, a mechanism of intertidal water exchange by wave action.  
*Marine Biology* **13**, 210-221.
- Riggs, SR, Snyder, SW, Hine, AC & Mearns, DL, 1996. Hardbottom morphology and relationship to the geologic framework - mid-Atlantic continental shelf.  
*Journal of Sedimentary Research Section A* **66**, 830-846.
- Ritzrau, W & Graf, G, 1992. Increase of microbial biomass in the benthic turbidity zone of Kiel Bight after resuspension by a storm event.  
*Limnology and Oceanography* **37**, 1081-1086.
- Rocha, C, 1998. Rhythmic ammonium regeneration and flushing in intertidal sediments of the Sado estuary.  
*Limnology and Oceanography* **43**, 823-831.
- Rowan, KS, 1989. Photosynthetic pigments of algae. Cambridge University Press.
- Rowe, GT, Boland, GS, Phoel, WC, Anderson, RF & Biscaye, PE, 1994. Deep-sea floor respiration as an indication of lateral input of biogenic detritus from continental margins.  
*Deep Sea Research II (Topical Studies in Oceanography)* **41**, 657-668.
- Rowe, GT, Clifford, CH, Smith, KLJ & Hamilton, PL, 1975. Benthic nutrient regeneration and its coupling to primary productivity in coastal waters.  
*Nature* **255**, 215-217.
- Rowe, GT, Smith, S, Falkowski, P, Whitledge, T, Theroux, R, Phoel, W & Ducklow, H, 1986. Do continental shelves export organic matter?  
*Nature* **324**, 559-561.
- Rowe, GT, Theroux, R, W., P, Quinby, H, Wilke, R, Koschoreck, D, Whitledge, TE, Falkowski, PG & Fray, C, 1988. Benthic carbon budgets for the continental shelf south of New England.  
*Continental Shelf Research* **8**, 511-527.
- Ruardij, P & van Raaphorst, W, 1995. Benthic nutrient regeneration in the ERSEM ecosystem model of the North Sea.  
*Netherlands Journal of Sea Research* **33**, 453-483.
- Saager, PM, Sweerts, J-P & Ellermeijer, HJ, 1990. A simple pore-water sampler for coarse, sandy sediments of low porosity.  
*Limnology and Oceanography* **35**, 747-751.

Sachs, L, 1997. *Angewandte Statistik*. Springer.

Sahm, K, MacGregor, BJ, Jørgensen, BB & Stahl, DA, 1999. Sulphate reduction and vertical distribution of sulphate-reducing bacteria quantified by rRNA slot-blot hybridization in a coastal marine sediment.

*Environmental Microbiology* **1**, 65-74.

Savant, SA, Reible, DD & Thibodeaux, LJ, 1987. Convective transport within stable river sediments.

*Water Resources Research* **23**, 1763-1768.

Schories, D, Albrecht, A & Lotze, H, 1997. Historical changes and inventory of macroalgae from Königshafen Bay in the northern Wadden Sea.

*Helgoländer Meeresuntersuchungen* **51**, 321-341.

Schovaert, D, Krishnaswamy, S, Couturier, M & Marano, F, 1988. Ciliary beat and cell motility of *Dunaliella* - computer analysis of high speed microcinematography.

*Biology of the Cell* **62**, 229-240.

Seitzinger, SP & Kroeze, C, 1998. Global distribution of nitrous oxide production and N inputs in freshwater and coastal ecosystems.

*Global Biogeochemical Cycles* **12**, 93-113.

Shepherd, RG, 1989. Correlations of permeability and grain size.

*Ground Water* **27**, 633-638.

Shum, KT, 1995. A numerical study of the wave-induced solute transport above a rippled bed.

*Journal of Fluid Mechanics* **299**, 267-288.

Shum, KT & Sundby, B, 1996. Organic matter processing in continental shelf sediments - the subtidal pump revisited.

*Marine Chemistry* **53**, 81-87.

Sievert, SM, Brinkhoff, T, Muyzer, G, Ziebis, W & Kuever, J, 1999. Spatial heterogeneity of bacterial populations along an environmental gradient at a shallow submarine hydrothermal vent near Milos Island (Greece).

*Applied and Environmental Microbiology* **65**, 3834-3842.

Sims, I, 1993. Measuring the growth of phytoplankton: The relationship between total organic carbon with three commonly used parameters of algal growth.

*Archives of Hydrobiology* **128**, 459-466.

Smayda, TJ, 1978. From phytoplankters to biomass.

In: Sournia, A (ed.). *Phytoplankton manual*. UNESCO.

Smith, DJ & Underwood, GJC, 1998. Exopolymer production by intertidal epipelagic diatoms. *Limnology and Oceanography* **43**, 1578-1591.

Staats, N, 1999. Exopolysaccharide production by marine benthic diatoms. Ph.D. thesis, University of Amsterdam.

Steenbergen, CLM, Korthals, HJ & Dobrynin, EG, 1994. Algal and bacterial pigments in non-laminated lacustrine sediment: studies of their sedimentation, degradation and stratigraphy. *FEMS Microbiology Ecology* **13**, 335-352.

Sun, M, Aller, RC & Lee, C, 1991. Early diagenesis of chlorophyll-a in Long Island Sound sediments: A measure of carbon flux and particle reworking. *Journal of Marine Research* **49**, 379-401.

Sun, M, Aller, RC & Lee, C, 1994. Spatial and temporal distributions of sedimentary chloropigments as indicators of benthic processes in Long Island Sound. *Journal of Marine Research* **52**, 149-176.

Tanoue, E & Handa, N, 1979. Differential sorption of organic matter by various sized sediment particles in recent sediment from the Bering Sea. *Journal of the Oceanographic Society of Japan* **35**, 199-208.

Thibodeaux, LJ & Boyle, JD, 1987. Bedform-generated convective transport in bottom sediment. *Nature* **325**, 341-343.

Turley, CM, Lochte, K & Lampitt, RS, 1995. Transformations of biogenic particles during sedimentation in the northeastern Atlantic. *Philosophical Transactions of the Royal Society of London Series B* **348**, 179-189.

Turley, CM & Mackie, PJ, 1994. Biogeochemical significance of attached and free-living bacteria and the flux of particles in the NE Atlantic Ocean. *Marine Ecology Progress Series* **115**, 191-203.

Underwood, GJC, Paterson, DM & Parkes, RJ, 1995. The measurement of microbial carbohydrate exopolymers from intertidal sediments. *Limnology and Oceanography* **40**, 1243-1253.

Upton, AC, Nedwell, DB, Parkes, RJ & Harvey, SM, 1993. Seasonal benthic microbial activity in the southern North Sea; oxygen uptake and sulphate reduction. *Marine Ecology Progress Series* **101**, 273-281.

van Raaphorst, W, Malschaert, H & van Haren, H, 1998. Tidal resuspension and deposition of particulate matter in the Oyster Grounds, North Sea. *Journal of Marine Research* **56**, 257-291.

- Verity, PGK, Stoecker, DE, Sieracki, MH, Burkill, PS, Edwards, E & Craig, RT, 1993. Abundance, biomass and distribution of heterotrophic dinoflagellates during the North Atlantic spring bloom. *Deep Sea Research II* **40**, 227-244.
- Walsh, JJ, 1988. On the nature of continental shelves. Academic Press.
- Webb, DG & Montagna, PA, 1993. Initial burial and subsequent degradation of sedimented phytoplankton - relative impact of macrobenthos and meiobenthos. *Journal of Experimental Marine Biology and Ecology* **166**, 151-163.
- Webb, JE & Theodor, J, 1968. Irrigation of submerged marine sands through wave action. *Nature* **220**, 682-685.
- Webster, IT & Taylor, JH, 1992. Rotational dispersion in porous media due to fluctuating flow. *Water Resources Research* **28**, 109-119.
- Wheatcroft, RA, Jumars, PA, Smith, CR & Nowell, ARM, 1990. A mechanistic view of the particulate biodiffusion coefficient: Step lengths, rest periods and transport directions. *Journal of Marine Research* **48**, 177-207.
- Wiesner, MG, Haake, B & Wirth, H, 1990. Organic facies of surface sediments in the North Sea. *Organic Geochemistry* **15**, 419-432.
- Wollast, R, 1991. The coastal organic carbon cycle: fluxes, sources, and sinks. In: Mantoura, RFC, Martin, JM & Wollast, R (ed.). *Ocean margin processes in global change*. John Wiley & Sons.
- Yallop, ML, de Winder, B, Paterson, DM & Stal, LJ, 1994. Comparative structure, primary production and biogenic stabilization of cohesive and non-cohesive marine sediments inhabited by microphytobenthos. *Estuarine, Coastal and Shelf Science* **39**, 565-582.
- Ziebis, W, Forster, S, Huettel, M & Jørgensen, BB, 1996a. Complex burrows of the mud shrimp *Callinassa truncata* and their geochemical impact in the sea bed. *Nature* **382**, 619-622.
- Ziebis, W, Huettel, M & Forster, S, 1996b. Impact of biogenic sediment topography on oxygen fluxes in permeable sediments. *Marine Ecology Progress Series* **140**, 227-237.

In dieser Reihe bereits erschienen:

- Nr. 1**      **Wefer, G., E. Suess und Fahrtteilnehmer**  
Bericht über die POLARSTERN-Fahrt ANT IV/2, Rio de Janeiro - Punta Arenas, 6.11. - 1.12.1985.  
60 Seiten, Bremen, 1986.
- Nr. 2**      **Hoffmann, G.**  
Holozänstratigraphie und Küstenlinienverlagerung an der andalusischen Mittelmeerküste.  
173 Seiten, Bremen, 1988. (vergriffen)
- Nr. 3**      **Wefer, G. und Fahrtteilnehmer**  
Bericht über die METEOR-Fahrt M 6/6, Libreville - Las Palmas, 18.2. - 23.3.1988.  
97 Seiten, Bremen, 1988.
- Nr. 4**      **Wefer, G., G.F. Lutze, T.J. Müller, O. Pfannkuche, W. Schenke, G. Siedler, W. Zenk**  
Kurzbericht über die METEOR-Expedition Nr. 6, Hamburg - Hamburg, 28.10.1987 - 19.5.1988.  
29 Seiten, Bremen, 1988. (vergriffen)
- Nr. 5**      **Fischer, G.**  
Stabile Kohlenstoff-Isotope in partikulärer organischer Substanz aus dem Südpolarmeer  
(Atlantischer Sektor). 161 Seiten, Bremen, 1989.
- Nr. 6**      **Berger, W.H. und G. Wefer**  
Partikelfluß und Kohlenstoffkreislauf im Ozean.  
Bericht und Kurzfassungen über den Workshop vom 3.-4. Juli 1989 in Bremen.  
57 Seiten, Bremen, 1989.
- Nr. 7**      **Wefer, G. und Fahrtteilnehmer**  
Bericht über die METEOR - Fahrt M 9/4, Dakar - Santa Cruz, 19.2. - 16.3.1989.  
103 Seiten, Bremen, 1989.
- Nr. 8**      **Kölling, M.**  
Modellierung geochemischer Prozesse im Sickerwasser und Grundwasser.  
135 Seiten, Bremen, 1990.
- Nr. 9**      **Heinze, P.-M.**  
Das Auftriebsgeschehen vor Peru im Spätquartär. 204 Seiten, Bremen, 1990. (vergriffen)
- Nr. 10**      **Willems, H., G. Wefer, M. Rinski, B. Donner, H.-J. Bellmann, L. Eißmann, A. Müller,  
B.W. Flemming, H.-C. Höfle, J. Merkt, H. Streif, G. Hertweck, H. Kuntze, J. Schwaar,  
W. Schäfer, M.-G. Schulz, F. Grube, B. Menke**  
Beiträge zur Geologie und Paläontologie Norddeutschlands: Exkursionsführer.  
202 Seiten, Bremen, 1990.
- Nr. 11**      **Wefer, G. und Fahrtteilnehmer**  
Bericht über die METEOR-Fahrt M 12/1, Kapstadt - Funchal, 13.3.1990 - 14.4.1990.  
66 Seiten, Bremen, 1990.
- Nr. 12**      **Dahmke, A., H.D. Schulz, A. Kölling, F. Kracht, A. Lücke**  
Schwermetallspuren und geochemische Gleichgewichte zwischen Porenlösung und Sediment  
im Wesermündungsgebiet. BMFT-Projekt MFU 0562, Abschlußbericht. 121 Seiten, Bremen, 1991.
- Nr. 13**      **Rostek, F.**  
Physikalische Strukturen von Tiefseesedimenten des Südatlantiks und ihre Erfassung in  
Echolotregistrierungen. 209 Seiten, Bremen, 1991.
- Nr. 14**      **Baumann, M.**  
Die Ablagerung von Tschernobyl-Radiocäsium in der Norwegischen See und in der Nordsee.  
133 Seiten, Bremen, 1991. (vergriffen)
- Nr. 15**      **Kölling, A.**  
Frühdiaagenetische Prozesse und Stoff-Flüsse in marinen und ästuarinen Sedimenten.  
140 Seiten, Bremen, 1991.
- Nr. 16**      **SFB 261 (Hrsg.)**  
1. Kolloquium des Sonderforschungsbereichs 261 der Universität Bremen (14.Juni 1991):  
Der Südatlantik im Spätquartär: Rekonstruktion von Stoffhaushalt und Stromsystemen.  
Kurzfassungen der Vorträge und Poster. 66 Seiten, Bremen, 1991.
- Nr. 17**      **Pätzold, J., T. Bickert, L. Brück, C. Gaedicke, K. Heidland, G. Meinecke, S. Mulitza**  
Bericht und erste Ergebnisse über die METEOR-Fahrt M 15/2, Rio de Janeiro - Vitoria,  
18.1. - 7.2.1991. 46 Seiten, Bremen, 1993.
- Nr. 18**      **Wefer, G. und Fahrtteilnehmer**  
Bericht und erste Ergebnisse über die METEOR-Fahrt M 16/1, Pointe Noire - Recife,  
27.3. - 25.4.1991. 120 Seiten, Bremen, 1991.
- Nr. 19**      **Schulz, H.D. und Fahrtteilnehmer**  
Bericht und erste Ergebnisse über die METEOR-Fahrt M 16/2, Recife - Belem, 28.4. - 20.5.1991.  
149 Seiten, Bremen, 1991.

- Nr. 20 Berner, H.**  
Mechanismen der Sedimentbildung in der Fram-Straße, im Arktischen Ozean und in der Norwegischen See. 167 Seiten, Bremen, 1991.
- Nr. 21 Schneider, R.**  
Spätquartäre Produktivitätsänderungen im östlichen Angola-Becken: Reaktion auf Variationen im Passat-Monsun-Windsystem und in der Advektion des Benguela-Küstenstroms. 198 Seiten, Bremen, 1991. (vergriffen)
- Nr. 22 Hebbeln, D.**  
Spätquartäre Stratigraphie und Paläozeanographie in der Fram-Straße. 174 Seiten, Bremen, 1991.
- Nr. 23 Lücke, A.**  
Umsetzungsprozesse organischer Substanz während der Frühdiagenese in ästuarinen Sedimenten. 137 Seiten, Bremen, 1991.
- Nr. 24 Wefer, G. und Fahrtteilnehmer**  
Bericht und erste Ergebnisse der METEOR-Fahrt M 20/1, Bremen - Abidjan, 18.11.- 22.12.1991. 74 Seiten, Bremen, 1992.
- Nr. 25 Schulz, H.D. und Fahrtteilnehmer**  
Bericht und erste Ergebnisse der METEOR-Fahrt M 20/2, Abidjan - Dakar, 27.12.1991 - 3.2.1992. 173 Seiten, Bremen, 1992.
- Nr. 26 Gingele, F.**  
Zur klimaabhängigen Bildung biogener und terrigener Sedimente und ihrer Veränderung durch die Frühdiagenese im zentralen und östlichen Südatlantik. 202 Seiten, Bremen, 1992.
- Nr. 27 Bickert, T.**  
Rekonstruktion der spätquartären Bodenwasserzirkulation im östlichen Südatlantik über stabile Isotope benthischer Foraminiferen. 205 Seiten, Bremen, 1992. (vergriffen)
- Nr. 28 Schmidt, H.**  
Der Benguela-Strom im Bereich des Walfisch-Rückens im Spätquartär. 172 Seiten, Bremen, 1992.
- Nr. 29 Meinecke, G.**  
Spätquartäre Oberflächenwassertemperaturen im östlichen äquatorialen Atlantik. 181 Seiten, Bremen, 1992.
- Nr. 30 Bathmann, U., U. Bleil, A. Dahmke, P. Müller, A. Nehr Korn, E.-M. Nöthig, M. Olesch, J. Pätzold, H.D. Schulz, V. Smetacek, V. Spieß, G. Wefer, H. Willems**  
Bericht des Graduierten Kollegs. Stoff-Flüsse in marinen Geosystemen. Berichtszeitraum Oktober 1990 - Dezember 1992. 396 Seiten, Bremen, 1992.
- Nr. 31 Damm, E.**  
Frühdiagenetische Verteilung von Schwermetallen in Schlicksedimenten der westlichen Ostsee. 115 Seiten, Bremen, 1992.
- Nr. 32 Antia, E.E.**  
Sedimentology, Morphodynamics and Facies Association of a mesotidal Barrier Island Shoreface (Spiekeroog, Southern North Sea). 370 Seiten, Bremen, 1993.
- Nr. 33 Duinker, J. und G. Wefer (Hrsg.)**  
Bericht über den 1. JGOFS-Workshop. 1./2. Dezember 1992 in Bremen. 83 Seiten, Bremen, 1993.
- Nr. 34 Kasten, S.**  
Die Verteilung von Schwermetallen in den Sedimenten eines stadtbremischen Hafenbeckens. 103 Seiten, Bremen, 1993.
- Nr. 35 Spieß, V.**  
Digitale Sedimentographie. Neue Wege zu einer hochauflösenden Akustostratigraphie. 199 Seiten, Bremen, 1993.
- Nr. 36 Schinzel, U.**  
Laborversuche zu frühdiagenetischen Reaktionen von Eisen (III) - Oxidhydraten in marinen Sedimenten. 189 Seiten, Bremen, 1993.
- Nr. 37 Sieger, R.**  
CoTAM - ein Modell zur Modellierung des Schwermetalltransports in Grundwasserleitern. 56 Seiten, Bremen, 1993. (vergriffen)
- Nr. 38 Willems, H. (Ed.)**  
Geoscientific Investigations in the Tethyan Himalayas. 183 Seiten, Bremen, 1993.
- Nr. 39 Hamer, K.**  
Entwicklung von Laborversuchen als Grundlage für die Modellierung des Transportverhaltens von Arsenat, Blei, Cadmium und Kupfer in wassergesättigten Säulen. 147 Seiten, Bremen, 1993.
- Nr. 40 Sieger, R.**  
Modellierung des Stofftransports in porösen Medien unter Ankopplung kinetisch gesteuerter Sorptions- und Redoxprozesse sowie thermischer Gleichgewichte. 158 Seiten, Bremen, 1993.

- Nr. 41 Thießen, W.**  
Magnetische Eigenschaften von Sedimenten des östlichen Südatlantiks und ihre paläozeanographische Relevanz. 170 Seiten, Bremen, 1993.
- Nr. 42 Spieß, V. und Fahrtteilnehmer**  
Report and preliminary results of METEOR-Cruise M 23/1, Kapstadt - Rio de Janeiro, 4.-25.2.1993. 139 Seiten, Bremen, 1994.
- Nr. 43 Bleil, U. und Fahrtteilnehmer**  
Report and preliminary results of METEOR-Cruise M 23/2, Rio de Janeiro - Recife, 27.2.-19.3.1993. 133 Seiten, Bremen, 1994.
- Nr. 44 Wefer, G. und Fahrtteilnehmer**  
Report and preliminary results of METEOR-Cruise M 23/3, Recife - Las Palmas, 21.3. - 12.4.1993. 71 Seiten, Bremen, 1994.
- Nr. 45 Giese, M. und G. Wefer (Hrsg.)**  
Bericht über den 2. JGOFs-Workshop. 18./19. November 1993 in Bremen. 93 Seiten, Bremen, 1994.
- Nr. 46 Balzer, W. und Fahrtteilnehmer**  
Report and preliminary results of METEOR-Cruise M 22/1, Hamburg - Recife, 22.9. - 21.10.1992. 24 Seiten, Bremen, 1994.
- Nr. 47 Stax, R.**  
Zyklische Sedimentation von organischem Kohlenstoff in der Japan See: Anzeiger für Änderungen von Paläozeanographie und Paläoklima im Spätkänozoikum. 150 Seiten, Bremen, 1994.
- Nr. 48 Skowronek, F.**  
Frühdiaogenetische Stoff-Flüsse gelöster Schwermetalle an der Oberfläche von Sedimenten des Weser Ästuares. 107 Seiten, Bremen, 1994.
- Nr. 49 Dersch-Hansmann, M.**  
Zur Klimaentwicklung in Ostasien während der letzten 5 Millionen Jahre: Terrigener Sedimenteintrag in die Japan See (ODP Ausfahrt 128). 149 Seiten, Bremen, 1994.
- Nr. 50 Zabel, M.**  
Frühdiaogenetische Stoff-Flüsse in Oberflächen-Sedimenten des äquatorialen und östlichen Südatlantik. 129 Seiten, Bremen, 1994.
- Nr. 51 Bleil, U. und Fahrtteilnehmer**  
Report and preliminary results of SONNE-Cruise SO 86, Buenos Aires - Capetown, 22.4. - 31.5.93. 116 Seiten, Bremen, 1994.
- Nr. 52 Symposium: The South Atlantic: Present and Past Circulation.**  
Bremen, Germany, 15 - 19 August 1994. Abstracts. 167 Seiten, Bremen, 1994.
- Nr. 53 Kretzmann, U.B.**  
57Fe-Mössbauer-Spektroskopie an Sedimenten - Möglichkeiten und Grenzen. 183 Seiten, Bremen, 1994.
- Nr. 54 Bachmann, M.**  
Die Karbonatrampe von Organyà im oberen Oberapt und unteren Unterapt (NE-Spanien, Prov. Lerida): Fazies, Zylo- und Sequenzstratigraphie. 147 Seiten, Bremen, 1994. (vergriffen)
- Nr. 55 Kemle-von Mücke, S.**  
Oberflächenwasserstruktur und -zirkulation des Südostatlantiks im Spätquartär. 151 Seiten, Bremen, 1994.
- Nr. 56 Petermann, H.**  
Magnetotaktische Bakterien und ihre Magnetosome in Oberflächensedimenten des Südatlantiks. 134 Seiten, Bremen, 1994.
- Nr. 57 Mulitza, S.**  
Spätquartäre Variationen der oberflächennahen Hydrographie im westlichen äquatorialen Atlantik. 97 Seiten, Bremen, 1994.
- Nr. 58 Segl, M. und Fahrtteilnehmer**  
Report and preliminary results of METEOR-Cruise M 29/1, Buenos-Aires - Montevideo, 17.6. - 13.7.1994. 94 Seiten, Bremen, 1994.
- Nr. 59 Bleil, U. und Fahrtteilnehmer**  
Report and preliminary results of METEOR-Cruise M 29/2, Montevideo - Rio de Janeiro 15.7. - 8.8.1994. 153 Seiten, Bremen, 1994.
- Nr. 60 Henrich, R. und Fahrtteilnehmer**  
Report and preliminary results of METEOR-Cruise M 29/3, Rio de Janeiro - Las Palmas 11.8. - 5.9.1994. Bremen, 1994. (vergriffen)

- Nr. 61 Sagemann, J.**  
Saisonale Variationen von Porenwasserprofilen, Nährstoff-Flüssen und Reaktionen in intertidalen Sedimenten des Weser-Ästuars. 110 Seiten, Bremen, 1994. (vergriffen)
- Nr. 62 Giese, M. und G. Wefer**  
Bericht über den 3. JGOFS-Workshop. 5./6. Dezember 1994 in Bremen. 84 Seiten, Bremen, 1995.
- Nr. 63 Mann, U.**  
Genese kretazischer Schwarzschiefer in Kolumbien: Globale vs. regionale/lokale Prozesse. 153 Seiten, Bremen, 1995. (vergriffen)
- Nr. 64 Willems, H., Wan X., Yin J., Dongdui L., Liu G., S. Dürr, K.-U. Gräfe**  
The Mesozoic development of the N-Indian passive margin and of the Xigaze Forearc Basin in southern Tibet, China. – Excursion Guide to IGCP 362 Working-Group Meeting "Integrated Stratigraphy". 113 Seiten, Bremen, 1995. (vergriffen)
- Nr. 65 Hünken, U.**  
Liefergebiets - Charakterisierung proterozoischer Goldseifen in Ghana anhand von Fluideinschluß - Untersuchungen. 270 Seiten, Bremen, 1995.
- Nr. 66 Nyandwi, N.**  
The Nature of the Sediment Distribution Patterns in the Spiekeroog Backbarrier Area, the East Frisian Islands. 162 Seiten, Bremen, 1995.
- Nr. 67 Isenbeck-Schröter, M.**  
Transportverhalten von Schwermetallkationen und Oxoanionen in wassergesättigten Sanden. - Laborversuche in Säulen und ihre Modellierung - 182 Seiten, Bremen, 1995.
- Nr. 68 Hebbeln, D. und Fahrtteilnehmer**  
Report and preliminary results of SONNE-Cruise SO 102, Valparaiso - Valparaiso, 95 134 Seiten, Bremen, 1995.
- Nr. 69 Willems, H. (Sprecher), U. Bathmann, U. Bleil, T. v. Dobeneck, K. Herterich, B.B. Jorgensen, E.-M. Nöthig, M. Olesch, J. Pätzold, H.D. Schulz, V. Smetacek, V. Spieß. G. Wefer**  
Bericht des Graduierten-Kollegs Stoff-Flüsse in marine Geosystemen. Berichtszeitraum Januar 1993 - Dezember 1995. 45 & 468 Seiten, Bremen, 1995.
- Nr. 70 Giese, M. und G. Wefer**  
Bericht über den 4. JGOFS-Workshop. 20./21. November 1995 in Bremen. 60 Seiten, Bremen, 1996. (vergriffen)
- Nr. 71 Meggers, H.**  
Pliozän-quartäre Karbonatsedimentation und Paläozeanographie des Nordatlantiks und des Europäischen Nordmeeres - Hinweise aus planktischen Foraminiferengemeinschaften. 143 Seiten, Bremen, 1996. (vergriffen)
- Nr. 72 Teske, A.**  
Phylogenetische und ökologische Untersuchungen an Bakterien des oxidativen und reduktiven marinen Schwefelkreislaufs mittels ribosomaler RNA.. 220 Seiten, Bremen, 1996. (vergriffen)
- Nr. 73 Andersen, N.**  
Biogeochemische Charakterisierung von Sinkstoffen und Sedimenten aus ostatlantischen Produktions-Systemen mit Hilfe von Biomarkern. 215 Seiten, Bremen, 1996.
- Nr. 74 Treppke, U.**  
Saisonalität im Diatomeen- und Silikoflagellatenfluß im östlichen tropischen und subtropischen Atlantik. 200 Seiten, Bremen, 1996.
- Nr. 75 Schüring, J.**  
Die Verwendung von Steinkohlebergematerialien im Deponiebau im Hinblick auf die Pyritverwitterung und die Eignung als geochemische Barriere. 110 Seiten, Bremen, 1996.
- Nr. 76 Pätzold, J. und Fahrtteilnehmer**  
Report and preliminary results of VICTOR HENSEN cruise JOPS II, Leg 6, Fortaleza - Recife. 10.3. - 26.3. 1995 and Leg 8, Vitória - Vitória, 10.4. - 23.4.1995. 87 Seiten, Bremen, 1996.
- Nr. 77 Bleil, U. und Fahrtteilnehmer**  
Report and preliminary results of METEOR-Cruise M 34/1, Cape Town - Walvis Bay, 3.-26.1.1996. 129 Seiten, Bremen, 1996.
- Nr. 78 Schulz, H.D. und Fahrtteilnehmer**  
Report and preliminary results of METEOR-Cruise M 34/2, Walvis Bay - Walvis Bay, 29.1.-18.2.96 133 Seiten, Bremen, 1996.
- Nr. 79 Wefer, G. und Fahrtteilnehmer**  
Report and preliminary results of METEOR-Cruise M 34/3, Walvis Bay - Recife, 21.2.-17.3.1996. 168 Seiten, Bremen, 1996.

- Nr. 80** **Fischer, G. und Fahrtteilnehmer**  
Report and preliminary results of METEOR-Cruise M 34/4, Recife - Bridgetown, 19.3.-15.4.1996.  
105 Seiten, Bremen, 1996.
- Nr. 81** **Kulbrok, F.**  
Biostratigraphie, Fazies und Sequenzstratigraphie einer Karbonatrampe in den Schichten der Oberkreide und des Alttertiärs Nordost-Ägyptens (Eastern Desert, N' Golf von Suez, Sinai).  
153 Seiten, Bremen, 1996.
- Nr. 82** **Kasten, S.**  
Early Diagenetic Metal Enrichments in Marine Sediments as Documents of Nonsteady-State Depositional Conditions. Bremen, 1996.
- Nr. 83** **Holmes, M.E.**  
Reconstruction of Surface Ocean Nitrate Utilization in the Southeast Atlantic Ocean Based on Stable Nitrogen Isotopes. 113 Seiten, Bremen, 1996.
- Nr. 84** **Rühlemann, C.**  
Akkumulation von Carbonat und organischem Kohlenstoff im tropischen Atlantik: Spätquartäre Produktivitäts-Variationen und ihre Steuerungsmechanismen.  
139 Seiten, Bremen, 1996.
- Nr. 85** **Ratmeyer, V.**  
Untersuchungen zum Eintrag und Transport lithogener und organischer partikulärer Substanz im östlichen subtropischen Nordatlantik. 154 Seiten, Bremen, 1996.
- Nr. 86** **Cepek, M.**  
Zeitliche und räumliche Variationen von Coccolithophoriden-Gemeinschaften im subtropischen Ost-Atlantik: Untersuchungen an Plankton, Sinkstoffen und Sedimenten. 156 Seiten, Bremen, 1996.
- Nr. 87** **Otto, S.**  
Die Bedeutung von gelöstem organischen Kohlenstoff (DOC) für den Kohlenstofffluß im Ozean. 150 Seiten, Bremen, 1996.
- Nr. 88** **Hensen, C.**  
Frühdiaagenetische Prozesse und Quantifizierung benthischer Stoff-Flüsse in Oberflächensedimenten des Südatlantiks. 132 Seiten, Bremen, 1996.
- Nr. 89** **Giese, M. und G. Wefer**  
Bericht über den 5. JGOFS-Workshop. 27./28. November 1996 in Bremen. 73 Seiten, Bremen, 1997.
- Nr. 90** **Wefer, G. und Fahrtteilnehmer**  
Report and preliminary results of METEOR-Cruise M 37/1, Lisbon - Las Palmas, 4.-23.12.1996.  
79 Seiten, Bremen, 1997.
- Nr. 91** **Isenbeck-Schröter, M., E. Bedbur, M. Kofod, B. König, T. Schramm & G. Mattheß**  
Occurrence of Pesticide Residues in Water - Assessment of the Current Situation in Selected EU Countries. 65 Seiten, Bremen 1997.
- Nr. 92** **Kühn, M.**  
Geochemische Folgereaktionen bei der hydrogeothermalen Energiegewinnung.  
129 Seiten, Bremen 1997.
- Nr. 93** **Determann, S. & K. Herterich**  
JGOFS-A6 "Daten und Modelle": Sammlung JGOFS-relevanter Modelle in Deutschland.  
26 Seiten, Bremen, 1997.
- Nr. 94** **Fischer, G. und Fahrtteilnehmer**  
Report and preliminary results of METEOR-Cruise M 38/1, Las Palmas - Recife, 25.1.-1.3.1997, with Appendix: Core Descriptions from METEOR Cruise M 37/1. Bremen, 1997.
- Nr. 95** **Bleil, U. und Fahrtteilnehmer**  
Report and preliminary results of METEOR-Cruise M 38/2, Recife - Las Palmas, 4.3.-14.4.1997.  
126 Seiten, Bremen, 1998.
- Nr. 96** **Neuer, S. und Fahrtteilnehmer**  
Report and preliminary results of VICTOR HENSEN-Cruise 96/1, Las Palmas - Las Palmas, 10.1. - 4-3.1996. 76 Seiten, Bremen, 1997.
- Nr. 97** **Villinger, H. und Fahrtteilnehmer**  
Fahrtbericht SO 111, 20.8. - 16.9.1996. 115 Seiten, Bremen, 1997.
- Nr. 98** **Lüning, S.**  
Late Cretaceous - Early Tertiary sequence stratigraphy, paleoecology and geodynamics of Eastern Sinai, Egypt. 218 Seiten, Bremen, 1997.
- Nr. 99** **Haese, R.R.**  
Beschreibung und Quantifizierung frühdiaagenetischer Reaktionen des Eisens in Sedimenten des Südatlantiks. 118 Seiten, Bremen, 1997.

- Nr. 100**     **Lührte, R. von**  
Verwertung von Bremer Baggergut als Material zur Oberflächenabdichtung von Deponien - Geochemisches Langzeitverhalten und Schwermetall-Mobilität (Cd, Cu, Ni, Pb, Zn). Bremen, 1997.
- Nr. 101**     **Ebert, M.**  
Der Einfluß des Redoxmilieus auf die Mobilität von Chrom im durchströmten Aquifer. 135 Seiten, Bremen, 1997.
- Nr. 102**     **Krögel, F.**  
Einfluß von Viskosität und Dichte des Seewassers auf Transport und Ablagerung von Wattsedimenten (Langeooger Rückseitenwatt, südliche Nordsee). 168 Seiten, Bremen, 1997.
- Nr. 103**     **Kerntopf, B.**  
Dinoflagellate Distribution Patterns and Preservation in the Equatorial Atlantic and Offshore North-West Africa. 137 Seiten, Bremen, 1997.
- Nr. 104**     **Breitzke, M.**  
Elastische Wellenausbreitung in marinen Sedimenten - Neue Entwicklungen der Ultraschall Sedimentphysik und Sedimentechographie. 298 Seiten, Bremen, 1997.
- Nr. 105**     **Marchant, M.**  
Rezente und spätquartäre Sedimentation planktischer Foraminiferen im Peru-Chile Strom. 115 Seiten, Bremen, 1997.
- Nr. 106**     **Habicht, K.S.**  
Sulfur isotope fractionation in marine sediments and bacterial cultures. 125 Seiten, Bremen, 1997.
- Nr. 107**     **Hamer, K., R.v. Lührte, G. Becker, T. Felis, S. Keffel, B. Strotmann, C. Waschkowitz, M. Kölling, M. Isenbeck-Schröter, H.D. Schulz**  
Endbericht zum Forschungsvorhaben 060 des Landes Bremen: Baggergut der Hafengruppe Bremen-Stadt: Modelluntersuchungen zur Schwermetallmobilität und Möglichkeiten der Verwertung von Hafenschlick aus Bremischen Häfen. 98 Seiten, Bremen, 1997.
- Nr. 108**     **Greeff, O.W.**  
Entwicklung und Erprobung eines benthischen Landersystemes zur *in situ*-Bestimmung von Sulfatreduktionsraten mariner Sedimente. 121 Seiten, Bremen, 1997.
- Nr. 109**     **Pätzold, M. und G. Wefer**  
Bericht über den 6. JGOFS-Workshop am 4./5.12.1997 in Bremen. Im Anhang: Publikationen zum deutschen Beitrag zur Joint Global Ocean Flux Study (JGOFS), Stand 1/1998. 122 Seiten, Bremen, 1998.
- Nr. 110**     **Landenberger, H.**  
CoTRem, ein Multi-Komponenten Transport- und Reaktions-Modell. 142 Seiten, Bremen, 1998.
- Nr. 111**     **Villinger, H. und Fahrtteilnehmer**  
Fahrtbericht SO 124, 4.10. - 16.10.1997. 90 Seiten, Bremen, 1997.
- Nr. 112**     **Gietl, R.**  
Biostratigraphie und Sedimentationsmuster einer nordostägyptischen Karbonatrampe unter Berücksichtigung der Alveolinen-Faunen. 142 Seiten, Bremen, 1998.
- Nr. 113**     **Ziebis, W.**  
The Impact of the Thalassinidean Shrimp *Callinassa truncata* on the Geochemistry of permeable, coastal Sediments. 158 Seiten, Bremen 1998.
- Nr. 114**     **Schulz, H.D. und Fahrtteilnehmer**  
Report and preliminary results of METEOR-Cruise M 41/1, Málaga - Libreville, 13.2.-15.3.1998. Bremen, 1998.
- Nr. 115**     **Völker, D.J.**  
Untersuchungen an strömungsbeeinflussten Sedimentationsmustern im Südozean. Interpretation sedimentechographischer Daten und numerische Modellierung. 152 Seiten, Bremen, 1998.
- Nr. 116**     **Schlünz, B.**  
Riverine Organic Carbon Input into the Ocean in Relation to Late Quaternary Climate Change. 136 Seiten, Bremen, 1998.
- Nr. 117**     **Kuhnert, H.**  
Aufzeichnung des Klimas vor Westaustralien in stabilen Isotopen in Korallenskeletten. 109 Seiten, Bremen, 1998.
- Nr. 118**     **Kirst, G.**  
Rekonstruktion von Oberflächenwassertemperaturen im östlichen Südatlantik anhand von Alkenonen. 130 Seiten, Bremen, 1998.
- Nr. 119**     **Dürkoop, A.**  
Der Brasil-Strom im Spätquartär: Rekonstruktion der oberflächennahen Hydrographie während der letzten 400 000 Jahre. 121 Seiten, Bremen, 1998.

- Nr. 120**     **Lamy, F.**  
Spätquartäre Variationen des terrigenen Sedimenteintrags entlang des chilenischen Kontinentalhangs als Abbild von Klimavariabilität im Milanković- und Sub-Milanković-Zeitbereich. 141 Seiten, Bremen, 1998.
- Nr. 121**     **Neuer, S. und Fahrtteilnehmer**  
Report and preliminary results of POSEIDON-Cruise Pos 237/2, Vigo – Las Palmas, 18.3.-31.3.1998. 39 Seiten, Bremen, 1998.
- Nr. 122**     **Romero, O.E.**  
Marine planktonic diatoms from the tropical and equatorial Atlantic: temporal flux patterns and the sediment record. 205 Seiten, Bremen, 1998.
- Nr. 123**     **Spiess, V. und Fahrtteilnehmer**  
Report and preliminary results of RV SONNE Cruise 125, Cochín – Chittagong, 17.10.-17.11.1997. 128 Seiten, Bremen, 1998.
- Nr. 124**     **Arz, H.W.**  
Dokumentation von kurzfristigen Klimaschwankungen des Spätquartärs in Sedimenten des westlichen äquatorialen Atlantiks. 96 Seiten, Bremen, 1998.
- Nr. 125**     **Wolff, T.**  
Mixed layer characteristics in the equatorial Atlantic during the late Quaternary as deduced from planktonic foraminifera. 132 Seiten, Bremen, 1998.
- Nr. 126**     **Dittert, N.**  
Late Quaternary Planktic Foraminifera Assemblages in the South Atlantic Ocean: Quantitative Determination and Preservational Aspects. 165 Seiten, Bremen, 1998.
- Nr. 127**     **Höll, C.**  
Kalkige und organisch-wandige Dinoflagellaten-Zysten in Spätquartären Sedimenten des tropischen Atlantiks und ihre palökologische Auswertbarkeit. 121 Seiten, Bremen, 1998.
- Nr. 128**     **Hencke, J.**  
Redoxreaktionen im Grundwasser: Etablierung und Verlagerung von Reaktionsfronten und ihre Bedeutung für die Spurenelement-Mobilität. 122 Seiten, Bremen 1998.
- Nr. 129**     **Pätzold, J. und Fahrtteilnehmer**  
Report and preliminary results of METEOR-Cruise M 41/3, Vitoria, Brasilien – Salvador de Bahia, Brasilien, 18.4. - 15.5.1998. Bremen, 1999.
- Nr. 130**     **Fischer, G. und Fahrtteilnehmer**  
Report and preliminary results of METEOR-Cruise M 41/4, Salvador de Bahia, Brasilien – Las Palmas, Spanien, 18.5. – 13.6.1998. Bremen, 1999.
- Nr. 131**     **Schlünz, B. und G. Wefer**  
Bericht über den 7. JGOFS-Workshop am 3. und 4.12.1998 in Bremen. Im Anhang: Publikationen zum deutschen Beitrag zur Joint Global Ocean Flux Study (JGOFS), Stand 1/ 1999. 100 Seiten, Bremen, 1999.
- Nr. 132**     **Wefer, G. und Fahrtteilnehmer**  
Report and preliminary results of METEOR-Cruise M 42/4, Las Palmas - Las Palmas - Viena do Castelo; 26.09.1998 - 26.10.1998. 104 Seiten, Bremen, 1999.
- Nr. 133**     **Felis, T.**  
Climate and ocean variability reconstructed from stable isotope records of modern subtropical Corals (Northern Red Sea). 111 Seiten, Bremen, 1999.
- Nr. 134**     **Draschba, S.**  
North Atlantic climate variability recorded in reef corals from Bermuda. 108 Seiten, Bremen, 1999.
- Nr. 135**     **Schmieder, F.**  
Magnetic Cyclostratigraphy of South Atlantic Sediments. 82 Seiten, Bremen, 1999.
- Nr. 136**     **Rieß, W.**  
In situ measurements of respiration and mineralisation processes – Interaction between fauna and geochemical fluxes at active interfaces. 68 Seiten, Bremen, 1999.
- Nr. 137**     **Devey, C.W. und Fahrtteilnehmer**  
Report and shipboard results from METEOR-cruise M 41/2, Libreville – Vitoria, 18.3. – 15.4.98. 59 Seiten, Bremen, 1999.
- Nr. 138**     **Wenzhöfer, F.**  
Biogeochemical processes at the sediment water interface and quantification of metabolically driven calcite dissolution in deep sea sediments. 103 Seiten, Bremen, 1999.

- Nr. 139 Klump, J.**  
Biogenic barite as a proxy of paleoproductivity variations in the Southern Peru-Chile Current. 107 Seiten, Bremen, 1999.
- Nr. 140 Huber, R.**  
Carbonate sedimentation in the northern Northatlantic since the late pliocene. 103 Seiten, Bremen, 1999.
- Nr. 141 Schulz, H.**  
Nitrate-storing sulfur bacteria in sediments of coastal upwelling. 94 Seiten, Bremen, 1999.
- Nr. 142 Mai, S.**  
Die Sedimentverteilung im Wattenmeer: ein Simulationsmodell. 114 Seiten, Bremen, 1999.
- Nr. 143 Neuer, S. und Fahrtteilnehmer**  
Report and preliminary results of Poseidon Cruise 248, Las Palmas - Las Palmas, 15.2.-26.2.1999. 45 Seiten, Bremen, 1999.
- Nr. 144 Weber, A.**  
Schwefelkreislauf in marinen Sedimenten und Messung von *in situ* Sulfatreduktionsraten. 122 Seiten, Bremen, 1999.
- Nr. 145 Haderler, A.**  
Sorptionenreaktionen im Grundwasser: Unterschiedliche Aspekte bei der Modellierung des Transportverhaltens von Zink. 122 Seiten, Bremen, 1999.
- Nr. 146 Dierßen, H.**  
Zum Kreislauf ausgewählter Spurenmetalle im Südatlantik: Vertikaltransport und Wechselwirkung zwischen Partikeln und Lösung. 167 Seiten, Bremen, 1999.
- Nr. 147 Zühlsdorff, L.**  
High resolution multi-frequency seismic surveys at the Eastern Juan de Fuca Ridge Flank and the Cascadia Margin – Evidence for thermally and tectonically driven fluid upflow in marine sediments. 118 Seiten, Bremen 1999.
- Nr. 148 Kinkel, H.**  
Living and late Quaternary Coccolithophores in the equatorial Atlantic Ocean: response of Distribution and productivity patterns to changing surface water circulation. Bremen 2000.
- Nr. 149 Pätzold, J. und Fahrtteilnehmer**  
Report and preliminary results of METEOR Cruise M 44/3, Aqaba (Jordan) - Safaga (Egypt) - Dubá (Saudi Arabia) – Suez (Egypt) - Haifa (Israel), 12.3.-26.3.-2.4.-4.4.1999. 135 Seiten, Bremen, 2000.
- Nr. 150 Schlünz, B. und G. Wefer**  
Bericht über den 8. JGOFS-Workshop am 2. und 3.12.1999 in Bremen. Im Anhang: Publikationen zum deutschen Beitrag zur Joint Global Ocean Flux Study (JGOFS), Stand 1/ 2000. 95 Seiten, Bremen, 2000.
- Nr. 151 Schnack, K.**  
Biostratigraphie und fazielle Entwicklung in der Oberkreide und im Alttertiär im Bereich der Kharga Schwelle, Westliche Wüste, SW-Ägypten. 142 Seiten, Bremen, 2000.
- Nr. 152 Karwath, B.**  
Ecological studies on living and fossil calcareous dinoflagellates of the equatorial and tropical Atlantic Ocean. 175 Seiten, Bremen, 2000.
- Nr. 153 Moustafa, Y.**  
Paleoclimatic reconstructions of the Northern Red Sea during the Holocene inferred from stable isotope records of modern and fossil corals and molluscs. 102 Seiten, Bremen, 2000.
- Nr. 154 Villinger, H. and cruise participants**  
Report and preliminary results of SONNE-cruise 145-1 Balboa – Talcahuana, 21.12.1999 – 28.01.2000. 147 Seiten, Bremen, 2000.